

# Transparent boundary condition and its high frequency approximation for the Schrödinger equation on a rectangular computational domain

Samardhi Yadav<sup>a</sup>, Vishal Vaibhav<sup>a,b</sup>

<sup>a</sup>Department of Physics, Indian Institute of Technology Delhi, Hauz Khas, New Delhi–110016, India

<sup>b</sup>Optics and Photonics Center, Indian Institute of Technology Delhi, Hauz Khas, New Delhi–110016, India

## Abstract

This paper addresses the numerical implementation of the transparent boundary condition (TBC) and its various approximations for the free Schrödinger equation on a rectangular computational domain. In particular, we consider the exact TBC and its spatially local approximation under high frequency assumption along with an appropriate corner condition. For the spatial discretization, we use a Legendre-Galerkin spectral method where Lobatto polynomials serve as the basis. Within variational formalism, we first arrive at the time-continuous dynamical system using spatially discrete form of the initial boundary-value problem incorporating the boundary conditions. This dynamical system is then discretized using various time-stepping methods, namely, the backward-differentiation formula of order 1 and 2 (i.e., BDF1 and BDF2, respectively) and the trapezoidal rule (TR) to obtain a fully discrete system. Next, we extend this approach to the novel Padé based implementation of the TBC presented by Yadav and Vaibhav [[arXiv:2403.07787\(2024\)](https://arxiv.org/abs/2403.07787)]. Finally, several numerical tests are presented to demonstrate the effectiveness of the boundary maps (incorporating the corner conditions) where we study the stability and convergence behavior empirically.

**Keywords:** Transparent Boundary Conditions, Two-dimensional Schrödinger Equation, High Frequency Approximation, Legendre-Galerkin Spectral Method, Convolution-Quadrature, Padé Approximants

## Contents

<b>1</b>	<b>Introduction</b>	<b>2</b>
<b>2</b>	<b>Transparent Boundary Conditions</b>	<b>3</b>
2.1	High frequency approximation	4
2.2	Fractional operator based formulation	6
2.3	Novel Padé approach	7
<b>3</b>	<b>Variational Formulation: Preliminaries</b>	<b>9</b>
<b>4</b>	<b>Variational Formulation: HF</b>	<b>10</b>
4.1	Nonlocal temporal discretization: Convolution quadrature	12
4.1.1	CQ-BDF1	13
4.1.2	CQ-BDF2	13
4.1.3	CQ-TR	14
4.2	Local temporal discretization: Conventional Padé	14
4.2.1	CP-BDF1	16
4.2.2	CP-BDF2	18
4.2.3	CP-TR	18

Email addresses: Samardhi@physics.iitd.ac.in (Samardhi Yadav), vishal.vaibhav@gmail.com (Vishal Vaibhav)

Preprint submitted to Communications in Nonlinear Science and Numerical Simulation

May 28, 2024

<b>5</b>	<b>Variational Formulation: TBCs</b>	<b>19</b>
5.1	Nonlocal temporal discretization: Convolution quadrature	20
5.1.1	CQ-BDF1	21
5.1.2	CQ-TR	21
5.2	Local temporal discretization: Novel Padé	21
5.2.1	NP-BDF1	23
5.2.2	NP-TR	25
<b>6</b>	<b>Numerical Experiments</b>	<b>27</b>
6.1	Exact solutions	27
6.1.1	Chirped-Gaussian profile	27
6.1.2	Hermite-Gaussian profile	28
6.2	Tests for evolution error	29
6.3	Tests for convergence	32
<b>7</b>	<b>Conclusion</b>	<b>32</b>
<b>Appendix A</b>	<b>Autonomous System</b>	<b>36</b>

## Notations

The set of non-zero positive real numbers ( $\mathbb{R}$ ) is denoted by  $\mathbb{R}_+$ . For any complex number  $\zeta$ ,  $\text{Re}(\zeta)$  and  $\text{Im}(\zeta)$  refer to the real and the imaginary parts of  $\zeta$ , respectively. The open interval  $(-1, 1)$  is denoted by  $\mathbb{I}$ .

## 1. Introduction

In this article, we address the numerical solution of the initial value problem (IVP) corresponding to the free Schrödinger equation formulated on  $\mathbb{R}^2$  given by

$$i\partial_t u + \Delta u = 0, \quad (\mathbf{x}, t) \in \mathbb{R}^2 \times \mathbb{R}_+, \quad (1)$$

with initial condition  $u(\mathbf{x}, 0) = u_0(\mathbf{x})$  which is assumed to be compactly supported. A Sommerfeld-like radiation condition at infinity is imposed in order to avoid any incoming waves which in turn ensures the uniqueness of the solution [1]. We are interested in solving the IVP on a rectangular computational domain denoted by  $\Omega_i$  such that  $\text{supp } u_0(\mathbf{x}) \subset \Omega_i$ . The Schrödinger equation appears in many areas of physical and technological interests, for instance, in quantum mechanics, underwater acoustics [2], and electromagnetic wave propagation [3]. This simple model can be augmented with a space and time-varying potential and nonlinear terms to model various systems of physical interest such as optical fibers [4]. For the rectangular domain, development of an efficient numerical scheme for (1) which is capable of handling the boundary and corner conditions is key to addressing more general systems in this hierarchy.

The exact TBC for the free Schrödinger equation for convex computational domains with smooth boundaries have been developed by several authors [5–8]. Among the existing approaches for a more general version of the Schrödinger equation, the pseudo-differential approach provides an approximation for the exact nonreflecting boundary operators [7, 9–12] for convex computational domains with smooth boundaries. Let us emphasize that the aforementioned methods are incapable of treating the corners in the boundary of the computational domain which rules out the rectangular domain. To the best of our knowledge, within the class of methods which employ nonreflecting boundary maps, the problem of corners has only been addressed in [8, 13–15]. The transparent boundary operator for the Schrödinger equation on a rectangular domain has the form  $\sqrt{\partial_t - i\Delta_\Gamma}$  and is nonlocal, both in time as well as space. The earliest approach for the numerical implementation of this operator was given by Menza [13] which is based on Padé approximant for the square root function, however, this approach became problematic at the corners of the domain. This problem was resolved by Feshchenko and Popov [14] who developed a representation in terms of fractional operators. The numerical approach presented by Feshchenko and Popov becomes computationally expensive on account of the increasing number of linear systems to be solved on the boundary segments with increasing

time-steps. In the recent work of Yadav and Vaibhav [15], a novel-Padé approach was developed which happens to be computationally efficient and capable of handling the corners of the domain adequately. The generalization of the novel-Padé approach for more general systems (i.e., including exterior potentials and nonlinear terms) is yet to be explored. For such systems, the use of pseudo-differential approach leads to approximate boundary conditions (BCs) involving the operators of the form  $(\partial_t - i\Delta_\Gamma)^\alpha$ ,  $\alpha = 1/2, -1/2, -1, \dots$ , where  $\Delta_\Gamma$  is the Laplace-Beltrami operator. Implementation of such BCs is not yet addressed on a rectangular domain because of non-availability of the corner conditions which is an open problem. However, spatially local form of these BCs under high-frequency approximation readily offer the possibility of constructing the *corner conditions* for the case of free as well as general Schrödinger equation [8]. Let us emphasize the fact that the use of the high-frequency BCs may impact accuracy but they are easier to implement and affords comparatively lower computational complexity which makes them attractive<sup>1</sup>.

Having made the aforementioned observations, we now turn to the main objective of this work which is twofold: (i) We address the numerical solution of the IVP in (1) with the BCs obtained as a result high-frequency approximation of the transparent boundary operator of this problem on a rectangular domain, and, (ii) we discuss the novel-Padé based implementation of the TBCs which serves as golden standard for comparison<sup>2</sup>. For space discretization, we use a Legendre-Galerkin method where Lobatto polynomials serve as basis functions. Within the variational formalism, we present a time-continuous route to arrive at a fully discrete system for the IBVP in (2). To this end, we start with a spatially discrete form of the initial boundary-value problem to obtain a time-continuous dynamical system by incorporating the boundary conditions. This dynamical system is nonlocal on account of presence of time-fractional operators. Temporal discretization of this system is addressed with convolution quadrature and also by employing Padé approximant based rational approximation for these time-fractional operators. Note that the former remains nonlocal while the latter becomes effectively local. This formalism presents a straightforward way of arriving at a dynamical system which can be further studied using the theory of autonomous ODEs (discussed in Appendix A) to assess the stability of the overall system. Let us note that this new formalism presents the possibility of using any higher order time-stepping method for the temporal discretization which can improve the accuracy of overall system. Finally, we extend this approach to the novel-Padé based implementation of TBCs within variational formalism.

The paper is organized in the following manner: Sec. 2 presents high-frequency approximation of the TBCs followed by a discussion of numerically tractable forms of the TBCs. This section also addresses the development of corner conditions under high frequency approximation. In Sec. 3, we collect all the facts about the Lobatto polynomial based Legendre-Galerkin spectral method for the numerical solution of the initial boundary-value problem (IBVP). In Sec. 4, we discuss the numerical solution of the IBVP using the boundary maps obtained as a result of high-frequency approximation using Legendre-Galerkin method. In Sec. 5, we discuss the numerical solution of the IBVP (in context of a Galerkin method) with effectively local form of the TBCs obtained as a result of novel Padé approach. We test the efficiency of our numerical schemes and confirm the order of convergence empirically with several numerical tests presented in Sec. 6. Finally, we conclude this paper in Sec. 7.

## 2. Transparent Boundary Conditions

Consider a rectangular computational domain  $(\Omega_i)$  with boundary segments parallel to one of the axes (see Fig. 1) with  $\Omega_i = (x_l, x_r) \times (x_b, x_t)$  referred to as the *interior* domain. Consider the decomposition of the field  $u(\mathbf{x}, t)$  such that  $u(\mathbf{x}, t) \in L^2(\mathbb{R}^2) = L^2(\Omega_i) \oplus L^2(\Omega_e)$  where  $\Omega_e = \mathbb{R}^2 \setminus \overline{\Omega_i}$  is referred to as the *exterior* domain. An equivalent formulation of the IVP in (1) on the computational domain  $\Omega_i$  can be stated as [8, 15]:

$$\begin{cases} i\partial_t u + \Delta u = 0, & (\mathbf{x}, t) \in \Omega_i \times \mathbb{R}_+, \\ u(\mathbf{x}, 0) = u_0(\mathbf{x}) \in L^2(\Omega_i), & \text{supp } u_0 \subset \Omega_i, \\ \partial_n u + e^{-i\pi/4}(\partial_t - i\partial_{x_2}^2)^{1/2} u = 0, & \mathbf{x} \in \Gamma_l \cup \Gamma_r, t > 0, \\ \partial_n u + e^{-i\pi/4}(\partial_t - i\partial_{x_1}^2)^{1/2} u = 0, & \mathbf{x} \in \Gamma_b \cup \Gamma_t, t > 0. \end{cases} \quad (2)$$

<sup>1</sup>Note that use of certain type of time-stepping methods are only possible under periodic or Dirichlet BCs which require sufficiently large computational domain. In this work, we would like to explore if high-frequency BCs can offer a better trade-off between complexity and accuracy.

<sup>2</sup>The method of perfectly matched layers will not be considered in this work for the purpose of comparison because it belongs to a different class of methods than presented in this article. Besides, a fair comparison can only be made if we consider an IVP that is fairly general so that no specific method has any distinct advantage. Therefore, this comparison is outside the scope of this article.

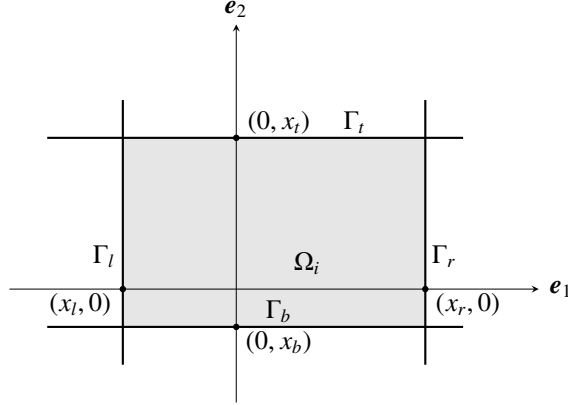


Figure 1: The figure shows a rectangular domain with boundary segments parallel to one of the axes.

Recalling from [15], the operator  $(\partial_t - i\partial_{x_1}^2)^{1/2}$  is defined as

$$(\partial_t - i\partial_{x_2}^2)^{1/2} f = (\partial_t - i\partial_{x_2}^2)[(\partial_t - i\partial_{x_2}^2)^{-1/2} f], \quad (3)$$

where

$$(\partial_t - i\partial_{x_2}^2)^{-1/2} f(x_2, t) = \frac{1}{\sqrt{\pi}} \int_0^t \int_{\mathbb{R}} f(x'_2, \tau) \frac{\mathcal{G}(x_2 - x'_2, t - \tau)}{\sqrt{t - \tau}} dx'_2 d\tau, \quad (4)$$

with the kernel  $\mathcal{G}$  function given by

$$\mathcal{G}(x_2, t) = \frac{e^{-i\pi/4}}{\sqrt{4\pi t}} \exp\left[i\frac{x_2^2}{4t}\right]. \quad (5)$$

Let us note that the fractional operators present in the DtN maps are non-local both in space and time. For an efficient numerical implementation of the IBVP (2), we present a spatially local form of these DtN-maps by employing a high-frequency approximation with respect to temporal frequencies. This approach is presented in Sec. 2.1 which also includes corner conditions obtained as a result of high-frequency approximation. Before we address the numerical aspects, we revisit various numerically tractable representations for these operators at the continuous level in Sec. 2.2 and Sec. 2.3. Finally, we present our main contribution from Sec. 3 onward where a numerical recipe is described to arrive at a spatially discrete time-continuous dynamical system in context of variational formulation. This dynamical system can be further discretized temporally with any choice of time-stepping method to arrive at a fully discrete system for the IBVP (2).

### 2.1. High frequency approximation

The boundary conditions in (2) can be further simplified by making them local in terms of spatial variables under high-frequency approximation with respect to the temporal frequencies. We reproduce the steps from [8] for the sake of completeness. Let  $(\zeta_1, \zeta_2)$  be the covariables corresponding to  $(x_1, x_2)$  to be used in the two dimensional Fourier transform. Let  $z$  denote the complex variable in the Laplace transform. The operator  $(\partial_t - i\partial_{x_1}^2)^{-1/2}$  in the transformed space is  $1/\sqrt{z + i\zeta_1^2}$  such that  $\sqrt{\cdot}$  denotes the branch with  $\text{Im}(\alpha) > 0$ . Consider

$$\mathcal{L}^{-1}\left[\frac{1}{\sqrt{z + i\zeta_2^2}}\right] = \frac{1}{2\pi i} \int \frac{e^{zt}}{\sqrt{z + i\zeta_2^2}} dz. \quad (6)$$

Setting  $\xi = zt$ , we have

$$\begin{aligned}\mathcal{L}^{-1}\left[\frac{1}{\sqrt{z+i\zeta_2^2}}\right] &= \frac{t^{-\frac{1}{2}}}{2\pi i} \int_{a+i\mathbb{R}} \frac{e^\xi}{\sqrt{\xi+i\zeta_2^2 t}} d\xi = \frac{t^{-\frac{1}{2}}}{2\pi i} \int_{a+i\mathbb{R}} \left(1 + \frac{i\zeta_2^2 t}{\xi}\right)^{-\frac{1}{2}} \frac{e^\xi d\xi}{\sqrt{\xi}} \quad (a > 0) \\ &\sim \frac{t^{-\frac{1}{2}}}{2\pi i} \int_{a+i\mathbb{R}} \left(\frac{1}{\xi^{\frac{1}{2}}} - \frac{i\zeta_2^2 t}{2\xi^{\frac{3}{2}}} - \frac{3\zeta_2^4 t^2}{8\xi^{\frac{5}{2}}} + \dots\right) e^\xi d\xi \sim \frac{1}{\Gamma(\frac{1}{2})} t^{-\frac{1}{2}} - \frac{i}{2\Gamma(\frac{3}{2})} t^{\frac{1}{2}} \zeta_2^2 - \frac{3}{8\Gamma(\frac{5}{2})} t^{\frac{3}{2}} \zeta_2^4 + \dots\end{aligned}$$

which yields the expansion

$$\begin{aligned}(\partial_t - i\partial_{x_1}^2)^{-1/2} &\sim \partial_t^{-1/2} + i\frac{1}{2}\partial_t^{-3/2}\partial_{x_2}^2 - \frac{3}{8}\partial_t^{-5/2}\partial_{x_2}^4 + \dots, \\ (\partial_t - i\partial_{x_1}^2)^{1/2} &= (\partial_t - i\partial_{x_1}^2)^{-1/2}(\partial_t - i\partial_{x_1}^2) \sim \partial_t^{1/2} - i\frac{1}{2}\partial_t^{-1/2}\partial_{x_2}^2 + \frac{1}{8}\partial_t^{-3/2}\partial_{x_2}^4 + \dots\end{aligned}$$

We obtain the following form of DtN map as a result of high-frequency approximation on  $\Gamma_r$ :

$$\partial_{x_1} u + e^{-i\pi/4} \partial_t^{1/2} u - e^{i\pi/4} \frac{1}{2} \partial_{x_2}^2 \partial_t^{-1/2} u = 0 \quad \text{mod } (\partial_t^{-3/2}). \quad (7)$$

Following a similar approach for rest of the segments of the rectangular domain, we obtain the following approximate BCs:

$$\begin{aligned}\partial_n u + e^{-i\pi/4} \partial_t^{1/2} u - e^{i\pi/4} \frac{1}{2} \partial_{x_2}^2 \partial_t^{-1/2} u &= 0, \quad \mathbf{x} \in \Gamma_r \cup \Gamma_l, \\ \partial_n u + e^{-i\pi/4} \partial_t^{1/2} u - e^{i\pi/4} \frac{1}{2} \partial_{x_1}^2 \partial_t^{-1/2} u &= 0, \quad \mathbf{x} \in \Gamma_b \cup \Gamma_t.\end{aligned} \quad (8)$$

These boundary conditions do not take into account the corners of the rectangular domain and become problematic at corners. To understand this, we consider the weak formulation of the original IVP as follows: Consider a test function  $\psi(\mathbf{x}) \in L^2(\Omega_i)$ , taking the inner product with the equation (1), we have

$$\int_{\Omega_i} (i\partial_t u + \nabla^2 u) \psi d^2 \mathbf{x} = i\partial_t \int_{\Omega_i} u \psi d^2 \mathbf{x} - \int_{\Omega_i} (\nabla u) \cdot (\nabla \psi) d^2 \mathbf{x} + \int_{\partial\Omega_i} \psi (\nabla u) \cdot d\sigma. \quad (9)$$

The boundary integrals on top and right segments are given by

$$\begin{aligned}\int_{\Gamma_r} \psi \partial_{x_1} u dx_2 + \int_{\Gamma_t} \psi \partial_{x_2} u dx_1 &= -e^{-i\pi/4} \int_{\Gamma_r \cup \Gamma_t} \psi \partial_t^{1/2} u + \frac{1}{2} e^{i\pi/4} \left[ \int_{\Gamma_r} \psi \partial_{x_2}^2 \partial_t^{-1/2} u dx_2 + \int_{\Gamma_t} \psi \partial_{x_1}^2 \partial_t^{-1/2} u dx_1 \right] \\ &= -e^{-i\pi/4} \int_{\Gamma_r \cup \Gamma_t} \psi \partial_t^{1/2} u + \frac{1}{2} e^{i\pi/4} \left[ \psi \partial_{x_2} \partial_t^{-1/2} u \Big|_{x_2=x_b}^{x_t} + \psi \partial_{x_1} \partial_t^{-1/2} u \Big|_{x_1=x_l}^{x_r} \right. \\ &\quad \left. - \int_{\Gamma_r} (\partial_{x_2} \psi) (\partial_{x_2} \partial_t^{-1/2} u) dx_2 - \int_{\Gamma_t} (\partial_{x_1} \psi) (\partial_{x_1} \partial_t^{-1/2} u) dx_1 \right].\end{aligned}$$

Consider the terms which correspond to the top-right corner in the above equation:

$$(\partial_{x_2} \partial_t^{-1/2} u + \partial_{x_1} \partial_t^{-1/2} u)_{\Gamma_r \cap \Gamma_t} = \partial_t^{-1/2} (\partial_{x_2} u + \partial_{x_1} u)_{\Gamma_r \cap \Gamma_t}. \quad (10)$$

They are problematic on account of the fact that the BCs in the current form cannot be used to evaluate them. We can evaluate these terms by applying  $\partial_t^{-1/2}$  to the IVP in (1) as

$$i\partial_t^{1/2} u + (\partial_{x_1}^2 + \partial_{x_2}^2) \partial_t^{-1/2} u = 0, \quad (x_1, x_2) \in \Gamma_r \cap \Gamma_t. \quad (11)$$

Here, the fact that the field is zero at the corner at  $t = 0$  is explicitly used to arrive at the fractional derivative. Using BCs in (8) and the last equation, we get the following corner condition:

$$\partial_{x_1} u + \partial_{x_2} u + \frac{3}{2} e^{-i\pi/4} \partial_t^{1/2} u = 0, \quad (x_1, x_2) \in \Gamma_r \cap \Gamma_t. \quad (12)$$

Following a similar approach, we can construct the corner conditions for rest of the corners of the rectangular domain:

$$\partial_n u|_{\Gamma_i} + \partial_n u|_{\Gamma_j} + \frac{3}{2} e^{-i\pi/4} \partial_t^{1/2} u = 0, \quad (x_1, x_2) \in \Gamma_i \cap \Gamma_j, \quad (13)$$

where  $i \neq j$  and  $i, j \in \{r, t, l, b\}$ . Let us introduce the set of corner points of the computational domain as  $\Gamma_C = \{\Gamma_{rt}, \Gamma_{rb}, \Gamma_{lt}, \Gamma_{lb}\}$  where  $\Gamma_{ij} = \Gamma_i \cap \Gamma_j$  with  $i, j \in \{r, t, l, b\}$ . Under high-frequency approximation, we have the following equivalent formulation for (2) on  $\Omega_i$ :

$$\begin{cases} i\partial_t u + \Delta u = 0, & (\mathbf{x}, t) \in \Omega_i \times \mathbb{R}_+, \\ u(\mathbf{x}, 0) = u_0(\mathbf{x}) \in L^2(\Omega_i), & \text{supp } u_0 \subset \Omega_i, \\ \partial_n u + e^{-i\pi/4} \partial_t^{1/2} u - e^{i\pi/4} \frac{1}{2} \Delta_\Gamma \partial_t^{-\frac{1}{2}} u = 0, & \mathbf{x} \in \Gamma \setminus \Gamma_C, \\ \partial_{n_1} u + \partial_{n_2} u + \frac{3}{2} e^{-i\pi/4} \partial_t^{\frac{1}{2}} u = 0, & \mathbf{x} \in \Gamma_C, t > 0. \end{cases} \quad (14)$$

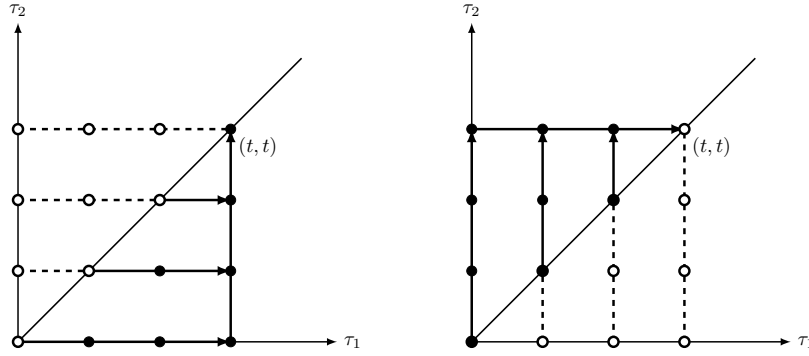


Figure 2: A schematic depiction of the evolution of the auxiliary field  $\varphi(x_1, x_2, \tau_1, \tau_2)$  in the  $(\tau_1, \tau_2)$ -plane is provided in this figure where the plot on the right corresponds  $\mathbf{x} \in \Gamma_r \cup \Gamma_l$  and the plot on the left corresponds  $\mathbf{x} \in \Gamma_t \cup \Gamma_b$ . The filled circles depict the evolution of the auxiliary field  $\varphi(x_1, x_2, \tau_1, \tau_2)$  either above or below the diagonal in the  $(\tau_1, \tau_2)$ -plane starting from the diagonal which also serves as initial conditions for solving IVPs corresponding to the auxiliary function. The TBCs for the auxiliary field require the history of the auxiliary field at the corner points which makes empty circles relevant. Note that these values at the corners can be taken from the adjacent segment of the boundary where it is already being computed and this is depicted by broken lines. Note that the vertical/horizontal lines where the arrows end corresponds to the history of the auxiliary field needed for the TBCs on  $\partial\Omega_i$  in the current time ( $t$ ).

## 2.2. Fractional operator based formulation

In this section, we provide a summary of the fractional operator based approach which we presented in [15]. The DtN maps in terms of a time-fractional derivative operator for the IVP (2) can be expressed as

$$\begin{aligned} \partial_{x_1} u(\mathbf{x}, t) &= -e^{-i\pi/4} \partial_{\tau_1}^{1/2} \varphi(x_1, x_2, \tau_1, \tau_2) \Big|_{\tau_1, \tau_2=t}, & (x_1, x_2) \in \Gamma_r, \\ \partial_{x_1} u(\mathbf{x}, t) &= +e^{-i\pi/4} \partial_{\tau_1}^{1/2} \varphi(x_1, x_2, \tau_1, \tau_2) \Big|_{\tau_1, \tau_2=t}, & (x_1, x_2) \in \Gamma_l, \\ \partial_{x_2} u(\mathbf{x}, t) &= -e^{-i\pi/4} \partial_{\tau_2}^{1/2} \varphi(x_1, x_2, \tau_1, \tau_2) \Big|_{\tau_1, \tau_2=t}, & (x_1, x_2) \in \Gamma_t, \\ \partial_{x_2} u(\mathbf{x}, t) &= +e^{-i\pi/4} \partial_{\tau_2}^{1/2} \varphi(x_1, x_2, \tau_1, \tau_2) \Big|_{\tau_1, \tau_2=t}, & (x_1, x_2) \in \Gamma_b. \end{aligned} \quad (15)$$

the auxiliary functions satisfy the IVPs given by

$$\begin{aligned} [i\partial_{\tau_1} + \partial_{x_1}^2] \varphi(x_1, x_2, \tau_1, \tau_2) &= 0, & (x_1, x_2) \in \Gamma_t \cup \Gamma_b, \tau_1 \in (\tau_2, t], \\ [i\partial_{\tau_2} + \partial_{x_2}^2] \varphi(x_1, x_2, \tau_1, \tau_2) &= 0, & (x_1, x_2) \in \Gamma_l \cup \Gamma_r, \tau_2 \in (\tau_1, t], \end{aligned} \quad (16)$$

with the initial condition  $\varphi(x_1, x_2, \tau_1, \tau_1) = u(x_1, x_2, \tau_1)$  and  $\varphi(x_1, x_2, \tau_2, \tau_2) = u(x_1, x_2, \tau_2)$ . Let us introduce the set of corner points of the computational domain as  $\Gamma_C = \{\Gamma_{rt}, \Gamma_{rb}, \Gamma_{lt}, \Gamma_{lb}\}$  where  $\Gamma_{ij} = \Gamma_i \cap \Gamma_j$  with  $i, j \in \{r, t, l, b\}$ . The transparent boundary conditions at corner points for the IVPs listed in (16) are as follows

$$\begin{aligned} \partial_{x_1} \varphi(x_1, x_2, \tau_1, \tau_2) + e^{-i\pi/4} \partial_{\tau_1}^{1/2} \varphi(x_1, x_2, \tau_1, \tau_2) &= 0, & (x_1, x_2) \in \{\Gamma_{rt}, \Gamma_{rb}\}, \\ \partial_{x_1} \varphi(x_1, x_2, \tau_1, \tau_2) - e^{-i\pi/4} \partial_{\tau_1}^{1/2} \varphi(x_1, x_2, \tau_1, \tau_2) &= 0, & (x_1, x_2) \in \{\Gamma_{lt}, \Gamma_{lb}\}, \\ \partial_{x_2} \varphi(x_1, x_2, \tau_1, \tau_2) + e^{-i\pi/4} \partial_{\tau_2}^{1/2} \varphi(x_1, x_2, \tau_1, \tau_2) &= 0, & (x_1, x_2) \in \{\Gamma_{rt}, \Gamma_{lt}\}, \\ \partial_{x_2} \varphi(x_1, x_2, \tau_1, \tau_2) - e^{-i\pi/4} \partial_{\tau_2}^{1/2} \varphi(x_1, x_2, \tau_1, \tau_2) &= 0. & (x_1, x_2) \in \{\Gamma_{rb}, \Gamma_{lb}\}. \end{aligned} \quad (17)$$

The history required for the fractional derivatives present in the DtN maps can be understood with the help of the schematic shown in Fig. 2. The two IVPs for the auxiliary field  $\varphi(x_1, x_2, \tau_1, \tau_2)$  advances the field either above or below the diagonal in the  $(\tau_1, \tau_2)$ -plane starting from the diagonal which also serves as initial conditions for solving IVPs. This is depicted by filled circles where arrows denote the direction of evolution. The TBCs present in (17) to solve the IVPs for the auxiliary functions on the boundary segments require the history of the auxiliary function at corners from the start of the computations which makes the empty circles relevant. Note that these values at the corners can be taken from the adjacent segment of the boundary where it is already being computed. This is depicted by broken lines in Fig. 2.

### 2.3. Novel Padé approach

In this section, we provide a summary of the novel-Padé approach which we presented in [15]. This approach relies on the Padé approximant based representation for the  $1/2$ -order temporal derivative in (15). Let the  $K$ -th order diagonal Padé approximant based rational approximation for the function  $\sqrt{z}$  be denoted by  $R_K^{(1/2)}(z)$  is given by

$$R_K^{(1/2)}(z) = b_0 - \sum_{k=1}^K \frac{b_k}{z + \eta_k^2}, \quad \text{where} \quad \begin{cases} b_0 = 2K + 1, & b_k = \frac{2\eta_k^2(1 + \eta_k^2)}{2K + 1}, \\ \eta_k = \tan \theta_k, & \theta_k = \frac{k\pi}{2K + 1}, \quad k = 1, 2, \dots, K. \end{cases} \quad (18)$$

Following [15], we introduce the following notations for the auxiliary function:

$$\begin{aligned} \varphi_{a_1}(x_2, \tau_1, \tau_2) &= \varphi(x_{a_1}, x_2, \tau_1, \tau_2), & a_1 \in \{l, r\}, \\ \varphi_{a_2}(x_1, \tau_1, \tau_2) &= \varphi(x_1, x_{a_2}, \tau_1, \tau_2), & a_2 \in \{b, t\}. \end{aligned} \quad (19)$$

Corresponding to the each of the partial fractions in (18), we introduce the auxiliary functions  $\varphi_{k,a_1}$  and  $\varphi_{k,a_2}$  such that they satisfy the following ODEs:

$$\begin{aligned} (\partial_{\tau_1} + \eta_k^2) \varphi_{k,a_1}(x_2, \tau_1, \tau_2) &= \varphi_{a_1}(x_2, \tau_1, \tau_2), \\ (\partial_{\tau_2} + \eta_k^2) \varphi_{k,a_2}(x_1, \tau_1, \tau_2) &= \varphi_{a_2}(x_1, \tau_1, \tau_2), \end{aligned} \quad (20)$$

with the initial conditions assumed to be  $\varphi_{k,a_1}(x_2, 0, \tau_2) = 0$  and  $\varphi_{k,a_2}(x_1, \tau_1, 0) = 0$ , respectively. The solution can be stated as

$$\begin{aligned} \varphi_{k,a_1}(x_2, \tau_1, \tau_2) &= \int_0^{\tau_1} e^{-\eta_k^2(\tau_1-s_1)} \varphi_{a_1}(x_2, s_1, \tau_2) ds_1, & a_1 \in \{l, r\}, \\ \varphi_{k,a_2}(x_1, \tau_1, \tau_2) &= \int_0^{\tau_2} e^{-\eta_k^2(\tau_2-s_2)} \varphi_{a_2}(x_1, \tau_1, s_2) ds_2, & a_2 \in \{t, b\}. \end{aligned} \quad (21)$$

The DtN maps for the interior problem present in (15) now reads as

$$\begin{aligned} \partial_{x_1} u(\mathbf{x}, t) \pm e^{-i\pi/4} \left[ b_0 u(\mathbf{x}, t) - \sum_{k=1}^K b_k \varphi_{k,a_1}(x_2, t, t) \right] &\approx 0, \\ \partial_{x_2} u(\mathbf{x}, t) \pm e^{-i\pi/4} \left[ b_0 u(\mathbf{x}, t) - \sum_{k=1}^K b_k \varphi_{k,a_2}(x_1, t, t) \right] &\approx 0. \end{aligned} \quad (22)$$

It is straightforward to conclude that auxiliary fields satisfy the same IVPs which are satisfied by auxiliary function

$$\begin{aligned} [i\partial_{\tau_2} + \partial_{x_2}^2]\varphi_{k,a_1}(x_2, \tau_1, \tau_2) &= 0, \quad (x_1, x_2) \in \Gamma_l \cup \Gamma_r, \quad \tau_2 \in (\tau_1, t], \\ [i\partial_{\tau_1} + \partial_{x_1}^2]\varphi_{k,a_2}(x_1, \tau_1, \tau_2) &= 0, \quad (x_1, x_2) \in \Gamma_t \cup \Gamma_b, \quad \tau_1 \in (\tau_2, t]. \end{aligned} \quad (23)$$

The transparent boundary conditions for these IVPs can be written as:

$$\begin{aligned} \partial_{x_2}\varphi_{k,a_1}(x_b, \tau_1, \tau_2) - e^{-i\pi/4}\partial_{\tau_2}^{1/2}\varphi_{k,a_1}(x_b, \tau_1, \tau_2) &= 0, \\ \partial_{x_2}\varphi_{k,a_1}(x_t, \tau_1, \tau_2) + e^{-i\pi/4}\partial_{\tau_2}^{1/2}\varphi_{k,a_1}(x_t, \tau_1, \tau_2) &= 0, \\ \partial_{x_1}\varphi_{k,a_2}(x_l, \tau_1, \tau_2) - e^{-i\pi/4}\partial_{\tau_1}^{1/2}\varphi_{k,a_2}(x_l, \tau_1, \tau_2) &= 0, \\ \partial_{x_1}\varphi_{k,a_2}(x_r, \tau_1, \tau_2) + e^{-i\pi/4}\partial_{\tau_1}^{1/2}\varphi_{k,a_2}(x_r, \tau_1, \tau_2) &= 0. \end{aligned} \quad (24)$$

Once again, we use the Padé approximants based representation for the 1/2-order temporal derivative operator present in the TBCs for the auxiliary fields described in (24). Introducing the auxiliary fields  $\psi_{k,k',a_1,a_2}(\tau_1, \tau_2)$  and  $\psi_{k,k',a_2,a_1}(\tau_1, \tau_2)$  at the end points of the boundary segments  $\Gamma_{a_1}$  and  $\Gamma_{a_2}$ , respectively, such that In the physical space, every  $\psi_{k,k',a_1,a_2}$  and  $\psi_{k,k',a_2,a_1}$  satisfy the following ODEs:

$$\begin{aligned} (\partial_{\tau_2} + \eta_{k'}^2)\psi_{k,k',a_1,a_2}(\tau_1, \tau_2) &= \varphi_{k,a_1}(x_{a_2}, \tau_1, \tau_2), \\ (\partial_{\tau_1} + \eta_{k'}^2)\psi_{k,k',a_2,a_1}(\tau_1, \tau_2) &= \varphi_{k,a_2}(x_{a_1}, \tau_1, \tau_2), \end{aligned} \quad (25)$$

with the initial conditions assumed to be  $\psi_{k,k',a_1,a_2}(\tau_1, 0) = 0$  and  $\psi_{k,k',a_2,a_1}(0, \tau_2) = 0$ , respectively. The solution to the ODEs (25) reads as

$$\begin{aligned} \psi_{k,k',a_1,a_2}(\tau_1, \tau_2) &= \int_0^{\tau_2} e^{-\eta_{k'}^2(\tau_2-s_2)} \varphi_{k,a_1}(x_{a_2}, \tau_1, s_2) ds_2, \\ \psi_{k,k',a_2,a_1}(\tau_1, \tau_2) &= \int_0^{\tau_1} e^{-\eta_{k'}^2(\tau_1-s_1)} \varphi_{k,a_2}(x_{a_1}, s_1, \tau_2) ds_1. \end{aligned} \quad (26)$$

The DtN maps for the auxiliary fields (24) now reads as

$$\begin{aligned} \partial_{x_2}\varphi_{k,a_1}(x_{a_2}, \tau_1, \tau_2) \pm e^{-i\pi/4} \left[ b_0\varphi_{k,a_1}(x_{a_2}, \tau_1, \tau_2) - \sum_{k'=1}^K b_{k'}\psi_{k,k',a_1,a_2}(\tau_1, \tau_2) \right] &= 0, \\ \partial_{x_1}\varphi_{k,a_2}(x_{a_1}, \tau_1, \tau_2) \pm e^{-i\pi/4} \left[ b_0\varphi_{k,a_2}(x_{a_1}, \tau_1, \tau_2) - \sum_{k'=1}^K b_{k'}\psi_{k,k',a_2,a_1}(\tau_1, \tau_2) \right] &= 0. \end{aligned} \quad (27)$$

It is interesting to note that fields  $\psi_{k,k',a_1,a_2}(\tau_1, \tau_2)$  and  $\psi_{k,k',a_2,a_1}(\tau_1, \tau_2)$  are transpose of each other [15]. This observation allows us to develop a rather efficient numerical scheme from a storage point of view. These ODEs for the auxiliary fields can now be summarized as

$$\begin{aligned} (\partial_{\tau_1} + \eta_k^2)\psi_{k,k',a_1,a_2}(\tau_1, \tau_2) &= \varphi_{k',a_2}(x_{a_1}, \tau_1, \tau_2), \\ (\partial_{\tau_2} + \eta_k^2)\psi_{k,k',a_2,a_1}(\tau_1, \tau_2) &= \varphi_{k',a_1}(x_{a_2}, \tau_1, \tau_2). \end{aligned} \quad (28)$$

The evolution of the auxiliary fields  $\varphi_{k,a_1}(x_2, \tau_1, \tau_2)$ ,  $\varphi_{k,a_2}(x_1, \tau_1, \tau_2)$  and  $\psi_{k,k',a_1,a_2}(\tau_1, \tau_2)$  in the  $(\tau_1, \tau_2)$ -plane can be understood with the help of the schematic shown in Fig. 3. In this schematic, Fig. 3(A) and Fig. 3(B) depict the evolution of the fields  $\varphi_{k,a_2}(x_1, \tau_1, \tau_2)$  and  $\varphi_{k,a_1}(x_2, \tau_1, \tau_2)$  on the boundary segments  $\Gamma_{a_2}$  and  $\Gamma_{a_1}$ , respectively. The diagonal to diagonal computation of the fields  $\varphi_{k,a_1}(x_2, \tau_1, \tau_2)$  and  $\varphi_{k,a_2}(x_1, \tau_1, \tau_2)$  consists of first advancing the fields using the IVPs established in (23) and then using the ODEs in (20) for the second movement. Our novel Padé approach makes the numerical scheme efficient from a storage point of view which is obvious from the schematic presented. Similarly, Fig. 3(C) depicts the evolution of the field  $\psi_{k,k',a_1,a_2}(\tau_1, \tau_2)$  which can be achieved by moving either below or above the diagonal.



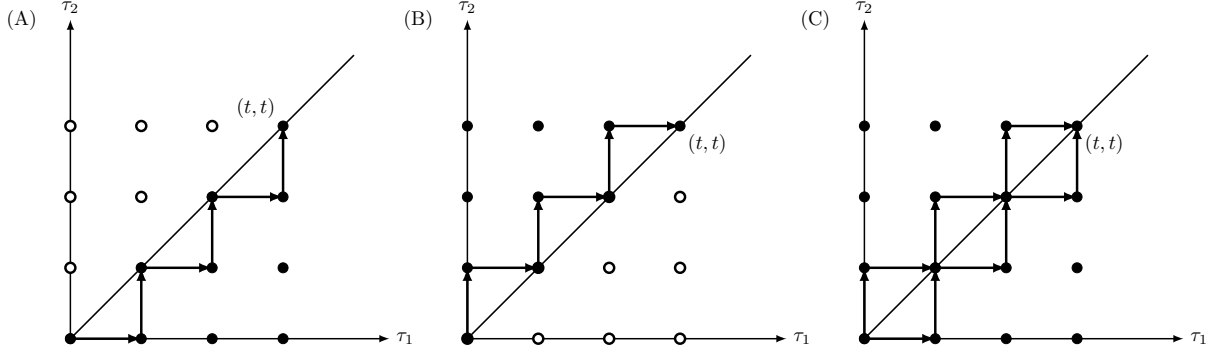


Figure 3: A schematic depiction of the evolution of the auxiliary fields  $\varphi_{k,a_1}(x_2, \tau_1, \tau_2)$ ,  $\varphi_{k,a_2}(x_1, \tau_1, \tau_2)$  and  $\psi_{k,k',a_1,a_2}(\tau_1, \tau_2)$  in the  $(\tau_1, \tau_2)$ -plane is provided in this figure. The plots (A) and (B) depict the evolution of the fields  $\varphi_{k,a_2}(x_1, \tau_1, \tau_2)$  and  $\varphi_{k,a_1}(x_2, \tau_1, \tau_2)$  on the boundary segments  $\Gamma_{a_2}$  and  $\Gamma_{a_1}$ , respectively. The plot (C) depicts the evolution of the field  $\psi_{k,k',a_1,a_2}(\tau_1, \tau_2)$  which can be achieved by moving either below or above the diagonal.

### 3. Variational Formulation: Preliminaries

In this section, we recall certain preliminary facts about the Lobatto polynomials based Legendre-Galerkin spectral method for the numerical solution of the initial boundary-value problem (IBVP) stated in (2). For the computational domain  $\Omega_i$ , we introduce a reference domain  $\Omega_i^{\text{ref.}} = \mathbb{I} \times \mathbb{I}$  where  $\mathbb{I} = (-1, 1)$ . In order to describe the associated linear maps between the reference domain and the actual computational domain, we introduce the variables  $y_1, y_2 \in \Omega_i^{\text{ref.}}$  such that

$$\begin{cases} x_1 = J_1 y_1 + \bar{x}_1, & J_1 = \frac{1}{2}(x_r - x_l), & \bar{x}_1 = \frac{1}{2}(x_l + x_r), & \beta_1 = J_1^{-2}, \\ x_2 = J_2 y_2 + \bar{x}_2, & J_2 = \frac{1}{2}(x_t - x_b), & \bar{x}_2 = \frac{1}{2}(x_b + x_t), & \beta_2 = J_2^{-2}. \end{cases} \quad (29)$$

Let  $L_n(y)$  denotes the Legendre polynomial of degree  $n$ , then the Lobatto polynomials can be defined as

$$\begin{aligned} \phi_0(y) &= \frac{1}{2}[L_0(y) - L_1(y)], & \phi_1(y) &= \frac{1}{2}[L_0(y) + L_1(y)], \\ \phi_k(y) &= \frac{1}{\sqrt{2(2k-1)}} [L_k(y) - L_{k-2}(y)] = c_k [L_k(y) - L_{k-2}(y)], & k &\geq 2. \end{aligned} \quad (30)$$

Observe that  $\phi_k(\pm 1) = 0$ ,  $k \geq 2$ . Introduce the polynomial space

$$\mathbf{P}_N = \text{Span}\{\phi_p(y) \mid p = 0, 1, \dots, N, y \in \mathbb{I}\}. \quad (31)$$

Let the index set  $\{0, 1, \dots, N_p\}$  be denoted by  $\mathbb{J}_p$  where  $p = 1, 2$ . The mass matrix and the stiffness matrix for the Lobatto basis are denoted by  $M_p = (m_{kj})_{k,j \in \mathbb{J}_p}$  and  $S_p = (s_{kj})_{k,j \in \mathbb{J}_p}$  for  $p = 1, 2$ , respectively. For  $j, k \geq 2$ , the matrix entries are given by

$$s_{jk} = (\phi'_j, \phi'_k)_{\mathbb{I}} = \begin{cases} 1, & j = k, \\ 0, & \text{otherwise} \end{cases}, \quad m_{jk} = (\phi_j, \phi_k)_{\mathbb{I}} = \begin{cases} -\frac{1}{\sqrt{(2k-1)(2k-5)}}, & j = k-2, \\ \frac{2}{(2k+1)(2k-3)}, & j = k, \\ -\frac{1}{\sqrt{(2k-1)(2k+3)}}, & j = k+2, \\ 0 & \text{otherwise.} \end{cases} \quad (32)$$

The remaining matrix entries are

$$\begin{aligned} s_{00} &= s_{11} = 1/2, & s_{01} &= s_{10} = -1/2, \\ m_{00} &= m_{11} = 2/3, & m_{01} &= m_{10} = 1/3. \end{aligned} \quad (33)$$

For the 2D problem, we consider the tensor product space  $\mathbf{P}_{N_1} \otimes \mathbf{P}_{N_2}$  of the Lobatto polynomial spaces  $\mathbf{P}_{N_j}$ ,  $j = 1, 2$ . The basis for the tensor product space  $\mathbf{P}_{N_1} \otimes \mathbf{P}_{N_2}$  can be written as

$$\theta_{p_1, p_2}(y_1, y_2) = \phi_{p_1}(y_1)\phi_{p_2}(y_2), \quad p_1 \in \mathbb{J}_1, \quad p_2 \in \mathbb{J}_2. \quad (34)$$

Within the variational formulation, our goal is to find the approximate solution  $u_{N_1, N_2} \in \mathbf{P}_{N_1} \otimes \mathbf{P}_{N_2}$  for the interior problem in (2):

$$\left(i\partial_t u_{N_1, N_2}, \theta_{p_1, p_2}\right)_{\Omega_i^{\text{ref}}} + \left(J_1^{-2} \partial_{y_1}^2 u_{N_1, N_2}, \theta_{p_1, p_2}\right)_{\Omega_i^{\text{ref}}} + \left(J_2^{-2} \partial_{y_2}^2 u_{N_1, N_2}, \theta_{p_1, p_2}\right)_{\Omega_i^{\text{ref}}} = 0, \quad (35)$$

where  $(u, \theta)_{\Omega_i^{\text{ref}}} = \int_{\Omega_i^{\text{ref}}} u \theta d^2 \mathbf{y}$  is the scalar product in  $L^2(\Omega_i^{\text{ref}})$ . The variational formulation defined above can be restated in terms of field  $u$  (dropping the subscripts ' $N_1$ ' and ' $N_2$ ' for the sake of brevity) as

$$\begin{aligned} & \left(i\partial_t u, \theta_{p_1, p_2}\right)_{\Omega_i^{\text{ref}}} + \left(J_1^{-2} \partial_{y_1}^2 u, \theta_{p_1, p_2}\right)_{\Omega_i^{\text{ref}}} + \left(J_2^{-2} \partial_{y_2}^2 u, \theta_{p_1, p_2}\right)_{\Omega_i^{\text{ref}}} \\ & = i\partial_t (u, \theta_{p_1, p_2})_{\Omega_i^{\text{ref}}} - J_1^{-2} (\partial_{y_1} u, \phi'_{p_1} \phi_{p_2})_{\Omega_i^{\text{ref}}} - J_2^{-2} (\partial_{y_2} u, \phi_{p_1} \phi'_{p_2})_{\Omega_i^{\text{ref}}} + \mathcal{I}_1 + \mathcal{I}_2, \end{aligned} \quad (36)$$

where the integrals labelled  $\mathcal{I}_1$  and  $\mathcal{I}_2$  are

$$\begin{aligned} \mathcal{I}_1 &= J_1^{-2} \int_{\mathbb{I}} ([\theta_{p_1, p_2} \partial_{y_1} u]_{+1} - [\theta_{p_1, p_2} \partial_{y_1} u]_{-1}) dy_2, \\ \mathcal{I}_2 &= J_2^{-2} \int_{\mathbb{I}} ([\theta_{p_1, p_2} \partial_{y_2} u]_{+1} - [\theta_{p_1, p_2} \partial_{y_2} u]_{-1}) dy_1. \end{aligned} \quad (37)$$

These terms correspond to the boundary segments so that the boundary conditions can be used to arrive at the complete variational form for the IBVP. Let  $\widehat{u}_{p_1, p_2}$  denote the expansion coefficients in the Lobatto basis so that

$$u_{N_1, N_2}(y_1, y_2, t) = \sum_{p_1 \in \mathbb{J}_1} \sum_{p_2 \in \mathbb{J}_2} \widehat{u}_{p_1, p_2} \phi_{p_1}(y_1) \phi_{p_2}(y_2). \quad (38)$$

Let us introduce the matrix  $\widehat{U} = (\widehat{u}_{p_1, p_2})_{p_1 \in \mathbb{J}_1, p_2 \in \mathbb{J}_2}$  to represent the field in the Lobatto basis on  $\Omega_{\text{ref}}$ . Further, let  $\Lambda_p = \text{diag}(1, 1, 0, \dots, 0) \in \mathbb{R}^{(N_p+1) \times (N_p+1)}$ ,  $p = 1, 2$ , then the representation of the restriction of the field on the boundary segments is given by

$$\left. \begin{aligned} u_l &= u|_{y_1=-1} = \sum_{p_2 \in \mathbb{J}_2} \widehat{u}_{0, p_2}(t) \phi_{p_2}(y_2), \\ u_r &= u|_{y_1=+1} = \sum_{p_2 \in \mathbb{J}_2} \widehat{u}_{1, p_2}(t) \phi_{p_2}(y_2) \end{aligned} \right\} \rightarrow \Lambda_1 \widehat{U}(t); \quad \left. \begin{aligned} u_b &= u|_{y_2=-1} = \sum_{p_1 \in \mathbb{J}_1} \widehat{u}_{p_1, 0}(t) \phi_{p_1}(y_1), \\ u_t &= u|_{y_2=+1} = \sum_{p_1 \in \mathbb{J}_1} \widehat{u}_{p_1, 1}(t) \phi_{p_1}(y_1) \end{aligned} \right\} \rightarrow \widehat{U}(t) \Lambda_2. \quad (39)$$

For convenience, we introduce the vectors:

$$\begin{aligned} \widehat{\mathbf{u}}_l &= (\widehat{u}_{0,1}, \widehat{u}_{0,2}, \dots, \widehat{u}_{0, N_2})^\top, & \widehat{\mathbf{u}}_b &= (\widehat{u}_{1,0}, \widehat{u}_{2,0}, \dots, \widehat{u}_{N_1,0})^\top, \\ \widehat{\mathbf{u}}_r &= (\widehat{u}_{1,1}, \widehat{u}_{1,2}, \dots, \widehat{u}_{0, N_2})^\top, & \widehat{\mathbf{u}}_t &= (\widehat{u}_{1,1}, \widehat{u}_{2,1}, \dots, \widehat{u}_{N_1,1})^\top. \end{aligned} \quad (40)$$

This is made possible on account of the observation:  $\phi_0(+1) = 0$ ,  $\phi_0(-1) = 1$ ,  $\phi_1(-1) = 0$  and  $\phi_1(+1) = 1$ . The field at the corners of  $\Omega_{\text{ref}}$  can be represented by

$$\left. \begin{aligned} u|_{y_1=-1, y_2=-1} &= \widehat{u}_{0,0}(t), & u|_{y_1=+1, y_2=-1} &= \widehat{u}_{1,0}(t), \\ u|_{y_1=-1, y_2=+1} &= \widehat{u}_{0,1}(t), & u|_{y_1=+1, y_2=+1} &= \widehat{u}_{1,1}(t), \end{aligned} \right\} \rightarrow \Lambda_1 \widehat{U}(t) \Lambda_2. \quad (41)$$

#### 4. Variational Formulation: HF

In this section, we consider the numerical solution of the IBVP in (14) using a Legendre-Galerkin method as laid out in Sec. 3. The variational formulation begins with (36) where the boundary terms, namely,  $\mathcal{I}_1$  and  $\mathcal{I}_2$ , need to

incorporate the boundary conditions in (14). Starting the with the segments denoted by  $\Gamma_{a_1}$ ,  $a_1 \in \{l, r\}$ , we have

$$\begin{aligned}
\mathcal{I}_1 &= J_1^{-2} \int_{\mathbb{I}} ([\theta_{p_1, p_2} \partial_{y_1} u]_{+1} - [\theta_{p_1, p_2} \partial_{y_1} u]_{-1}) dy_2 \\
&= J_1^{-1} \int_{\mathbb{I}} \phi_{p_1}(+1) \phi_{p_2}(y_2) \left( -e^{-i\pi/4} \partial_t^{1/2} u + e^{i\pi/4} \frac{1}{2} J_2^{-2} \partial_{y_2}^2 \partial_t^{-1/2} u \right) dy_2 \\
&\quad + J_1^{-1} \int_{\mathbb{I}} \phi_{p_1}(-1) \phi_{p_2}(y_2) \left( -e^{-i\pi/4} \partial_t^{1/2} u + e^{i\pi/4} \frac{1}{2} J_2^{-2} \partial_{y_2}^2 \partial_t^{-1/2} u \right) dy_2 \\
&= -e^{-i\pi/4} J_1^{-1} \partial_t^{1/2} \left[ \phi_{p_1}(+1) \int_{\mathbb{I}} \phi_{p_2}(y_2) (u)_{y_1=+1} dy_2 + \phi_{p_1}(-1) \int_{\mathbb{I}} \phi_{p_2}(y_2) (u)_{y_1=-1} dy_2 \right] \\
&\quad + e^{i\pi/4} \frac{1}{2} (J_1)^{-1} (J_2)^{-2} \partial_t^{-1/2} \left[ \underbrace{\phi_{p_1}(+1) \int_{\mathbb{I}} \phi_{p_2}(y_2) (\partial_{y_2}^2 u)_{y_1=+1} dy_2}_{\mathcal{I}_{1,r}} + \underbrace{\phi_{p_1}(-1) \int_{\mathbb{I}} \phi_{p_2}(y_2) (\partial_{y_2}^2 u)_{y_1=-1} dy_2}_{\mathcal{I}_{1,l}} \right].
\end{aligned} \tag{42}$$

Similarly, for the segments denoted by  $\Gamma_{a_2}$ ,  $a_2 \in \{b, t\}$ , we have

$$\begin{aligned}
\mathcal{I}_2 &= J_2^{-2} \int_{\mathbb{I}} ([\theta_{p_1, p_2} \partial_{y_2} u]_{+1} - [\theta_{p_1, p_2} \partial_{y_2} u]_{-1}) dy_1 \\
&= J_2^{-1} \int_{\mathbb{I}} \phi_{p_1}(y_1) \phi_{p_2}(+1) \left( -e^{-i\pi/4} \partial_t^{1/2} u + e^{i\pi/4} \frac{1}{2} J_1^{-2} \partial_{y_1}^2 \partial_t^{-1/2} u \right) dy_1 \\
&\quad + J_2^{-1} \int_{\mathbb{I}} \phi_{p_1}(y_1) \phi_{p_2}(-1) \left( -e^{-i\pi/4} \partial_t^{1/2} u + e^{i\pi/4} \frac{1}{2} J_1^{-2} \partial_{y_1}^2 \partial_t^{-1/2} u \right) dy_1 \\
&= -e^{-i\pi/4} J_2^{-1} \partial_t^{1/2} \left[ \phi_{p_2}(+1) \int_{\mathbb{I}} \phi_{p_1}(y_1) (u)_{y_2=+1} dy_1 + \phi_{p_2}(-1) \int_{\mathbb{I}} \phi_{p_1}(y_1) (u)_{y_2=-1} dy_1 \right] \\
&\quad + e^{i\pi/4} \frac{1}{2} (J_1)^{-2} (J_2)^{-1} \partial_t^{-1/2} \left[ \underbrace{\phi_{p_2}(+1) \int_{\mathbb{I}} \phi_{p_1}(y_1) (\partial_{y_1}^2 u)_{y_2=+1} dy_1}_{\mathcal{I}_{2,t}} + \underbrace{\phi_{p_2}(-1) \int_{\mathbb{I}} \phi_{p_1}(y_1) (\partial_{y_1}^2 u)_{y_2=-1} dy_1}_{\mathcal{I}_{2,b}} \right].
\end{aligned} \tag{43}$$

The terms involving second order derivatives acting on the field  $u$  in (42) and (43) need to be further simplified using integration by parts and invoking the corner conditions collectively. Consider the terms  $\mathcal{I}_{1,a_1}$  and  $\mathcal{I}_{2,a_2}$ , we have

$$\begin{aligned}
\mathcal{I}_{1,r} &= \phi_{p_1}(+1) \left[ \phi_{p_2}(+1) (\partial_{y_2} u)_{y_1=+1, y_2=+1} - \phi_{p_2}(-1) (\partial_{y_2} u)_{y_1=+1, y_2=-1} - \int_{\mathbb{I}} \partial_{y_2} \phi_{p_2}(y_2) (\partial_{y_2} u)_{y_1=+1} dy_2 \right], \\
\mathcal{I}_{1,l} &= \phi_{p_1}(-1) \left[ \phi_{p_2}(+1) (\partial_{y_2} u)_{y_1=-1, y_2=+1} - \phi_{p_2}(-1) (\partial_{y_2} u)_{y_1=-1, y_2=-1} - \int_{\mathbb{I}} \partial_{y_2} \phi_{p_2}(y_2) (\partial_{y_2} u)_{y_1=-1} dy_2 \right], \\
\mathcal{I}_{2,t} &= \phi_{p_2}(+1) \left[ \phi_{p_1}(+1) (\partial_{y_1} u)_{y_1=+1, y_2=+1} - \phi_{p_1}(-1) (\partial_{y_1} u)_{y_1=-1, y_2=+1} - \int_{\mathbb{I}} \partial_{y_1} \phi_{p_1}(y_1) (\partial_{y_1} u)_{y_2=+1} dy_1 \right], \\
\mathcal{I}_{2,b} &= \phi_{p_2}(-1) \left[ \phi_{p_1}(+1) (\partial_{y_1} u)_{y_1=+1, y_2=-1} - \phi_{p_1}(-1) (\partial_{y_1} u)_{y_1=-1, y_2=-1} - \int_{\mathbb{I}} \partial_{y_1} \phi_{p_1}(y_1) (\partial_{y_1} u)_{y_2=-1} dy_1 \right].
\end{aligned} \tag{44}$$

Collecting the corner terms from each of the expressions  $\mathcal{I}_{1,a_1}$  and  $\mathcal{I}_{2,a_2}$  and invoking the corner conditions from (14), we obtain

$$\begin{aligned}
e^{i\pi/4} \frac{1}{2} \partial_t^{-1/2} \left[ \phi_{p_1}(+1) \phi_{p_2}(+1) (+J_1^{-1} \partial_{y_1} u + J_2^{-1} \partial_{y_2} u)_{y_1=+1, y_2=+1} \right] &= -\frac{3}{4} \left[ \phi_{p_1}(+1) \phi_{p_2}(+1) (u)_{y_1=+1, y_2=+1} \right], \\
e^{i\pi/4} \frac{1}{2} \partial_t^{-1/2} \left[ \phi_{p_1}(-1) \phi_{p_2}(+1) (-J_1^{-1} \partial_{y_1} u + J_2^{-1} \partial_{y_2} u)_{y_1=-1, y_2=+1} \right] &= -\frac{3}{4} \left[ \phi_{p_1}(-1) \phi_{p_2}(+1) (u)_{y_1=-1, y_2=+1} \right], \\
e^{i\pi/4} \frac{1}{2} \partial_t^{-1/2} \left[ \phi_{p_1}(+1) \phi_{p_2}(-1) (+J_1^{-1} \partial_{y_1} u - J_2^{-1} \partial_{y_2} u)_{y_1=+1, y_2=-1} \right] &= -\frac{3}{4} \left[ \phi_{p_1}(+1) \phi_{p_2}(-1) (u)_{y_1=+1, y_2=-1} \right], \\
e^{i\pi/4} \frac{1}{2} \partial_t^{-1/2} \left[ \phi_{p_1}(-1) \phi_{p_2}(-1) (-J_1^{-1} \partial_{y_1} u - J_2^{-1} \partial_{y_2} u)_{y_1=-1, y_2=-1} \right] &= -\frac{3}{4} \left[ \phi_{p_1}(-1) \phi_{p_2}(-1) (u)_{y_1=-1, y_2=-1} \right].
\end{aligned} \tag{45}$$

Identifying the terms corresponding to the mass and stiffness matrices in (36) together with  $\mathcal{I}_{1,a_1}$  and  $\mathcal{I}_{2,a_2}$ , the dynamical system works out to be

$$\begin{aligned} iM_1\partial_t\widehat{U}M_2 &= J_1^{-2}S_1\widehat{U}M_2 + J_2^{-2}M_1\widehat{U}S_2 + e^{-i\pi/4}\partial_t^{1/2}\left[(J_1)^{-1}\Lambda_1\widehat{U}M_2 + (J_2)^{-1}M_1\widehat{U}\Lambda_2\right] \\ &+ e^{i\pi/4}\frac{1}{2}\partial_t^{-1/2}\left[(J_1)^{-1}(J_2)^{-2}\Lambda_1\widehat{U}S_2 + (J_1)^{-2}(J_2)^{-1}S_1\widehat{U}\Lambda_2\right] + \frac{3}{4}(J_1J_2)^{-1}\Lambda_1\widehat{U}\Lambda_2, \end{aligned} \quad (46)$$

where the last term contains all the contributions from the corners.

#### 4.1. Nonlocal temporal discretization: Convolution quadrature

In this section, we present various time-stepping methods to discretize the master equation (46). The standard recipe here is to use a linear multistep method (LMM) together with a compatible convolution quadrature (CQ) scheme for the fractional operators. Such a discretization is evidently nonlocal exhibiting the nonlocal nature of the dynamical system. To this end, let us identify the nonlocal terms in (46) as follows:

$$\begin{aligned} iM_1\partial_t\widehat{U}M_2 &= \beta_1S_1\widehat{U}M_2 + \beta_2M_1\widehat{U}S_2 + \frac{3}{4}\sqrt{\beta_1\beta_2}\Lambda_1\widehat{U}\Lambda_2 + \underbrace{\left[\partial_t^{1/2}\widehat{F}_+ + \partial_t^{-1/2}\widehat{F}_-\right]}_{\text{non-local terms}}, \\ \text{where } \begin{cases} \widehat{F}_+ &= e^{-i\pi/4}\left[\sqrt{\beta_1}\Lambda_1\widehat{U}M_2 + \sqrt{\beta_2}M_1\widehat{U}\Lambda_2\right], \\ \widehat{F}_- &= +e^{i\pi/4}\frac{1}{2}\left[\sqrt{\beta_1}\beta_2\Lambda_1\widehat{U}S_2 + \beta_1\sqrt{\beta_2}S_1\widehat{U}\Lambda_2\right]. \end{cases} \end{aligned} \quad (47)$$

Let  $\Delta t$  denote the time-step so that the temporal grid becomes  $t_j = j\Delta t$ ,  $j \in \mathbb{N}_0$ . The fractional operators  $\partial_t^{\pm 1/2}$  can be implemented using the LMM based CQ method. For a given LMM, let the CQ weights be denoted by  $\{\omega_k^{(\pm 1/2)} | k \in \mathbb{N}_0\}$ , then

$$[\partial_t^{\pm 1/2}\widehat{F}_\pm]^{j+1} = \rho^{\pm 1/2}F_\pm^{j+1} + \rho^{\pm 1/2}\sum_{k=1}^j\omega_{j+1-k}^{(\pm 1/2)}F_\pm^k, \quad (48)$$

where  $\rho$  is a function of  $\Delta t$  and it is chosen such that  $\omega_0^{(\pm 1/2)} = 1$ . In the following we restrict ourselves to the trapezoidal rule (TR) and backward differentiation formulae (BDF) of order 1 and 2. The recipe for computing the CQ weights for each of the time-stepping methods is enumerated below:

- CQ-BDF1 : The discretization scheme for the time-fractional operators is said to be ‘CQ-BDF1’ if the underlying time-stepping method used in designing the quadrature is BDF1. Let  $\nu \in \{+1/2, -1/2\}$  and  $\rho = 1/\Delta t$ , then the quadrature weights can be computed as follows

$$\omega_k^{(\nu)} = [(k-1-\nu)/k]\omega_{k-1}^{(\nu)}, \quad k \geq 1, \quad \text{with } \omega_0^{(\nu)} = 1. \quad (49)$$

- CQ-BDF2 : Let  $\rho = 3/(2\Delta t)$ , then the quadrature weights for BDF2 based CQ can be computed as

$$\omega_k^{(\nu)} = [4(k-1-\nu)/3k]\omega_{k-1}^{(\nu)} - [(k-2-2\nu)/3k]\omega_{k-2}^{(\nu)}, \quad k \geq 2, \quad \text{with } \omega_0^{(\nu)} = 1, \omega_1^{(\nu)} = -4\nu/3. \quad (50)$$

- CQ-TR : Let  $\rho = 2/\Delta t$ , then the quadrature weights for the TR based CQ scheme can be computed as

$$\omega_k^{(1/2)} = (-1)^j\omega_k^{(-1/2)}, \quad \omega_k^{(-1/2)} = \begin{cases} C_{k/2}, & k \text{ even}, \\ C_{(k-1)/2}, & k \text{ odd}, \end{cases} \quad \text{where } C_n = \frac{1 \cdot 3 \cdots (2n-1)}{n!2^n}. \quad (51)$$

The quadrature weights can also be generated using the following recurrence relation [16]:

$$(k+1)\omega_{k+1}^{(\nu)} = (k-1)\omega_{k-1}^{(\nu)} - 2\nu\omega_k^{(\nu)}, \quad k \geq 1, \quad \text{with } \omega_0^{(\nu)} = 1, \omega_1^{(\nu)} = -2\nu. \quad (52)$$

#### 4.1.1. CQ-BDF1

The discrete numerical scheme for the dynamical system (46) is labelled according to the CQ scheme used for the nonlocal terms. Therefore, the scheme ‘CQ-BDF1’ will use BDF1 for the time-stepping of the local terms in (46) which is discussed below.

Recalling  $\rho = 1/\Delta t$  and  $\alpha_k = \sqrt{\rho/\beta_k}e^{-i\pi/4}$  for  $k = 1, 2$  for the BDF1 scheme, the complete discretization of (46) reads as

$$\begin{aligned} & M_1 \widehat{U}^{j+1} M_2 + \alpha_1^{-2} S_1 \widehat{U}^{j+1} M_2 + \alpha_2^{-2} M_1 \widehat{U}^{j+1} S_2 + \left[ \alpha_1^{-1} \Lambda_1 \widehat{U}^{j+1} M_2 + \alpha_2^{-1} M_1 \widehat{U}^{j+1} \Lambda_2 \right] \\ & + \frac{1}{2} \left[ \alpha_1^{-1} \alpha_2^{-2} \Lambda_1 \widehat{U}^{j+1} S_2 + \alpha_1^{-2} \alpha_2^{-1} S_1 \widehat{U}^{j+1} \Lambda_2 \right] + \frac{3}{4} (\alpha_1 \alpha_2)^{-1} \Lambda_1 \widehat{U}^{j+1} \Lambda_2 = M_1 \widehat{U}^j M_2 + \mathcal{B}_+^{j+1} + \mathcal{B}_-^{j+1}, \end{aligned} \quad (53)$$

where the history terms are given by

$$\begin{cases} \mathcal{B}_+^{j+1} = \sum_{k=1}^j \omega_{j+1-k}^{(1/2)} \left[ \alpha_1^{-1} \Lambda_1 \widehat{U}^k M_2 + \alpha_2^{-1} M_1 \widehat{U}^k \Lambda_2 \right], \\ \mathcal{B}_-^{j+1} = \frac{1}{2} \sum_{k=1}^j \omega_{j+1-k}^{(-1/2)} \left[ \alpha_1^{-1} \alpha_2^{-2} \Lambda_1 \widehat{U}^k S_2 + \alpha_1^{-2} \alpha_2^{-1} S_1 \widehat{U}^k \Lambda_2 \right]. \end{cases} \quad (54)$$

We may refer to these functions as the *history functions* on account of the fact that, for the latest time-step, they can be assumed to be determined by the quantities that are already determined in the previous time-steps.

**Remark 1.** As noted in Sec. 3,  $\Lambda_1 \widehat{U}$  and  $\widehat{U} \Lambda_2$  denote the restrictions of the field  $\widehat{U}$  to the boundary segments. Therefore, for the numerical implementation we can rewrite the history terms defined above for each of the boundary segments separately as follows:

$$\begin{aligned} \widehat{\mathcal{B}}_{a_1,+}^{j+1} &= \sum_{k=1}^j \omega_{j+1-k}^{(1/2)} \widehat{\mathbf{u}}_{a_1}^k, & \widehat{\mathcal{B}}_{a_2,+}^{j+1} &= \sum_{k=1}^j \omega_{j+1-k}^{(1/2)} \widehat{\mathbf{u}}_{a_2}^k, & a_1 &\in \{l, r\}, \\ \widehat{\mathcal{B}}_{a_1,-}^{j+1} &= \sum_{k=1}^j \omega_{j+1-k}^{(-1/2)} \widehat{\mathbf{u}}_{a_1}^k, & \widehat{\mathcal{B}}_{a_2,-}^{j+1} &= \sum_{k=1}^j \omega_{j+1-k}^{(-1/2)} \widehat{\mathbf{u}}_{a_2}^k, & a_2 &\in \{b, t\}. \end{aligned}$$

It is straightforward to verify that the history terms,  $\mathcal{B}_+^{j+1}$  and  $\mathcal{B}_-^{j+1}$ , can now be efficiently computed as

$$\begin{aligned} \mathcal{B}_+^{j+1} &= \frac{1}{\alpha_1} \mathbf{e}_0^{(1)} \otimes \left[ \widehat{\mathcal{B}}_{l,+}^{j+1} \right]^\top M_2 + \frac{1}{\alpha_1} \mathbf{e}_1^{(1)} \otimes \left[ \widehat{\mathcal{B}}_{r,+}^{j+1} \right]^\top M_2 + \frac{1}{\alpha_2} \left[ M_1 \widehat{\mathcal{B}}_{b,+}^{j+1} \right] \otimes (\mathbf{e}_0^{(2)})^\top + \frac{1}{\alpha_2} \left[ M_1 \widehat{\mathcal{B}}_{t,+}^{j+1} \right] \otimes (\mathbf{e}_1^{(2)})^\top, \\ \mathcal{B}_-^{j+1} &= \frac{1}{2\alpha_1 \alpha_2^2} \left( \mathbf{e}_0^{(1)} \otimes \left[ \widehat{\mathcal{B}}_{l,+}^{j+1} \right]^\top S_2 + \mathbf{e}_1^{(1)} \otimes \left[ \widehat{\mathcal{B}}_{r,+}^{j+1} \right]^\top S_2 \right) + \frac{1}{2\alpha_1^2 \alpha_2} \left( \left[ S_1 \widehat{\mathcal{B}}_{b,+}^{j+1} \right] \otimes (\mathbf{e}_0^{(2)})^\top + \left[ S_1 \widehat{\mathcal{B}}_{t,+}^{j+1} \right] \otimes (\mathbf{e}_1^{(2)})^\top \right). \end{aligned} \quad (55)$$

where  $\mathbf{e}_0^{(p)} = (\delta_{k,0})_{k \in \mathbb{J}_p}$  and  $\mathbf{e}_1^{(p)} = (\delta_{k,1})_{k \in \mathbb{J}_p}$  for  $p = 1, 2$  are the orthogonal unit vectors in  $\mathbb{R}^{N_p+1}$ .

#### 4.1.2. CQ-BDF2

The discrete numerical scheme for the dynamical system (46) is labelled as ‘CQ-BDF2’ if the underlying time-stepping method is BDF2 and rest of the labels follow the convention defined above. Recalling  $\rho = 3/2\Delta t$ , the complete discretization of the dynamical system in (46) reads as

$$\begin{aligned} & M_1 \widehat{U}^{j+2} M_2 + \alpha_1^{-2} S_1 \widehat{U}^{j+2} M_2 + \alpha_2^{-2} M_1 \widehat{U}^{j+2} S_2 + \frac{1}{2} \left[ \alpha_1^{-1} \alpha_2^{-2} \Lambda_1 \widehat{U}^{j+2} S_2 + \alpha_1^{-2} \alpha_2^{-1} S_1 \widehat{U}^{j+2} \Lambda_2 \right] \\ & + \left[ \alpha_1^{-1} \Lambda_1 \widehat{U}^{j+2} M_2 + \alpha_2^{-1} M_1 \widehat{U}^{j+2} \Lambda_2 \right] + \frac{3}{4} (\alpha_1 \alpha_2)^{-1} \Lambda_1 \widehat{U}^{j+2} \Lambda_2 = \left[ \frac{4}{3} M_1 \widehat{U}^{j+1} M_2 - \frac{1}{3} M_1 \widehat{U}^j M_2 \right] + \mathcal{B}_+^{j+2} + \mathcal{B}_-^{j+2}, \end{aligned}$$

where the history terms are computed in similar manner as evaluated in BDF1 case.

#### 4.1.3. CQ-TR

The discrete numerical scheme for the dynamical system (46) is labelled as ‘CQ-TR’ if the underlying time-stepping method is TR and rest of the labels follow the convention defined above. Recalling  $\rho = 2/\Delta t$  and setting  $\widehat{V}^{j+1} = (\widehat{U}^{j+1} + \widehat{U}^j)/2$ , the complete discretization of the dynamical system in (46) reads as

$$\begin{aligned} & M_1 \widehat{V}^{j+1} M_2 + \alpha_1^{-2} S_1 \widehat{V}^{j+1} M_2 + \alpha_2^{-2} M_1 \widehat{V}^{j+1} S_2 + \left[ \alpha_1^{-1} \Lambda_1 \widehat{V}^{j+1} M_2 + \alpha_2^{-1} M_1 \widehat{V}^{j+1} \Lambda_2 \right] \\ & + \frac{1}{2} \left[ \alpha_1^{-1} \alpha_2^{-2} \Lambda_1 \widehat{V}^{j+1} S_2 + \alpha_1^{-2} \alpha_2^{-1} S_1 \widehat{V}^{j+1} \Lambda_2 \right] + \frac{3}{4} (\alpha_1 \alpha_2)^{-1} \Lambda_1 \widehat{V}^{j+1} \Lambda_2 = M_1 \widehat{U}^j M_2 + \mathcal{B}_+^{j+1/2} + \mathcal{B}_-^{j+1/2}, \end{aligned}$$

where the history terms are computed as  $\mathcal{B}_\pm^{j+1/2} = (\mathcal{B}_\pm^{j+1} + \mathcal{B}_\pm^j)/2$ .

#### 4.2. Local temporal discretization: Conventional Padé

In this section, we present an effectively local form of the (nonlocal) dynamical system stated in (47). This is accomplished by employing a Padé approximant based representation for the time-fractional operators in (47) to obtain a system of ODEs which approximate the original system.

Let the  $K$ -th order diagonal Padé approximant based rational approximation for the function  $\sqrt{z}$  is denoted by  $R_K^{(1/2)}(z)$  defined in (18). Here, we choose the rational approximation for the function  $1/\sqrt{z}$ , denoted by  $R_K^{(-1/2)}(z)$ , to ensure that

$$\left[ \frac{R_K^{(1/2)}(z)}{R_K^{(-1/2)}(z)} \right] = z \implies R_K^{(-1/2)}(z) = \frac{R_K^{(1/2)}(z)}{z}, \quad (56)$$

yielding

$$R_K^{(-1/2)}(z) = \frac{b_0}{z} - \sum_{k=1}^K \frac{b_k}{z(z + \eta_k^2)} = \frac{b_0}{z} - \sum_{k=1}^K \frac{b_k}{\eta_k^2} \left[ \frac{1}{z} - \frac{1}{z + \eta_k^2} \right] = \frac{d_0}{z} - \sum_{k=1}^K \frac{d_k}{z + \eta_k^2}, \quad (57)$$

where  $d_0 = b_0 - \sum_{k=1}^K b_k/\eta_k^2$  and  $d_k = -b_k/\eta_k^2$ .

Let  $I_k$  be the identity matrix of dimension  $(N_k + 1) \times (N_k + 1)$  for  $k = 1, 2$ . In order to write the rational approximations for the time-fractional operators present in (47), we introduce the auxiliary fields  $\widehat{\mathcal{A}}_{k,1}$  and  $\widehat{\mathcal{A}}_{k,2}$  where  $k = 0, 1, \dots, K$  such that

$$\begin{aligned} \partial_t^{1/2} [\Lambda_1 \widehat{U}] &\approx b_0 \Lambda_1 \widehat{U} - \sum_{k=1}^K b_k \widehat{\mathcal{A}}_{k,1} = b_0 \Lambda_1 \widehat{U} - (\mathbf{b}^\top \otimes I_1) \widehat{\mathcal{A}}_1, \\ \partial_t^{1/2} [\widehat{U} \Lambda_2] &\approx b_0 \widehat{U} \Lambda_2 - \sum_{k=1}^K b_k \widehat{\mathcal{A}}_{k,2} = b_0 \widehat{U} \Lambda_2 - \widehat{\mathcal{A}}_2 (\mathbf{b} \otimes I_2), \\ \partial_t^{-1/2} [\Lambda_1 \widehat{U}] &\approx d_0 \widehat{\mathcal{A}}_{0,1} - \sum_{k=1}^K d_k \widehat{\mathcal{A}}_{k,1} = d_0 \widehat{\mathcal{A}}_{0,1} - (\mathbf{d}^\top \otimes I_1) \widehat{\mathcal{A}}_1, \\ \partial_t^{-1/2} [\widehat{U} \Lambda_2] &\approx d_0 \widehat{\mathcal{A}}_{0,2} - \sum_{k=1}^K d_k \widehat{\mathcal{A}}_{k,2} = d_0 \widehat{\mathcal{A}}_{0,2} - \widehat{\mathcal{A}}_2 (\mathbf{d} \otimes I_2), \end{aligned} \quad (58)$$

where  $\mathbf{b} = (b_1, b_2, \dots, b_K)^\top$ ,  $\mathbf{d} = (d_1, d_2, \dots, d_K)^\top$  and ‘ $\otimes$ ’ denotes the Kronecker product. Note that the index  $k$  of the auxiliary fields correspond to the  $k$ -th partial fraction of the Padé approximant (with the exception of  $b_0$ ).

Let us now discuss the structure of the matrices  $\widehat{\mathcal{A}}_{k,1}$  and  $\widehat{\mathcal{A}}_{k,2}$  introduced above. In Sec. 3, we discussed how to obtain the representation of the restriction of the field  $u_{N_1, N_2}(\mathbf{y}, t)$  to the boundary segments in the Lobatto basis. Following the same convention, we observe from (39) that  $\Lambda_1 \widehat{U}$  and  $\widehat{U} \Lambda_2$  are representations of the restriction of the field to the boundary segments. Therefore, the auxiliary fields  $\mathcal{A}_{k,1}$  and  $\mathcal{A}_{k,2}$  are functions on the boundary segments

so that their expansion in the Lobatto basis reads as follows:

$$\begin{aligned}\mathcal{A}_{k,1}(\pm 1, y_2, t) &= \sum_{p_1=0,1} \sum_{p_2=0}^{N_2} \widehat{\mathcal{A}}_{p_1,p_2}^{(k,1)} \phi_{p_1}(\pm 1) \phi_{p_2}(y_2), \\ \mathcal{A}_{k,2}(y_1, \pm 1, t) &= \sum_{p_1=0}^{N_1} \sum_{p_2=0,1} \widehat{\mathcal{A}}_{p_1,p_2}^{(k,2)} \phi_{p_2}(y_1) \phi_{p_2}(\pm 1),\end{aligned}\tag{59}$$

where we have exploited the property of Lobatto polynomials to establish that only first two rows of the matrices  $\widehat{\mathcal{A}}_{k,1}$  are non-zero while only first two columns of the matrices  $\widehat{\mathcal{A}}_{k,2}$  are non-zero. Next, we introduce a block matrix  $\widehat{\mathcal{A}}_1$  with the matrix entries  $\widehat{\mathcal{A}}_{k,1}$  defined as follows:

$$\widehat{\mathcal{A}}_1 = \begin{pmatrix} \widehat{\mathcal{A}}_{1,1} \\ \widehat{\mathcal{A}}_{2,1} \\ \vdots \\ \widehat{\mathcal{A}}_{K,1} \end{pmatrix} \quad \text{where} \quad \widehat{\mathcal{A}}_{k,1} = \begin{pmatrix} \widehat{\mathcal{A}}_{0,0} & \widehat{\mathcal{A}}_{0,1} & \dots & \widehat{\mathcal{A}}_{0,N_2} \\ \widehat{\mathcal{A}}_{1,0} & \widehat{\mathcal{A}}_{1,1} & \dots & \widehat{\mathcal{A}}_{1,N_2} \\ 0 & 0 & \dots & 0 \\ \vdots & \vdots & & \vdots \\ 0 & 0 & \dots & 0 \end{pmatrix}^{(k,1)} \in \mathbb{C}^{(N_1+1) \times (N_2+1)}.\tag{60}$$

Similarly, we introduce a block matrix  $\widehat{\mathcal{A}}_2$  with the matrix entries  $\widehat{\mathcal{A}}_{k,2} \in \mathbb{C}^{(N_1+1) \times (N_2+1)}$  defined as follows:

$$\widehat{\mathcal{A}}_2 = \begin{pmatrix} \widehat{\mathcal{A}}_{1,2} & \dots & \widehat{\mathcal{A}}_{K,2} \end{pmatrix} \quad \text{where} \quad \widehat{\mathcal{A}}_{k,2} = \begin{pmatrix} \widehat{\mathcal{A}}_{0,0} & \widehat{\mathcal{A}}_{0,1} & 0 & \dots & 0 \\ \widehat{\mathcal{A}}_{1,0} & \widehat{\mathcal{A}}_{1,1} & 0 & \dots & 0 \\ \vdots & \vdots & \vdots & & \vdots \\ \widehat{\mathcal{A}}_{N_1,0} & \widehat{\mathcal{A}}_{N_1,1} & 0 & \dots & 0 \end{pmatrix}^{(k,2)}.\tag{61}$$

Let us recall that the index  $k$  of the auxiliary fields correspond to the  $k$ -th partial fraction of the Padé approximant so that one can identify the ODE satisfied by each of the auxiliary fields:

$$\begin{aligned}\partial_t \widehat{\mathcal{A}}_{0,1} &= \Lambda_1 \widehat{U}, & \partial_t \widehat{\mathcal{A}}_{0,2} &= \widehat{U} \Lambda_2, \\ \partial_t \widehat{\mathcal{A}}_{k,1} &= -\eta_k^2 \widehat{\mathcal{A}}_{k,1} + \Lambda_1 \widehat{U}, & \partial_t \widehat{\mathcal{A}}_{k,2} &= -\eta_k^2 \widehat{\mathcal{A}}_{k,2} + \widehat{U} \Lambda_2.\end{aligned}\tag{62}$$

Let us introduce the matrices  $\mathcal{E}_K = \text{diag}(\eta_1^2, \eta_2^2, \dots, \eta_K^2) \in \mathbb{R}^{(K \times K)}$  and  $\mathbf{1}_K = (1, 1, \dots, 1)^\top \in \mathbb{R}^K$  which can be used to rewrite the ODEs as follows:

$$\begin{aligned}\partial_t \widehat{\mathcal{A}}_{0,1} &= \Lambda_1 \widehat{U}, & \partial_t \widehat{\mathcal{A}}_{0,2} &= \widehat{U} \Lambda_2, \\ \partial_t \widehat{\mathcal{A}}_1 &= -(\mathcal{E}_K \otimes I_1) \widehat{\mathcal{A}}_1 + \mathbf{1}_K \otimes (\Lambda_1 \widehat{U}), & \partial_t \widehat{\mathcal{A}}_2 &= -\widehat{\mathcal{A}}_2 (\mathcal{E}_K \otimes I_2) + \mathbf{1}_K^\top \otimes (\widehat{U} \Lambda_2).\end{aligned}\tag{63}$$

Employing the approximations developed in (58) in the (non-local) dynamical system stated in (47), we obtain an effectively local system given by

$$\begin{aligned}iM_1 \partial_t \widehat{U} M_2 &= \beta_1 S_1 \widehat{U} M_2 + \beta_2 M_1 \widehat{U} S_2 + e^{-i\pi/4} b_0 \left[ \sqrt{\beta_1} \Lambda_1 \widehat{U} M_2 + \sqrt{\beta_2} M_1 \widehat{U} \Lambda_2 \right] \\ &\quad - e^{-i\pi/4} \left[ \sqrt{\beta_1} (\mathbf{b}^\top \otimes I_1) \widehat{\mathcal{A}}_1 M_2 + \sqrt{\beta_2} M_1 \widehat{\mathcal{A}}_2 (\mathbf{b} \otimes I_2) \right] + d_0 e^{i\pi/4} \frac{1}{2} \left[ \sqrt{\beta_1} \beta_2 \widehat{\mathcal{A}}_{0,1} S_2 + \beta_1 \sqrt{\beta_2} S_1 \widehat{\mathcal{A}}_{0,2} \right] \\ &\quad - e^{i\pi/4} \frac{1}{2} \left[ \sqrt{\beta_1} \beta_2 (\mathbf{d}^\top \otimes I_1) \widehat{\mathcal{A}}_1 S_2 + \beta_1 \sqrt{\beta_2} S_1 \widehat{\mathcal{A}}_2 (\mathbf{d} \otimes I_2) \right] + \frac{3}{4} \sqrt{\beta_1 \beta_2} \Lambda_1 \widehat{U} \Lambda_2.\end{aligned}\tag{64}$$

This dynamical system together with (63) can be solved further with any choice of temporal discretization methods (namely, one-step and multistep methods).

**Remark 2.** For the numerical implementation, only the non-zero entries of  $\widehat{\mathcal{A}}_{k,1}$  and  $\widehat{\mathcal{A}}_{k,2}$  are relevant. Therefore, we may introduce auxiliary functions

$$\begin{aligned}\Gamma_l : \varphi_{k,l}(y_2, t) &= \mathcal{A}_{k,1}(-1, y_2, t), & \Gamma_r : \varphi_{k,r}(y_2, t) &= \mathcal{A}_{k,1}(+1, y_2, t), \\ \Gamma_b : \varphi_{k,b}(y_1, t) &= \mathcal{A}_{k,1}(y_1, -1, t), & \Gamma_t : \varphi_{k,t}(y_1, t) &= \mathcal{A}_{k,1}(y_1, +1, t).\end{aligned}$$

Recalling  $a_1 \in \{l, r\}$  and  $a_2 \in \{b, t\}$ , the expansion in terms of Lobatto basis reads as

$$\varphi_{k,a_1}(y_2, t) = \sum_{p_2=0}^{N_2} \widehat{\varphi}_{k,p_2,a_1}(t) \phi_{p_2}(y_2), \quad \varphi_{k,a_2}(y_1, t) = \sum_{p_1=0}^{N_1} \widehat{\varphi}_{k,p_1,a_2}(t) \phi_{p_1}(y_1),$$

so that

$$\begin{aligned}\widehat{\mathcal{A}}_{k,1} &= \begin{pmatrix} \widehat{\varphi}_{k,0,l} & \widehat{\varphi}_{k,1,l} & \cdots & \widehat{\varphi}_{k,N_2,l} \\ \widehat{\varphi}_{k,0,r} & \widehat{\varphi}_{k,1,r} & \cdots & \widehat{\varphi}_{k,N_2,r} \\ 0 & 0 & \cdots & 0 \\ \vdots & \vdots & \cdots & \vdots \\ 0 & 0 & \cdots & 0 \end{pmatrix} = \begin{pmatrix} \widehat{\varphi}_{k,l}^\top \\ \widehat{\varphi}_{k,r}^\top \\ Z_1 \end{pmatrix}, & \widehat{\varphi}_{k,a_1} &= \begin{pmatrix} \widehat{\varphi}_{k,0,a_1} \\ \widehat{\varphi}_{k,1,a_1} \\ \vdots \\ \widehat{\varphi}_{k,N_2,a_1} \end{pmatrix}, \\ \widehat{\mathcal{A}}_{k,2} &= \begin{pmatrix} \widehat{\varphi}_{k,0,b} & \widehat{\varphi}_{k,0,t} & 0 & \cdots & 0 \\ \widehat{\varphi}_{k,1,b} & \widehat{\varphi}_{k,1,t} & 0 & \cdots & 0 \\ \vdots & \vdots & \vdots & \ddots & \vdots \\ \widehat{\varphi}_{k,N_1,b} & \widehat{\varphi}_{k,N_1,t} & 0 & \cdots & 0 \end{pmatrix} = \begin{pmatrix} \widehat{\varphi}_{k,b} & \widehat{\varphi}_{k,t} & Z_2 \end{pmatrix}, & \widehat{\varphi}_{k,a_2} &= \begin{pmatrix} \widehat{\varphi}_{k,0,a_2} \\ \widehat{\varphi}_{k,1,a_2} \\ \vdots \\ \widehat{\varphi}_{k,N_1,a_2} \end{pmatrix},\end{aligned}$$

where  $Z_1 = 0_{(N_1-1) \times (N_2+1)}$  and  $Z_2 = 0_{(N_1+1) \times (N_2-1)}$ .

The approach presented here is referred to as the *conventional Padé* approach. Each of the methods discussed below is derived by applying a particular time-stepping scheme to the conventional Padé approach, therefore, we label them as ‘CP-’ followed by the acronym for the time-stepping method.

#### 4.2.1. CP-BDF1

The discrete numerical scheme for the dynamical system defined in (63) and (64) is labelled as ‘CP-BDF1’ if the underlying time-stepping method is BDF1.

Recalling  $\rho = 1/(\Delta t)$ , the BDF1-based discretization of the dynamical system in (64) reads as

$$\begin{aligned}& i\rho M_1 \widehat{U}^{j+1} M_2 - i\rho M_1 \widehat{U}^j M_2 \\ &= \beta_1 S_1 \widehat{U}^{j+1} M_2 + \beta_2 M_1 \widehat{U}^{j+1} S_2 + e^{-i\pi/4} b_0 \left[ \sqrt{\beta_1} \Lambda_1 \widehat{U}^{j+1} M_2 + \sqrt{\beta_2} M_1 \widehat{U}^{j+1} \Lambda_2 \right] + \frac{3}{4} (J_1 J_2)^{-1} \Lambda_1 \widehat{U}^{j+1} \Lambda_2 \\ & \quad - e^{-i\pi/4} \left[ \sqrt{\beta_1} (\mathbf{b}^\top \otimes I_1) \widehat{\mathcal{A}}_1^{j+1} M_2 + \sqrt{\beta_2} M_1 \widehat{\mathcal{A}}_2^{j+1} (\mathbf{b} \otimes I_2) \right] + d_0 e^{i\pi/4} \frac{1}{2} \left[ \sqrt{\beta_1} \beta_2 \widehat{\mathcal{A}}_{0,1}^{j+1} S_2 + \beta_1 \sqrt{\beta_2} S_1 \widehat{\mathcal{A}}_{0,2}^{j+1} \right] \\ & \quad - e^{i\pi/4} \frac{1}{2} \left[ \sqrt{\beta_1} \beta_2 (\mathbf{d}^\top \otimes I_1) \widehat{\mathcal{A}}_1^{j+1} S_2 + \beta_1 \sqrt{\beta_2} S_1 \widehat{\mathcal{A}}_2^{j+1} (\mathbf{d} \otimes I_2) \right],\end{aligned} \tag{65}$$

and that of the auxiliary fields in (63) reads as

$$\begin{aligned}\widehat{\mathcal{A}}_{0,1}^{j+1} &= \frac{1}{\rho} \Lambda_1 \widehat{U}^{j+1} + \widehat{\mathcal{A}}_{0,1}^j, & \widehat{\mathcal{A}}_{0,2}^{j+1} &= \frac{1}{\rho} \widehat{U}^{j+1} \Lambda_2 + \widehat{\mathcal{A}}_{0,2}^j, \\ \widehat{\mathcal{A}}_1^{j+1} &= (\mathcal{G}_K \otimes I_1) \left[ \frac{1}{\rho} \mathbf{1}_K \otimes (\Lambda_1 \widehat{U}^{j+1}) + \widehat{\mathcal{A}}_1^j \right], & \widehat{\mathcal{A}}_2^{j+1} &= \left[ \frac{1}{\rho} \mathbf{1}_K^\top \otimes (\widehat{U}^{j+1} \Lambda_2) + \widehat{\mathcal{A}}_2^j \right] (\mathcal{G}_K \otimes I_2),\end{aligned} \tag{66}$$

where we have introduced

$$\mathcal{G}_K = \text{diag} \left( \frac{1}{1 + \bar{\eta}_1^2}, \frac{1}{1 + \bar{\eta}_2^2}, \dots, \frac{1}{1 + \bar{\eta}_K^2} \right) \in \mathbb{R}^{(K \times K)}, \quad \bar{\eta}_k = \eta_k / \sqrt{\rho}. \tag{67}$$



Plugging-in the updates for the auxiliary fields from (66) in the discrete system (65) and simplifying, we obtain

$$\begin{aligned}
& M_1 \widehat{U}^{j+1} M_2 - M_1 \widehat{U}^j M_2 \\
&= -\alpha_1^{-2} S_1 \widehat{U}^{j+1} M_2 - \alpha_2^{-2} M_1 \widehat{U}^{j+1} S_2 - \bar{b}_0 \left[ \alpha_1^{-1} \Lambda_1 \widehat{U}^{j+1} M_2 + \alpha_2^{-1} M_1 \widehat{U}^{j+1} \Lambda_2 \right] - \frac{3}{4\alpha_1\alpha_2} \Lambda_1 \widehat{U}^{j+1} \Lambda_2 \\
&+ \alpha_1^{-1} \left[ \frac{1}{\rho} (\bar{\mathbf{b}}^\top \mathcal{G}_K \mathbf{1}_K) \otimes (\Lambda_1 \widehat{U}^{j+1}) + (\bar{\mathbf{b}}^\top \mathcal{G}_K \otimes I_1) \widehat{\mathcal{A}}_1^j \right] M_2 + \alpha_2^{-1} M_1 \left[ \frac{1}{\rho} (\mathbf{b}^\top \mathcal{G}_K \mathbf{1}_K) \otimes (\widehat{U}^{j+1} \Lambda_2) + \widehat{\mathcal{A}}_2^j (\mathcal{G}_K \mathbf{b} \otimes I_2) \right] \\
&+ \frac{1}{2} \alpha_1^{-1} \alpha_2^{-2} \left[ \left( \frac{1}{\rho} (\mathbf{d}^\top \mathcal{G}_K \mathbf{1}_K) \otimes (\Lambda_1 \widehat{U}^{j+1}) + (\mathbf{d}^\top \mathcal{G}_K \otimes I_1) \widehat{\mathcal{A}}_1^j \right) - \bar{d}_0 \left( \frac{1}{\rho} \Lambda_1 \widehat{U}^{j+1} + \widehat{\mathcal{A}}_{0,1}^j \right) \right] S_2 \\
&+ \frac{1}{2} \alpha_2^{-1} \alpha_1^{-2} S_1 \left[ \left( \frac{1}{\rho} (\mathbf{d}^\top \mathcal{G}_K \mathbf{1}_K) \otimes (\widehat{U}^{j+1} \Lambda_2) + \widehat{\mathcal{A}}_2^j (\mathcal{G}_K \mathbf{d} \otimes I_2) \right) - \bar{d}_0 \left( \frac{1}{\rho} \widehat{U}^{j+1} \Lambda_2 + \widehat{\mathcal{A}}_{0,2}^j \right) \right].
\end{aligned}$$

Introducing the quantities

$$\begin{cases} \Gamma_k^{(1/2)} = \frac{\bar{b}_k}{1 + \bar{\eta}_k^2}, & k = 1, \dots, K, & \Gamma_k^{(-1/2)} = \frac{\bar{d}_k}{1 + \bar{\eta}_k^2}, & k = 1, \dots, K, \\ \varpi^{(1/2)} = \bar{b}_0 - \frac{1}{\rho} \bar{\mathbf{b}}^\top (\mathcal{G}_K \mathbf{1}_K) = \bar{b}_0 - \frac{1}{\rho} \sum_{k=1}^K \Gamma_k^{(1/2)}, & \varpi^{(-1/2)} = \frac{\bar{d}_0}{\rho} - \frac{1}{\rho} \bar{\mathbf{d}}^\top (\mathcal{G}_K \mathbf{1}_K) = \frac{\bar{d}_0}{\rho} - \frac{1}{\rho} \sum_{k=1}^K \Gamma_k^{(-1/2)}. \end{cases} \quad (68)$$

and identifying the terms with the latest time-step of the field,  $\widehat{U}^{j+1}$ , we obtain

$$\begin{aligned}
& M_1 \widehat{U}^{j+1} M_2 + \alpha_1^{-2} S_1 \widehat{U}^{j+1} M_2 + \alpha_2^{-2} M_1 \widehat{U}^{j+1} S_2 + \varpi^{(1/2)} \left[ \alpha_1^{-1} \Lambda_1 \widehat{U}^{j+1} M_2 + \alpha_2^{-1} M_1 \widehat{U}^{j+1} \Lambda_2 \right] \\
&+ \frac{1}{2} \varpi^{(-1/2)} \left[ \alpha_1^{-1} \alpha_2^{-2} \Lambda_1 \widehat{U}^{j+1} S_2 + \alpha_1^{-2} \alpha_2^{-1} S_1 \widehat{U}^{j+1} \Lambda_2 \right] + \frac{3}{4\alpha_1\alpha_2} \Lambda_1 \widehat{U}^{j+1} \Lambda_2 = M_1 \widehat{U}^j M_2 + \mathcal{B}_+^{j+1} + \mathcal{B}_-^{j+1},
\end{aligned} \quad (69)$$

where the history terms are given by

$$\begin{cases} \mathcal{B}_+^{j+1} = \alpha_1^{-1} \left[ (\bar{\mathbf{b}}^\top \mathcal{G}_K) \otimes I_1 \right] \widehat{\mathcal{A}}_1^j M_2 + \alpha_2^{-1} M_1 \widehat{\mathcal{A}}_2^j \left[ (\mathcal{G}_K \bar{\mathbf{b}}) \otimes I_2 \right], \\ \mathcal{B}_-^{j+1} = \frac{1}{2} \alpha_1^{-1} \alpha_2^{-2} \left[ (\bar{\mathbf{d}}^\top \mathcal{G}_K \otimes I_1) \widehat{\mathcal{A}}_1^j - \bar{d}_0 \widehat{\mathcal{A}}_{0,1}^j \right] S_2 + \frac{1}{2} \alpha_1^{-2} \alpha_2^{-1} S_1 \left[ \widehat{\mathcal{A}}_2^j (\mathcal{G}_K \bar{\mathbf{d}} \otimes I_2) - \widehat{\mathcal{A}}_{0,2}^j \bar{d}_0 \right]. \end{cases} \quad (70)$$

The latest value,  $\widehat{U}^{j+1}$ , can then be used to carry out the updates for the auxiliary fields as in (66) which will be used to compute the history terms in the next time-step.

**Remark 3.** As noted in Remark 2, only the non-zero entries of  $\widehat{\mathcal{A}}_1$  and  $\widehat{\mathcal{A}}_2$  are relevant for the numerical implementation so that we may rewrite the history terms defined above for each of the boundary segments separately as follows:

$$\begin{aligned} \widehat{\mathcal{B}}_{a_1,+}^{j+1} &= \sum_{k=1}^K \Gamma_k^{(1/2)} \widehat{\varphi}_{k,a_1}, & \widehat{\mathcal{B}}_{a_2,+}^{j+1} &= \sum_{k=1}^K \Gamma_k^{(1/2)} \widehat{\varphi}_{k,a_2}, \\ \widehat{\mathcal{B}}_{a_1,-}^{j+1} &= \sum_{k=1}^K \Gamma_k^{(-1/2)} \widehat{\varphi}_{k,a_1} - \bar{d}_0 \widehat{\varphi}_{0,a_1}, & \widehat{\mathcal{B}}_{a_2,-}^{j+1} &= \sum_{k=1}^K \Gamma_k^{(-1/2)} \widehat{\varphi}_{k,a_2} - \bar{d}_0 \widehat{\varphi}_{0,a_2}. \end{aligned}$$

It is straightforward to verify that the history terms,  $\mathcal{B}_+^{j+1}$  and  $\mathcal{B}_-^{j+1}$ , can now be efficiently computed as

$$\begin{aligned} \mathcal{B}_+^{j+1} &= \frac{1}{\alpha_1} \mathbf{e}_0^{(1)} \otimes \left[ \widehat{\mathcal{B}}_{l,+}^{j+1} \right]^\top M_2 + \frac{1}{\alpha_1} \mathbf{e}_1^{(1)} \otimes \left[ \widehat{\mathcal{B}}_{r,+}^{j+1} \right]^\top M_2 + \frac{1}{\alpha_2} \left[ M_1 \widehat{\mathcal{B}}_{b,+}^{j+1} \right] \otimes (\mathbf{e}_0^{(2)})^\top + \frac{1}{\alpha_2} \left[ M_1 \widehat{\mathcal{B}}_{l,+}^{j+1} \right] \otimes (\mathbf{e}_1^{(2)})^\top, \\ \mathcal{B}_-^{j+1} &= \frac{1}{2\alpha_1\alpha_2} \left( \mathbf{e}_0^{(1)} \otimes \left[ \widehat{\mathcal{B}}_{l,+}^{j+1} \right]^\top S_2 + \mathbf{e}_1^{(1)} \otimes \left[ \widehat{\mathcal{B}}_{r,+}^{j+1} \right]^\top S_2 \right) + \frac{1}{2\alpha_1\alpha_2} \left( \left[ S_1 \widehat{\mathcal{B}}_{b,+}^{j+1} \right] \otimes (\mathbf{e}_0^{(2)})^\top + \left[ S_1 \widehat{\mathcal{B}}_{l,+}^{j+1} \right] \otimes (\mathbf{e}_1^{(2)})^\top \right). \end{aligned} \quad (71)$$

#### 4.2.2. CP-BDF2

The discrete numerical scheme for the dynamical system defined in (63) and (64) is labelled as ‘CP-BDF2’ if the underlying time-stepping method is BDF2.

Recalling  $\rho = 3/(2\Delta t)$ , the BDF2-based discretization of the dynamical system in (64) reads as

$$\begin{aligned} & i\rho M_1 \widehat{U}^{j+2} M_2 - i\rho M_1 \left( \frac{4}{3} \widehat{U}^{j+1} - \frac{1}{3} \widehat{U}^j \right) M_2 \\ &= \beta_1 S_1 \widehat{U}^{j+2} M_2 + \beta_2 M_1 \widehat{U}^{j+2} S_2 + e^{-i\pi/4} b_0 \left[ \sqrt{\beta_1} \Lambda_1 \widehat{U}^{j+2} M_2 + \sqrt{\beta_2} M_1 \widehat{U}^{j+2} \Lambda_2 \right] + \frac{3}{4} (J_1 J_2)^{-1} \Lambda_1 \widehat{U}^{j+2} \Lambda_2 \\ & \quad - e^{-i\pi/4} \left[ \sqrt{\beta_1} (\mathbf{b}^\top \otimes I_1) \widehat{\mathcal{A}}_1^{j+2} M_2 + \sqrt{\beta_2} M_1 \widehat{\mathcal{A}}_2^{j+2} (\mathbf{b} \otimes I_2) \right] + d_0 e^{i\pi/4} \frac{1}{2} \left[ \sqrt{\beta_1} \beta_2 \widehat{\mathcal{A}}_{0,1}^{j+2} S_2 + \beta_1 \sqrt{\beta_2} S_1 \widehat{\mathcal{A}}_{0,2}^{j+2} \right] \\ & \quad - e^{i\pi/4} \frac{1}{2} \left[ \sqrt{\beta_1} \beta_2 (\mathbf{d}^\top \otimes I_1) \widehat{\mathcal{A}}_1^{j+2} S_2 + \beta_1 \sqrt{\beta_2} S_1 \widehat{\mathcal{A}}_2^{j+2} (\mathbf{d} \otimes I_2) \right], \end{aligned} \quad (72)$$

and that of the auxiliary fields in (63) reads as

$$\begin{aligned} \widehat{\mathcal{A}}_{0,1}^{j+2} &= \frac{1}{\rho} \Lambda_1 \widehat{U}^{j+2} + \frac{4}{3} \widehat{\mathcal{A}}_{0,1}^{j+1} - \frac{1}{3} \widehat{\mathcal{A}}_{0,1}^j, & \widehat{\mathcal{A}}_{0,2}^{j+2} &= \frac{1}{\rho} \widehat{U}^{j+2} \Lambda_2 + \frac{4}{3} \widehat{\mathcal{A}}_{0,2}^{j+1} - \frac{1}{3} \widehat{\mathcal{A}}_{0,2}^j, \\ \widehat{\mathcal{A}}_1^{j+2} &= (\mathcal{G}_K \otimes I_1) \left[ \frac{1}{\rho} \mathbf{1}_K \otimes (\Lambda_1 \widehat{U}^{j+2}) + \frac{4}{3} \widehat{\mathcal{A}}_1^{j+1} - \frac{1}{3} \widehat{\mathcal{A}}_1^j \right], & \widehat{\mathcal{A}}_2^{j+2} &= \left[ \frac{1}{\rho} \mathbf{1}_K^\top \otimes (\widehat{U}^{j+2} \Lambda_2) + \frac{4}{3} \widehat{\mathcal{A}}_2^{j+1} - \frac{1}{3} \widehat{\mathcal{A}}_2^j \right] (\mathcal{G}_K \otimes I_2). \end{aligned} \quad (73)$$

Following along similar lines as in BDF1, the discrete linear system corresponding to (64) turns out to be

$$\begin{aligned} & M_1 \widehat{U}^{j+2} M_2 + \alpha_1^{-2} S_1 \widehat{U}^{j+2} M_2 + \alpha_2^{-2} M_1 \widehat{U}^{j+2} S_2 + \varpi^{(1/2)} \left[ \alpha_1^{-1} \Lambda_1 \widehat{U}^{j+2} M_2 + \alpha_2^{-1} M_1 \widehat{U}^{j+2} \Lambda_2 \right] + \frac{3}{4\alpha_1\alpha_2} \Lambda_1 \widehat{U}^{j+2} \Lambda_2 \\ & + \frac{1}{2} \varpi^{(-1/2)} \left[ \alpha_1^{-1} \alpha_2^{-2} \Lambda_1 \widehat{U}^{j+2} S_2 + \alpha_1^{-2} \alpha_2^{-1} S_1 \widehat{U}^{j+2} \Lambda_2 \right] = M_1 \left( \frac{4}{3} \widehat{U}^{j+1} - \frac{1}{3} \widehat{U}^j \right) M_2 + \mathcal{B}_+^{j+2} + \mathcal{B}_-^{j+2}, \end{aligned} \quad (74)$$

where the history terms are given given by

$$\begin{cases} \mathcal{B}_+^{j+2} = \alpha_1^{-1} \left[ (\bar{\mathbf{b}}^\top \mathcal{G}_K) \otimes I_1 \right] \left( \frac{4}{3} \widehat{\mathcal{A}}_1^{j+1} - \frac{1}{3} \widehat{\mathcal{A}}_1^j \right) M_2 + \alpha_2^{-1} M_1 \left( \frac{4}{3} \widehat{\mathcal{A}}_2^{j+1} - \frac{1}{3} \widehat{\mathcal{A}}_2^j \right) \left[ (\mathcal{G}_K \bar{\mathbf{b}}) \otimes I_2 \right], \\ \mathcal{B}_-^{j+2} = \frac{1}{2} \alpha_1^{-1} \alpha_2^{-2} \left[ (\bar{\mathbf{d}}^\top \mathcal{G}_K \otimes I_1) \left( \frac{4}{3} \widehat{\mathcal{A}}_1^{j+1} - \frac{1}{3} \widehat{\mathcal{A}}_1^j \right) - \bar{d}_0 \left( \frac{4}{3} \widehat{\mathcal{A}}_{0,1}^{j+1} - \frac{1}{3} \widehat{\mathcal{A}}_{0,1}^j \right) \right] S_2 \\ \quad + \frac{1}{2} \alpha_1^{-2} \alpha_2^{-1} S_1 \left[ \left( \frac{4}{3} \widehat{\mathcal{A}}_2^{j+1} - \frac{1}{3} \widehat{\mathcal{A}}_2^j \right) (\mathcal{G}_K \bar{\mathbf{d}} \otimes I_2) - \left( \frac{4}{3} \widehat{\mathcal{A}}_{0,2}^{j+1} - \frac{1}{3} \widehat{\mathcal{A}}_{0,2}^j \right) \bar{d}_0 \right]. \end{cases} \quad (75)$$

The simplifications noted in Remark 3 can also be applied here for the history terms. We omit the details because the adaption is straightforward.

#### 4.2.3. CP-TR

The discrete numerical scheme for the dynamical system is labelled as ‘CP-TR’ if the underlying time-stepping method is TR.

Recalling  $\rho = 2/(\Delta t)$ , the TR based discretization of the dynamical system in (64) reads as

$$\begin{aligned} & i\rho M_1 \widehat{U}^{j+1/2} M_2 - i\rho M_1 \widehat{U}^j M_2 \\ &= \beta_1 S_1 \widehat{U}^{j+1/2} M_2 + \beta_2 M_1 \widehat{U}^{j+1/2} S_2 + e^{-i\pi/4} b_0 \left[ \sqrt{\beta_1} \Lambda_1 \widehat{U}^{j+1/2} M_2 + \sqrt{\beta_2} M_1 \widehat{U}^{j+1/2} \Lambda_2 \right] + \frac{3}{4} (J_1 J_2)^{-1} \Lambda_1 \widehat{U}^{j+1/2} \Lambda_2 \\ & \quad - e^{-i\pi/4} \left[ \sqrt{\beta_1} (\mathbf{b}^\top \otimes I_1) \widehat{\mathcal{A}}_1^{j+1/2} M_2 + \sqrt{\beta_2} M_1 \widehat{\mathcal{A}}_2^{j+1/2} (\mathbf{b} \otimes I_2) \right] + d_0 e^{i\pi/4} \frac{1}{2} \left[ \sqrt{\beta_1} \beta_2 \widehat{\mathcal{A}}_{0,1}^{j+1/2} S_2 + \beta_1 \sqrt{\beta_2} S_1 \widehat{\mathcal{A}}_{0,2}^{j+1/2} \right] \\ & \quad - e^{i\pi/4} \frac{1}{2} \left[ \sqrt{\beta_1} \beta_2 (\mathbf{d}^\top \otimes I_1) \widehat{\mathcal{A}}_1^{j+1/2} S_2 + \beta_1 \sqrt{\beta_2} S_1 \widehat{\mathcal{A}}_2^{j+1/2} (\mathbf{d} \otimes I_2) \right], \end{aligned} \quad (76)$$

and that of the auxiliary fields in (63) reads as

$$\begin{aligned}\widehat{\mathcal{A}}_{0,1}^{j+1/2} &= \frac{1}{\rho} \Lambda_1 \widehat{U}^{j+1/2} + \widehat{\mathcal{A}}_{0,1}^j, & \widehat{\mathcal{A}}_{0,2}^{j+1/2} &= \frac{1}{\rho} \widehat{U}^{j+1/2} \Lambda_2 + \widehat{\mathcal{A}}_{0,2}^j, \\ \widehat{\mathcal{A}}_1^{j+1/2} &= (\mathcal{G}_K \otimes I_1) \left[ \frac{1}{\rho} \mathbf{1}_K \otimes (\Lambda_1 \widehat{U}^{j+1/2}) + \widehat{\mathcal{A}}_1^j \right], & \widehat{\mathcal{A}}_2^{j+1/2} &= \left[ \frac{1}{\rho} \mathbf{1}_K^\top \otimes (\widehat{U}^{j+1/2} \Lambda_2) + \widehat{\mathcal{A}}_2^j \right] (\mathcal{G}_K \otimes I_2).\end{aligned}\quad (77)$$

Next, we plug-in these updates for auxiliary fields from (77) in the discrete system (76) to obtain

$$\begin{aligned}M_1 \widehat{U}^{j+1/2} M_2 + \alpha_1^{-2} S_1 \widehat{U}^{j+1/2} M_2 + \alpha_2^{-2} M_1 \widehat{U}^{j+1/2} S_2 + \varpi^{(1/2)} \left[ \alpha_1^{-1} \Lambda_1 \widehat{U}^{j+1/2} M_2 + \alpha_2^{-1} M_1 \widehat{U}^{j+1/2} \Lambda_2 \right] \\ + \frac{1}{2} \varpi^{(-1/2)} \left[ \alpha_1^{-1} \alpha_2^{-2} \Lambda_1 \widehat{U}^{j+1/2} S_2 + \alpha_1^{-2} \alpha_2^{-1} S_1 \widehat{U}^{j+1/2} \Lambda_2 \right] + \frac{3}{4\alpha_1\alpha_2} \Lambda_1 \widehat{U}^{j+1/2} \Lambda_2 = M_1 \widehat{U}^j M_2 + \mathcal{B}_+^{j+1/2} + \mathcal{B}_-^{j+1/2},\end{aligned}\quad (78)$$

where the history terms are given by

$$\begin{cases} \mathcal{B}_+^{j+1/2} = \alpha_1^{-1} \left[ (\bar{\mathbf{b}}^\top \mathcal{G}_K) \otimes I_1 \right] \widehat{\mathcal{A}}_1^j M_2 + \alpha_2^{-1} M_1 \widehat{\mathcal{A}}_2^j \left[ (\mathcal{G}_K \bar{\mathbf{b}}) \otimes I_2 \right], \\ \mathcal{B}_-^{j+1/2} = \frac{1}{2} \alpha_1^{-1} \alpha_2^{-2} \left[ (\bar{\mathbf{d}}^\top \mathcal{G}_K \otimes I_1) \widehat{\mathcal{A}}_1^j - \bar{d}_0 \widehat{\mathcal{A}}_{0,1}^j \right] S_2 + \frac{1}{2} \alpha_1^{-2} \alpha_2^{-1} S_1 \left[ \widehat{\mathcal{A}}_2^j (\mathcal{G}_K \bar{\mathbf{d}} \otimes I_2) - \widehat{\mathcal{A}}_{0,2}^j \bar{d}_0 \right]. \end{cases}\quad (79)$$

Once again, simplification of the history terms is possible along the lines of Remark 3 but we omit the discussion for the sake of brevity of presentation.

The computation of the history terms in the next time-step requires values of the auxiliary fields on the temporal grid which can be facilitated by the TR-based discretization of the ODEs in (63) as follows

$$\begin{aligned}\widehat{\mathcal{A}}_{0,1}^{j+1} &= \frac{2}{\rho} \Lambda_1 \widehat{U}^{j+1/2} + \widehat{\mathcal{A}}_{0,1}^j, & \widehat{\mathcal{A}}_{0,2}^{j+1} &= \frac{2}{\rho} \widehat{U}^{j+1/2} \Lambda_2 + \widehat{\mathcal{A}}_{0,2}^j, \\ \widehat{\mathcal{A}}_1^{j+1} &= \left[ \frac{2}{\rho} (\mathcal{G}_K \mathbf{1}_K) \otimes (\Lambda_1 \widehat{U}^{j+1/2}) + (\mathcal{H}_K \otimes I_1) \widehat{\mathcal{A}}_1^j \right], & \widehat{\mathcal{A}}_2^{j+1} &= \left[ \frac{2}{\rho} (\mathcal{G}_K \mathbf{1}_K)^\top \otimes (\widehat{U}^{j+1/2} \Lambda_2) + \widehat{\mathcal{A}}_2^j (\mathcal{H}_K \otimes I_2) \right],\end{aligned}\quad (80)$$

where

$$\mathcal{H}_K = \text{diag} \left( \frac{1 - \bar{\eta}_1^2}{1 + \bar{\eta}_1^2}, \frac{1 - \bar{\eta}_2^2}{1 + \bar{\eta}_2^2}, \dots, \frac{1 - \bar{\eta}_K^2}{1 + \bar{\eta}_K^2} \right) \in \mathbb{R}^{(K \times K)}.\quad (81)$$

## 5. Variational Formulation: TBCs

In this section, we consider the numerical solution of the IBVP in (2) using a Legendre-Galerkin method as laid out in Sec. 3. The variational formulation begins with (36) where the boundary terms, namely,  $\mathcal{I}_1$  and  $\mathcal{I}_2$ , need to incorporate the transparent boundary conditions stated in (15). In the following, we suppress the independent variables in the auxiliary function  $\varphi(y_1, y_2, \tau_1, \tau_2)$  for the sake of brevity of presentation. Starting with the segments denoted by  $\Gamma_{a_1}$ ,  $a_1 \in \{l, r\}$ , we have

$$\begin{aligned}\mathcal{I}_1 &= J_1^{-2} \int_{\mathbb{I}} \left( [\theta_{p_1, p_2} \partial_{y_1} u]_{+1} - [\theta_{p_1, p_2} \partial_{y_1} u]_{-1} \right) dy_2 \\ &= J_1^{-1} \int_{\mathbb{I}} \left[ \phi_{p_1}(+1) \left( -e^{-i\pi/4} \partial_{\tau_1}^{1/2} \varphi \Big|_{\tau_1, \tau_2=t} \right)_{y_1=+1} + \phi_{p_1}(-1) \left( -e^{-i\pi/4} \partial_{\tau_1}^{1/2} \varphi \Big|_{\tau_1, \tau_2=t} \right)_{y_1=-1} \right] \phi_{p_2}(y_2) dy_2 \\ &= -e^{-i\pi/4} J_1^{-1} \partial_{\tau_1}^{1/2} \left[ \phi_{p_1}(+1) \int_{\mathbb{I}} \phi_{p_2}(y_2) (\varphi)_{y_1=+1} dy_2 + \phi_{p_1}(-1) \int_{\mathbb{I}} \phi_{p_2}(y_2) (\varphi)_{y_1=-1} dy_2 \right] \Big|_{\tau_1, \tau_2=t}.\end{aligned}\quad (82)$$

Similarly, for the segments denoted by  $\Gamma_{a_2}$ ,  $a_2 \in \{b, t\}$ , we have

$$\begin{aligned}\mathcal{I}_2 &= J_2^{-2} \int_{\mathbb{I}} \left( [\theta_{p_1, p_2} \partial_{y_2} u]_{+1} - [\theta_{p_1, p_2} \partial_{y_2} u]_{-1} \right) dy_1 \\ &= J_2^{-1} \int_{\mathbb{I}} \left[ \phi_{p_2}(+1) \left( -e^{-i\pi/4} \partial_{\tau_2}^{1/2} \varphi \Big|_{\tau_1, \tau_2=t} \right)_{y_2=+1} + \phi_{p_2}(-1) \left( -e^{-i\pi/4} \partial_{\tau_2}^{1/2} \varphi \Big|_{\tau_1, \tau_2=t} \right)_{y_2=-1} \right] \phi_{p_1}(y_1) dy_1 \\ &= -e^{-i\pi/4} J_2^{-1} \partial_{\tau_2}^{1/2} \left[ \phi_{p_2}(+1) \int_{\mathbb{I}} \phi_{p_1}(y_1) (\varphi)_{y_2=+1} dy_1 + \phi_{p_2}(-1) \int_{\mathbb{I}} \phi_{p_1}(y_1) (\varphi)_{y_2=-1} dy_1 \right] \Big|_{\tau_1, \tau_2=t}.\end{aligned}\quad (83)$$

Let  $\widehat{\Phi}_{p_1, p_2}$  denote the expansion coefficient in the Lobatto basis for the auxiliary function  $\varphi(y_1, y_2, \tau_1, \tau_2)$  so that

$$\varphi(y_1, y_2, \tau_1, \tau_2) = \sum_{p_1=0}^{N_1} \sum_{p_2=0}^{N_2} \widehat{\Phi}_{p_1, p_2}(\tau_1, \tau_2) \phi_{p_1}(y_1) \phi_{p_2}(y_2). \quad (84)$$

We introduce the matrix  $\widehat{\Phi} = (\widehat{\Phi}_{p_1, p_2}) \in \mathbb{C}^{(N_1+1) \times (N_2+1)}$ . Restrictions of the auxiliary function on the boundary segments  $\Gamma_{a_1}$  and  $\Gamma_{a_2}$  require representation of  $\varphi(y_1 = \pm 1, y_2, \tau_1, \tau_2)$  and  $\varphi(y_1, y_2 = \pm 1, \tau_1, \tau_2)$ , respectively. Let  $\widehat{\Phi}_k$  denote the restriction of  $\widehat{\Phi}$  to  $\Gamma_{a_k}$  for  $k = 1, 2$ , then

$$\widehat{\Phi}_1 = \Lambda_1 \widehat{\Phi}, \quad \widehat{\Phi}_2 = \widehat{\Phi} \Lambda_2, \quad (85)$$

where  $\Lambda_1$  and  $\Lambda_2$  are defined in Sec. 3. The linear system corresponding to (36) turns out to be

$$iM_1 \partial_t \widehat{U} M_2 = J_1^{-2} S_1 \widehat{U} M_2 + J_2^{-2} M_1 \widehat{U} S_2 + e^{-i\pi/4} \left[ (J_1)^{-1} \partial_{\tau_1}^{1/2} \widehat{\Phi}_1(\tau_1, \tau_2) M_2 + (J_2)^{-1} M_1 \partial_{\tau_2}^{1/2} \widehat{\Phi}_2(\tau_1, \tau_2) \right] \Big|_{\tau_1, \tau_2 = t}. \quad (86)$$

Here, we observe that the implementation of the 1/2-order temporal derivatives require the history of the auxiliary function from the start of the computations which is facilitated by the IVPs in (16). The variational formulation for these IVPs can be written as:

$$\begin{aligned} \Gamma_{a_2} : \quad & (i\partial_{\tau_1} \varphi + J_1^{-2} \partial_{y_1}^2 \varphi, \phi_{p_1})_{\mathbb{I}} = i\partial_{\tau_1} (\varphi, \phi_{p_1})_{\mathbb{I}} - J_1^{-2} (\partial_{y_1} \varphi, \phi'_{p_1})_{\mathbb{I}} + J_1^{-2} ([\phi_{p_1} \partial_{y_1} \varphi]_{y_1=+1} - [\phi_{p_1} \partial_{y_1} \varphi]_{y_1=-1}), \\ \Gamma_{a_1} : \quad & (i\partial_{\tau_2} \varphi + J_2^{-2} \partial_{y_2}^2 \varphi, \phi_{p_2})_{\mathbb{I}} = i\partial_{\tau_2} (\varphi, \phi_{p_2})_{\mathbb{I}} - J_2^{-2} (\partial_{y_2} \varphi, \phi'_{p_2})_{\mathbb{I}} + J_2^{-2} ([\phi_{p_2} \partial_{y_2} \varphi]_{y_2=+1} - [\phi_{p_2} \partial_{y_2} \varphi]_{y_2=-1}). \end{aligned} \quad (87)$$

Supplying the maps present in (17) to the boundary terms for the segments  $\Gamma_{a_2}$  above, we have

$$\begin{aligned} J_1^{-2} ([\phi_{p_1} \partial_{y_1} \varphi]_{y_1=+1} - [\phi_{p_1} \partial_{y_1} \varphi]_{y_1=-1}) &= J_1^{-1} \left[ \phi_{p_1}(+1) (-e^{-i\pi/4} \partial_{\tau_1}^{1/2} \varphi)_{y_1=+1} + \phi_{p_1}(-1) (-e^{-i\pi/4} \partial_{\tau_1}^{1/2} \varphi)_{y_1=-1} \right] \\ &= -e^{-i\pi/4} J_1^{-1} \partial_{\tau_1}^{1/2} [\phi_{p_1}(+1) (\varphi)_{y_1=+1} + \phi_{p_1}(-1) (\varphi)_{y_1=-1}], \end{aligned} \quad (88)$$

Similarly, for the segments  $\Gamma_{a_1}$ , we have

$$\begin{aligned} J_2^{-2} ([\phi_{p_2} \partial_{y_2} \varphi]_{y_2=+1} - [\phi_{p_2} \partial_{y_2} \varphi]_{y_2=-1}) &= J_2^{-1} \left[ \phi_{p_2}(+1) (-e^{-i\pi/4} \partial_{\tau_2}^{1/2} \varphi)_{y_2=+1} + \phi_{p_2}(-1) (-e^{-i\pi/4} \partial_{\tau_2}^{1/2} \varphi)_{y_2=-1} \right] \\ &= -e^{-i\pi/4} J_2^{-1} \partial_{\tau_2}^{1/2} [\phi_{p_2}(+1) (\varphi)_{y_2=+1} + \phi_{p_2}(-1) (\varphi)_{y_2=-1}]. \end{aligned} \quad (89)$$

Introducing the appropriate mass and stiffness matrices, the variational form in (87) can be stated as

$$\begin{aligned} iM_1 \partial_{\tau_1} \widehat{\Phi}_2(\tau_1, \tau_2) &= J_1^{-2} S_1 \widehat{\Phi}_2(\tau_1, \tau_2) + e^{-i\pi/4} \left[ \partial_{\tau_1}^{1/2} (J_1)^{-1} \Lambda_1 \widehat{\Phi}_2(\tau_1, \tau_2) \right], \quad \tau_1 \in (\tau_2, t], \\ i\partial_{\tau_2} \widehat{\Phi}_1(\tau_1, \tau_2) M_2 &= J_2^{-2} \widehat{\Phi}_1(\tau_1, \tau_2) S_2 + e^{-i\pi/4} \left[ \partial_{\tau_2}^{1/2} (J_2)^{-1} \widehat{\Phi}_1(\tau_1, \tau_2) \Lambda_2 \right], \quad \tau_2 \in (\tau_1, t], \end{aligned} \quad (90)$$

where the initial conditions are  $\widehat{\Phi}_2(\tau_2, \tau_2) = \widehat{U}(\tau_2) \Lambda_2$  and  $\widehat{\Phi}_1(\tau_1, \tau_1) = \Lambda_1 \widehat{U}(\tau_1)$ .

### 5.1. Nonlocal temporal discretization: Convolution quadrature

In this section, we present various time-stepping method to discretize the dynamical system defined by (86) and (90). Here, we employ one-step methods, namely, BDF1 and TR, together with a compatible convolution quadrature scheme for the fractional operators. Such a discretization scheme is evidently nonlocal exhibiting the nonlocal nature of the dynamical system.

The recipe for handling the nonlocal terms in context of CQ is presented in Sec 4.1. The computation of quadrature sums require history of the auxiliary fields on the segments which can be facilitated by solving the dynamical systems established in (90). Each of the methods discussed below is derived by applying a particular time-stepping scheme to the CQ approach, therefore, we label them as ‘CQ–’ followed by the acronym for the time-stepping method.

### 5.1.1. CQ-BDF1

The discrete numerical scheme for the dynamical system (86) is labelled as ‘CQ-BDF1’ where the underlying one-step method is BDF1. Recalling  $\rho = 1/\Delta t$  and  $\alpha_k = \sqrt{\rho/\beta_k} e^{-i\pi/4}$  for  $k = 1, 2$ , the complete discretization of (86) reads as

$$M_1 \widehat{U}^{j+1} M_2 + \alpha_1^{-2} S_1 \widehat{U}^{j+1} M_2 + \alpha_2^{-2} M_1 \widehat{U}^{j+1} S_2 + \alpha_1^{-1} \Lambda_1 \widehat{U}^{j+1} M_2 + \alpha_2^{-1} M_1 \widehat{U}^{j+1} \Lambda_2 = M_1 \widehat{U}^j M_2 - \mathcal{B}^{j+1}, \quad (91)$$

where we have used the fact that  $\widehat{\Phi}_1^{j+1,j+1} = \Lambda_1 \widehat{U}^{j+1}$  and  $\widehat{\Phi}_2^{j+1,j+1} = \widehat{U}^{j+1} \Lambda_2$ . The history term is given by

$$\mathcal{B}^{j+1} = \sum_{k=1}^j \omega_{j+1-k}^{(1/2)} [\alpha_1^{-1} \widehat{\Phi}_1^{k,j+1} M_2 + \alpha_2^{-1} M_1 \widehat{\Phi}_2^{j+1,k}]. \quad (92)$$

The computation of the history term above requires the off-diagonal samples  $\widehat{\Phi}_1^{k,j+1}$  and  $\widehat{\Phi}_2^{j+1,k}$  which can be obtained by solving the dynamical system defined in (90) corresponding to the boundary segments. The BDF1-based temporal discretization of this system reads as

$$\begin{aligned} (M_1 + \alpha_1^{-2} S_1 + \alpha_1^{-1} \Lambda_1) \widehat{\Phi}_2^{j+1,p} &= M_1 \widehat{\Phi}_2^{j,p} - C_2^{j+1}, \quad p = 0, 1, \dots, j, \\ \widehat{\Phi}_1^{q,j+1} (M_2 + \alpha_2^{-2} S_2 + \alpha_2^{-1} \Lambda_2) &= \widehat{\Phi}_1^{q,j} M_2 - C_1^{j+1}, \quad q = 0, 1, \dots, j. \end{aligned} \quad (93)$$

where the history terms are given by

$$C_1^{j+1} = \sum_{k=1}^j \omega_{j+1-k}^{(1/2)} [\alpha_2^{-1} \widehat{\Phi}_1^{q,k} \Lambda_2], \quad C_2^{j+1} = \sum_{k=1}^j \omega_{j+1-k}^{(1/2)} [\alpha_1^{-1} \Lambda_1 \widehat{\Phi}_2^{k,p}]. \quad (94)$$

### 5.1.2. CQ-TR

The discrete numerical scheme for the dynamical system (86) is labelled as ‘CQ-TR’ where the underlying one-step method is TR. Recalling  $\rho = 2/\Delta t$ , the complete discretization of (86) reads as

$$M_1 \widehat{U}^{j+1/2} M_2 + \alpha_1^{-2} S_1 \widehat{U}^{j+1/2} M_2 + \alpha_2^{-2} M_1 \widehat{U}^{j+1/2} S_2 + \alpha_1^{-1} \Lambda_1 \widehat{U}^{j+1/2} M_2 + \alpha_2^{-1} M_1 \widehat{U}^{j+1/2} \Lambda_2 = M_1 \widehat{U}^j M_2 - \mathcal{B}^{j+1/2}, \quad (95)$$

where the history term is computed in the similar manner as done in BDF1. Here,  $\mathcal{B}^{j+1/2} = (\mathcal{B}^{j+1} + \mathcal{B}^j)/2$ .

In order to obtain the off-diagonal samples  $\widehat{\Phi}_1^{k,j+1}$  and  $\widehat{\Phi}_2^{j+1,k}$ , we solve the dynamical system defined in (90) corresponding to the boundary segments. The TR-based temporal discretization of this system reads as

$$\begin{aligned} (M_1 + \alpha_1^{-2} S_1 + \alpha_1^{-1} \Lambda_1) \widehat{\Phi}_2^{j+1/2,p} &= M_1 \widehat{\Phi}_2^{j,p} - C_2^{j+1/2}, \quad p = 0, 1, \dots, j, \\ \widehat{\Phi}_1^{q,j+1/2} (M_2 + \alpha_2^{-2} S_2 + \alpha_2^{-1} \Lambda_2) &= \widehat{\Phi}_1^{q,j} M_2 - C_1^{j+1/2}, \quad q = 0, 1, \dots, j. \end{aligned} \quad (96)$$

where the history terms corresponding to the corners are computed in the similar manner as done in BDF1. Here, we use the fact that  $C_k^{j+1/2} = (C_k^{j+1} + C_k^j)/2$  for  $k = 1, 2$ .

## 5.2. Local temporal discretization: Novel Padé

In this section, we present an effectively local form of the (nonlocal) dynamical system stated in (86) and (90). This is accomplished by employing a novel Padé approximant based representation for the time-fractional operators in (86) and (90) to obtain a system of ODEs which approximate the original system. This approach can be contrasted with the CQ-approach where the history grows with each time-step making it expensive computationally as well as from a storage point of view.

In order to write the rational approximations for the time-fractional operators present in (86), we introduce the auxiliary fields  $\mathcal{A}_{k,1}$  and  $\mathcal{A}_{k,2}$  where  $k = 1, 2, \dots, K$  such that

$$\begin{aligned} \partial_{\tau_1}^{1/2} \widehat{\Phi}_1 \Big|_{\tau_1, \tau_2=t} &= b_0 \Lambda_1 \widehat{U} - \sum_{k=1}^K b_k \widehat{\mathcal{A}}_{k,1}(t, t) = b_0 \Lambda_1 \widehat{U} - (\mathbf{b}^\top \otimes I_1) \widehat{\mathcal{A}}_1(t, t), \\ \partial_{\tau_2}^{1/2} \widehat{\Phi}_2 \Big|_{\tau_1, \tau_2=t} &= b_0 \widehat{U} \Lambda_2 - \sum_{k=1}^K b_k \widehat{\mathcal{A}}_{k,2}(t, t) = b_0 \widehat{U} \Lambda_2 - \widehat{\mathcal{A}}_2(t, t) (\mathbf{b} \otimes I_2). \end{aligned} \quad (97)$$

The auxiliary fields  $\mathcal{A}_{k,1}$  and  $\mathcal{A}_{k,2}$  can be expanded in the Lobatto basis as follows:

$$\begin{aligned}\mathcal{A}_{k,1}(\pm 1, y_2, \tau_1, \tau_2) &= \sum_{p_1=0,1} \sum_{p_2=0}^{N_2} \widehat{\mathcal{A}}_{p_1,p_2}^{(k,1)}(\tau_1, \tau_2) \phi_{p_1}(\pm 1) \phi_{p_2}(y_2), \\ \mathcal{A}_{k,2}(y_1, \pm 1, \tau_1, \tau_2) &= \sum_{p_1=0}^{N_1} \sum_{p_2=0,1} \widehat{\mathcal{A}}_{p_1,p_2}^{(k,2)}(\tau_1, \tau_2) \phi_{p_2}(y_1) \phi_{p_1}(\pm 1).\end{aligned}\tag{98}$$

The structure of the matrices  $\widehat{\mathcal{A}}_{k,1}$  and  $\widehat{\mathcal{A}}_{k,2}$  are same as that defined in Sec. 4.2. The structure of the block matrix  $\widehat{\mathcal{A}}_p$  with the matrix entries  $\widehat{\mathcal{A}}_{k,p}$  for  $p = 1, 2$  is also borrowed from the same section.

As noted before, the index  $k$  of the auxiliary fields correspond to the  $k$ -th partial fraction of the Padé approximant so that the ODE satisfied by each of the auxiliary fields reads as

$$\begin{aligned}\partial_{\tau_1} \widehat{\mathcal{A}}_{k,1}(\tau_1, \tau_2) &= -\eta_k^2 \widehat{\mathcal{A}}_{k,1}(\tau_1, \tau_2) + \widehat{\Phi}_1, & \partial_{\tau_2} \widehat{\mathcal{A}}_{k,2}(\tau_1, \tau_2) &= -\eta_k^2 \widehat{\mathcal{A}}_{k,2}(\tau_1, \tau_2) + \widehat{\Phi}_2, \\ \partial_{\tau_1} \widehat{\mathcal{A}}_1(\tau_1, \tau_2) &= -(\mathcal{E}_K \otimes I_1) \widehat{\mathcal{A}}_1(\tau_1, \tau_2) + \mathbf{1}_K \otimes \widehat{\Phi}_1, & \partial_{\tau_2} \widehat{\mathcal{A}}_2(\tau_1, \tau_2) &= -\widehat{\mathcal{A}}_2(\tau_1, \tau_2)(\mathcal{E}_K \otimes I_2) + \mathbf{1}_K^T \otimes \widehat{\Phi}_2.\end{aligned}\tag{99}$$

Let us observe that the non-zero entries of  $\widehat{\mathcal{A}}_{k,1}$  and  $\widehat{\mathcal{A}}_{k,2}$  are related to the auxiliary functions introduced in Sec. 2.3 as follows:

$$\begin{aligned}\Gamma_l : \varphi_{k,l}(y_2, \tau_1, \tau_2) &= \mathcal{A}_{k,1}(-1, y_2, \tau_1, \tau_2), & \Gamma_r : \varphi_{k,r}(y_2, \tau_1, \tau_2) &= \mathcal{A}_{k,1}(+1, y_2, \tau_1, \tau_2), \\ \Gamma_b : \varphi_{k,b}(y_1, \tau_1, \tau_2) &= \mathcal{A}_{k,1}(y_1, -1, \tau_1, \tau_2), & \Gamma_t : \varphi_{k,t}(y_1, \tau_1, \tau_2) &= \mathcal{A}_{k,1}(y_1, +1, \tau_1, \tau_2).\end{aligned}$$

Following the convention laid out in Remark (2), expansion of the auxiliary fields in the Lobatto basis read as

$$\begin{aligned}\varphi_{k,a_1}(y_2, \tau_1, \tau_2) &= \sum_{p_2=0}^{N_2} \widehat{\varphi}_{k,p_2,a_1}(\tau_1, \tau_2) \phi_{p_2}(y_2), & a_1 \in \{l, r\}, \\ \varphi_{k,a_2}(y_1, \tau_1, \tau_2) &= \sum_{p_1=0}^{N_1} \widehat{\varphi}_{k,p_1,a_2}(\tau_1, \tau_2) \phi_{p_1}(y_1), & a_2 \in \{b, t\},\end{aligned}\tag{100}$$

and the matrices  $\widehat{\mathcal{A}}_{k,1}$  and  $\widehat{\mathcal{A}}_{k,2}$  can be written as

$$\widehat{\mathcal{A}}_{k,1} = \begin{pmatrix} \widehat{\varphi}_{k,l}^T \\ \widehat{\varphi}_{k,r}^T \\ Z_1 \end{pmatrix}, \quad \widehat{\mathcal{A}}_{k,2} = \begin{pmatrix} \widehat{\varphi}_{k,b} & \widehat{\varphi}_{k,t} & Z_2 \end{pmatrix}.\tag{101}$$

Employing the approximations developed in (97) in the (non-local) dynamical system stated in (86), we obtain an effectively local system given by

$$\begin{aligned}iM_1 \partial_t \widehat{U} M_2 &= J_1^{-2} S_1 \widehat{U} M_2 + J_2^{-2} M_1 \widehat{U} S_2 + e^{-i\pi/4} b_0 \left[ (J_1)^{-1} \Lambda_1 \widehat{U} M_2 + (J_2)^{-1} M_1 \widehat{U} \Lambda_2 \right] \\ &\quad - e^{-i\pi/4} \left[ (J_1)^{-1} (\mathbf{b}^T \otimes I_1) \widehat{\mathcal{A}}_1(t, t) M_2 + (J_2)^{-1} M_1 \widehat{\mathcal{A}}_2(t, t) (\mathbf{b} \otimes I_2) \right].\end{aligned}\tag{102}$$

As noted in Sec. 2.3, the auxiliary fields  $\mathcal{A}_{k,1}$  and  $\mathcal{A}_{k,2}$  satisfy the same IVPs as that of  $\Phi_1$  and  $\Phi_2$  on the boundary segments. Therefore, the dynamical system for  $\mathcal{A}_{k,1}$  and  $\mathcal{A}_{k,2}$  work out to be (similar to that in (90)):

$$\begin{aligned}\Gamma_{a_1} : i \partial_{\tau_2} \widehat{\mathcal{A}}_{k,1}(\tau_1, \tau_2) M_2 &= J_2^{-2} \widehat{\mathcal{A}}_{k,1}(\tau_1, \tau_2) S_2 + e^{-i\pi/4} \left[ \partial_{\tau_2}^{1/2} (J_2)^{-1} \widehat{\mathcal{A}}_{k,1}(\tau_1, \tau_2) \Lambda_2 \right], \\ \Gamma_{a_2} : i \partial_{\tau_1} M_1 \widehat{\mathcal{A}}_{k,2}(\tau_1, \tau_2) &= J_1^{-2} S_1 \widehat{\mathcal{A}}_{k,2}(\tau_1, \tau_2) + e^{-i\pi/4} \left[ \partial_{\tau_1}^{1/2} (J_1)^{-1} \Lambda_1 \widehat{\mathcal{A}}_{k,2}(\tau_1, \tau_2) \right],\end{aligned}\tag{103}$$

which can be restated in terms of block matrices corresponding to these auxiliary fields as

$$\begin{aligned}\Gamma_{a_1} : i \partial_{\tau_2} \widehat{\mathcal{A}}_1(\tau_1, \tau_2) M_2 &= J_2^{-2} \widehat{\mathcal{A}}_1(\tau_1, \tau_2) S_2 + e^{-i\pi/4} \left[ \partial_{\tau_2}^{1/2} (J_2)^{-1} \widehat{\mathcal{A}}_1(\tau_1, \tau_2) \Lambda_2 \right], \\ \Gamma_{a_2} : i \partial_{\tau_1} M_1 \widehat{\mathcal{A}}_2(\tau_1, \tau_2) &= J_1^{-2} S_1 \widehat{\mathcal{A}}_2(\tau_1, \tau_2) + e^{-i\pi/4} \left[ \partial_{\tau_1}^{1/2} (J_1)^{-1} \Lambda_1 \widehat{\mathcal{A}}_2(\tau_1, \tau_2) \right].\end{aligned}\tag{104}$$

In order to write the rational approximations for the (non-local) time-fractional operators present in (103), we introduce the auxiliary fields  $C_{k,k'}$  where  $k = k' = 1, 2, \dots, K$  such that

$$\begin{aligned}\partial_{\tau_1}^{1/2}(\Lambda_1 \widehat{\mathcal{A}}_{k,2}) &= b_0 \Lambda_1 \widehat{\mathcal{A}}_{k,2} - \sum_{k'=1}^K b_{k'} \widehat{C}_{k',k}(\tau_1, \tau_2) = b_0 \Lambda_1 \widehat{\mathcal{A}}_2 - (\mathbf{b}^\top \otimes I_1) \widehat{C}(\tau_1, \tau_2), \\ \partial_{\tau_2}^{1/2}(\widehat{\mathcal{A}}_{k,1} \Lambda_2) &= b_0 \widehat{\mathcal{A}}_{k,1} \Lambda_2 - \sum_{k'=1}^K b_{k'} \widehat{C}_{k,k'}(\tau_1, \tau_2) = b_0 \widehat{\mathcal{A}}_1 \Lambda_2 - \widehat{C}(\tau_1, \tau_2)(\mathbf{b} \otimes I_2).\end{aligned}\quad (105)$$

The auxiliary field  $C_{k,k'}$  can be expanded in the Lobatto basis as follows:

$$C_{k,k'}(\pm 1, \pm 1, \tau_1, \tau_2) = \sum_{p_1=0,1} \sum_{p_2=0,1} \widehat{C}_{p_1,p_2}^{(k,k')} \phi_{p_1}(\pm 1) \phi_{p_2}(\pm 1), \quad (106)$$

Exploiting the property of Lobatto polynomials, we can establish that only four entries in the matrix  $\widehat{C}_{k,k'}$  are non-zero. Next we introduce a block matrix  $\widehat{C}$  with the matrix entries  $\widehat{C}_{k,k'} \in \mathbb{C}^{(N_1+1) \times (N_2+1)}$  defined as follows:

$$\widehat{C} = \begin{pmatrix} \widehat{C}_{1,1} & \widehat{C}_{1,2} & \dots & \widehat{C}_{1,K} \\ \widehat{C}_{2,1} & \widehat{C}_{2,2} & \dots & \widehat{C}_{2,K} \\ \vdots & \vdots & \ddots & \vdots \\ \widehat{C}_{K,1} & \widehat{C}_{K,2} & \dots & \widehat{C}_{K,K} \end{pmatrix}, \quad \widehat{C}_{k,k'} = \begin{pmatrix} \widehat{C}_{0,0} & \widehat{C}_{0,1} & \dots & 0 \\ \widehat{C}_{1,0} & \widehat{C}_{1,1} & \dots & 0 \\ 0 & 0 & \dots & 0 \\ \vdots & \vdots & \ddots & \vdots \\ 0 & 0 & \dots & 0 \end{pmatrix}^{(k,k')} = \begin{pmatrix} \psi_{k,k',lb} & \psi_{k,k',lt} & \dots & 0 \\ \psi_{k,k',rb} & \psi_{k,k',rt} & \dots & 0 \\ 0 & 0 & \dots & 0 \\ \vdots & \vdots & \ddots & \vdots \\ 0 & 0 & \dots & 0 \end{pmatrix}. \quad (107)$$

where the auxiliary functions  $\psi_{k,k',a_1 a_2}$  and  $\psi_{k,k',a_1 a_2}$  are defined in Sec. 2.3. Finally, identifying the correspondence with the partial fractions of the Padé approximant, the ODEs satisfied by the auxiliary field  $C_{k,k'}$  work out to be

$$\partial_{\tau_2} \widehat{C}_{k,k'}(\tau_1, \tau_2) = -\eta_k^2 \widehat{C}_{k,k'}(\tau_1, \tau_2) + \widehat{\mathcal{A}}_{k,1} \Lambda_2, \quad \partial_{\tau_1} \widehat{C}_{k,k'}(\tau_1, \tau_2) = -\eta_k^2 \widehat{C}_{k,k'}(\tau_1, \tau_2) + \Lambda_1 \widehat{\mathcal{A}}_{k',2}. \quad (108)$$

Introducing the block matrix  $\widehat{C}(\tau_1, \tau_2)$ , the above equations can be stated as follows:

$$\partial_{\tau_2} \widehat{C}(\tau_1, \tau_2) = -\widehat{C}(\tau_1, \tau_2)(\mathcal{E}_K \otimes I_2) + \mathbf{1}_K^\top \otimes (\widehat{\mathcal{A}}_1 \Lambda_2), \quad \partial_{\tau_1} \widehat{C}(\tau_1, \tau_2) = -(\mathcal{E}_K \otimes I_1) \widehat{C}(\tau_1, \tau_2) + \mathbf{1}_K \otimes (\Lambda_1 \widehat{\mathcal{A}}_2). \quad (109)$$

Employing the approximations developed in (105) in the (non-local) dynamical system stated in (104), we obtain an effectively local system given by

$$\begin{aligned}i \partial_{\tau_2} \widehat{\mathcal{A}}_1 M_2 &= J_2^{-2} \widehat{\mathcal{A}}_1 S_2 + e^{-i\pi/4} (J_2)^{-1} \left[ b_0 \widehat{\mathcal{A}}_1 \Lambda_2 - \widehat{C}(\tau_1, \tau_2)(\mathbf{b} \otimes I_2) \right], \\ i \partial_{\tau_1} M_1 \widehat{\mathcal{A}}_2 &= J_1^{-2} S_1 \widehat{\mathcal{A}}_2 + e^{-i\pi/4} (J_1)^{-1} \left[ b_0 \Lambda_1 \widehat{\mathcal{A}}_2 - (\mathbf{b}^\top \otimes I_1) \widehat{C}(\tau_1, \tau_2) \right].\end{aligned}\quad (110)$$

The approach presented here is referred to as the *novel Padé* approach. Each of the methods discussed below is derived by applying a particular time-stepping scheme to the novel Padé approach, therefore, we label them as ‘NP-’ followed by the acronym for the time-stepping method.

### 5.2.1. NP-BDF1

The discrete numerical scheme for the dynamical system defined in (102) and (110) is labelled as ‘NP-BDF1’ if the underlying time-stepping method is BDF1.

Recalling  $\rho = 1/(\Delta t)$ , the BDF1-based discretization of the dynamical system in (102) reads as

$$\begin{aligned}M_1 \widehat{U}^{j+1} M_2 - M_1 \widehat{U}^j M_2 &= -\alpha_1^{-2} S_1 \widehat{U}^{j+1} M_2 - \alpha_2^{-2} M_1 \widehat{U}^{j+1} S_2 - \bar{b}_0 \left[ \alpha_1^{-1} \Lambda_1 \widehat{U}^{j+1} M_2 + \alpha_2^{-1} M_1 \widehat{U}^{j+1} \Lambda_2 \right] \\ &\quad + \left[ \alpha_1^{-1} (\bar{\mathbf{b}}^\top \otimes I_1) \widehat{\mathcal{A}}_1^{j+1,j+1} M_2 + \alpha_2^{-1} M_1 \widehat{\mathcal{A}}_2^{j+1,j+1} (\bar{\mathbf{b}} \otimes I_2) \right],\end{aligned}\quad (111)$$

and that of the auxiliary fields in (99) reads as

$$\begin{aligned}\widehat{\mathcal{A}}_1^{j+1,j+1} &= (\mathcal{G}_K \otimes I_1) \left[ \frac{1}{\rho} \mathbf{1}_K \otimes (\Lambda_1 \widehat{U}^{j+1}) + \widehat{\mathcal{A}}_1^{j,j+1} \right] = \left[ \frac{1}{\rho} (\mathcal{G}_K \mathbf{1}_K) \otimes (\Lambda_1 \widehat{U}^{j+1}) + (\mathcal{G}_K \otimes I_1) \widehat{\mathcal{A}}_1^{j,j+1} \right], \\ \widehat{\mathcal{A}}_2^{j+1,j+1} &= \left[ \frac{1}{\rho} \mathbf{1}_K^\top \otimes (\widehat{U}^{j+1} \Lambda_2) + \widehat{\mathcal{A}}_2^{j+1,j} \right] (\mathcal{G}_K \otimes I_2) = \left[ \frac{1}{\rho} (\mathcal{G}_K \mathbf{1}_K)^\top \otimes (\widehat{U}^{j+1} \Lambda_2) + \widehat{\mathcal{A}}_2^{j+1,j} (\mathcal{G}_K \otimes I_2) \right].\end{aligned}\quad (112)$$

Plugging-in the updates for the auxiliary fields from (112) in the discrete system (111) to obtain

$$\begin{aligned}M_1 \widehat{U}^{j+1} M_2 + \alpha_1^{-2} S_1 \widehat{U}^{j+1} M_2 + \alpha_2^{-2} M_1 \widehat{U}^{j+1} S_2 + \bar{b}_0 \left[ \alpha_1^{-1} \Lambda_1 \widehat{U}^{j+1} M_2 + \alpha_2^{-1} M_1 \widehat{U}^{j+1} \Lambda_2 \right] \\ = M_1 \widehat{U}^j M_2 + \alpha_1^{-1} \left[ \left( \frac{1}{\rho} \mathbf{b}^\top \mathcal{G}_K \mathbf{1}_K \otimes \Lambda_1 \widehat{U}^{j+1} \right) M_2 + (\mathbf{b}^\top \mathcal{G}_K \otimes I_1) \widehat{\mathcal{A}}_1^{j,j+1} M_2 \right] \\ + \alpha_2^{-1} \left[ M_1 \left( \frac{1}{\rho} (\mathcal{G}_K \mathbf{1}_K)^\top \mathbf{b} \otimes (\widehat{U}^{j+1} \Lambda_2) \right) + M_1 \widehat{\mathcal{A}}_2^{j+1,j} (\mathcal{G}_K \mathbf{b} \otimes I_2) \right].\end{aligned}\quad (113)$$

Introducing  $\varpi^{(1/2)}$  as defined in (68) and collecting the terms containing  $\widehat{U}^{j+1}$ , the resulting discrete system becomes

$$M_1 \widehat{U}^{j+1} M_2 + \alpha_1^{-2} S_1 \widehat{U}^{j+1} M_2 + \alpha_2^{-2} M_1 \widehat{U}^{j+1} S_2 + \varpi^{(1/2)} \left[ \alpha_1^{-1} \Lambda_1 \widehat{U}^{j+1} M_2 + \alpha_2^{-1} M_1 \widehat{U}^{j+1} \Lambda_2 \right] = M_1 \widehat{U}^j M_2 + \mathcal{B}^{j+1}, \quad (114)$$

where the history term is given by

$$\mathcal{B}^{j+1} = \alpha_1^{-1} (\mathbf{b}^\top \mathcal{G}_K \otimes I_1) \widehat{\mathcal{A}}_1^{j,j+1} M_2 + \alpha_2^{-1} M_1 \widehat{\mathcal{A}}_2^{j+1,j} (\mathcal{G}_K \mathbf{b} \otimes I_2). \quad (115)$$

**Remark 4.** As noted in Remark 2, only the non-zero entries of  $\widehat{\mathcal{A}}_1$  and  $\widehat{\mathcal{A}}_2$  are relevant for the numerical implementation so that we may rewrite the history terms defined above for each of the boundary segments separately as follows:

$$\widehat{\mathcal{B}}_{a_1}^{j+1} = \sum_{k=1}^K \Gamma_k^{(1/2)} \widehat{\varphi}_{k,a_1}^{j,j+1}, \quad \widehat{\mathcal{B}}_{a_2}^{j+1} = \sum_{k=1}^K \Gamma_k^{(1/2)} \widehat{\varphi}_{k,a_2}^{j+1,j},$$

where the auxiliary fields are as defined in (100). It is straightforward to verify that the history term,  $\mathcal{B}^{j+1}$ , can now be efficiently computed as

$$\mathcal{B}^{j+1} = \frac{1}{\alpha_1} \mathbf{e}_0^{(1)} \otimes \left[ \widehat{\mathcal{B}}_l^{j+1} \right]^\top M_2 + \frac{1}{\alpha_1} \mathbf{e}_1^{(1)} \otimes \left[ \widehat{\mathcal{B}}_r^{j+1} \right]^\top M_2 + \frac{1}{\alpha_2} \left[ M_1 \widehat{\mathcal{B}}_b^{j+1} \right] \otimes (\mathbf{e}_0^{(2)})^\top + \frac{1}{\alpha_2} \left[ M_1 \widehat{\mathcal{B}}_t^{j+1} \right] \otimes (\mathbf{e}_1^{(2)})^\top.$$

where  $\mathbf{e}_0^{(p)} = (\delta_{k,0})_{k \in \mathbb{J}_p}$  and  $\mathbf{e}_1^{(p)} = (\delta_{k,1})_{k \in \mathbb{J}_p}$  for  $p = 1, 2$  are the orthogonal unit vectors in  $\mathbb{R}^{N_p+1}$ .

The computation of the history term above requires the off-diagonal samples  $\widehat{\mathcal{A}}_1^{j,j+1}$  and  $\widehat{\mathcal{A}}_2^{j+1,j}$  which can be obtained by advancing the corresponding IVPs satisfied by these auxiliary fields. The BDF1-based discretization of the dynamical system in (110) reads as

$$\begin{aligned}(M_1 + \alpha_1^{-2} S_1) \widehat{\mathcal{A}}_2^{j+1,j} &= M_1 \widehat{\mathcal{A}}_2^{j,j} - \alpha_1^{-1} \left[ b_0 \Lambda_1 \widehat{\mathcal{A}}_2^{j+1,j} - (\mathbf{b}^\top \otimes I_1) \widehat{\mathcal{C}}^{j+1,j} \right], \\ \widehat{\mathcal{A}}_1^{j,j+1} (M_2 + \alpha_2^{-2} S_2) &= \widehat{\mathcal{A}}_1^{j,j+1} M_2 - \alpha_2^{-1} \left[ b_0 \widehat{\mathcal{A}}_1^{j,j+1} \Lambda_2 - \widehat{\mathcal{C}}^{j,j+1} (\mathbf{b} \otimes I_2) \right],\end{aligned}\quad (116)$$

and that of the auxiliary fields in (109) work out to be

$$\begin{aligned}\widehat{\mathcal{C}}^{j+1,j} &= (\mathcal{G}_K \otimes I_1) \left[ \frac{1}{\rho} \mathbf{1}_K \otimes (\Lambda_1 \widehat{\mathcal{A}}_2^{j+1,j}) + \widehat{\mathcal{C}}^{j,j} \right] = \left[ \frac{1}{\rho} (\mathcal{G}_K \mathbf{1}_K) \otimes (\Lambda_1 \widehat{\mathcal{A}}_2^{j+1,j}) + (\mathcal{G}_K \otimes I_1) \widehat{\mathcal{C}}^{j,j} \right], \\ \widehat{\mathcal{C}}^{j,j+1} &= \left[ \frac{1}{\rho} \mathbf{1}_K^\top \otimes (\widehat{\mathcal{A}}_1^{j,j+1} \Lambda_2) + \widehat{\mathcal{C}}^{j,j} \right] (\mathcal{G}_K \otimes I_2) = \left[ \frac{1}{\rho} (\mathcal{G}_K \mathbf{1}_K)^\top \otimes (\widehat{\mathcal{A}}_1^{j,j+1} \Lambda_2) + \widehat{\mathcal{C}}^{j,j} (\mathcal{G}_K \otimes I_2) \right].\end{aligned}\quad (117)$$

Plugging-in these updates in the discrete system (116) and collecting the latest time-step of the field yields

$$\begin{aligned}\Gamma_{a_2} : \quad & (M_1 + \alpha_1^{-2} S_1 + \alpha_1^{-1} \varpi^{(1/2)} \Lambda_1) \widehat{\mathcal{A}}_2^{j+1,j} = M_1 \widehat{\mathcal{A}}_2^{j,j} - \alpha_1^{-1} (\mathbf{b}^\top \mathcal{G}_K \otimes I_1) \widehat{\mathcal{C}}^{j,j}, \\ \Gamma_{a_1} : \quad & \widehat{\mathcal{A}}_1^{j,j+1} (M_2 + \alpha_2^{-2} S_2 + \alpha_2^{-1} \varpi^{(1/2)} \Lambda_2) = \widehat{\mathcal{A}}_1^{j,j} M_2 - \alpha_2^{-1} \widehat{\mathcal{C}}^{j,j} (\mathcal{G}_K \mathbf{b} \otimes I_2).\end{aligned}\quad (118)$$



The computation of the history sums require diagonal-to-diagonal update of the field  $\widehat{\mathcal{C}}^{j,j}$  which can be achieved via  $\widehat{\mathcal{C}}^{j,j} \rightarrow \widehat{\mathcal{C}}^{j,j+1} \rightarrow \widehat{\mathcal{C}}^{j+1,j+1}$ . The BDF1-based discretization of the auxiliary field in (109) provides:

$$\widehat{\mathcal{C}}^{j+1,j+1} = (\mathcal{G}_K \otimes I_1) \left[ \frac{1}{\rho} \mathbf{1}_K \otimes (\Lambda_1 \widehat{\mathcal{A}}_2^{j+1,j+1}) + \widehat{\mathcal{C}}^{j,j+1} \right] = \left[ \frac{1}{\rho} (\mathcal{G}_K \mathbf{1}_K) \otimes (\Lambda_1 \widehat{\mathcal{A}}_2^{j+1,j+1}) + (\mathcal{G}_K \otimes I_1) \widehat{\mathcal{C}}^{j,j+1} \right]. \quad (119)$$

The algorithmic steps for the solving the IBVP in (2) using NP-BDF1 method are enumerated below.

**Step 1:** Solve the dynamical system in (118) corresponding to auxiliary fields for one step, say,  $j \rightarrow (j+1)$  using the previously computed values of the auxiliary field on the segments (as described in Fig. 3).

**Step 2:** Compute the history functions on each of the boundary segments of the domain  $\Omega_i$  as in Remark 4 to obtain

$$\mathcal{B}^{j+1} = \alpha_1^{-1} (\mathbf{b}^\top \mathcal{G}_K \otimes I_1) \widehat{\mathcal{A}}_1^{j,j+1} M_2 + \alpha_2^{-1} M_1 \widehat{\mathcal{A}}_2^{j+1,j} (\mathcal{G}_K \mathbf{b} \otimes I_2).$$

**Step 3:** Solve the discrete linear system in (114) to compute the solution at  $(j+1)$ -th time step, i.e.,  $\widehat{U}^{j+1}$ .

**Step 4:** Update the arrays storing the values of the auxiliary fields  $\widehat{\mathcal{A}}_1$  and  $\widehat{\mathcal{A}}_2$  with the  $(j+1)$ -th time step values using (112). The auxiliary field  $\widehat{\mathcal{C}}$  at the corners is updated using (119).

### 5.2.2. NP-TR

The discrete numerical scheme for the dynamical system defined in (102) and (110) is labelled as ‘NP-TR’ if the underlying time-stepping method is TR.

Recalling  $\rho = 2/(\Delta t)$ , the TR-based discretization of the dynamical system in (102) reads as

$$M_1 \widehat{U}^{j+1/2} M_2 - M_1 \widehat{U}^j M_2 = -\alpha_1^{-2} S_1 \widehat{U}^{j+1/2} M_2 - \alpha_2^{-2} M_1 \widehat{U}^{j+1/2} S_2 - \bar{b}_0 \left[ \alpha_1^{-1} \Lambda_1 \widehat{U}^{j+1/2} M_2 + \alpha_2^{-1} M_1 \widehat{U}^{j+1/2} \Lambda_2 \right] + \left[ \alpha_1^{-1} (\bar{\mathbf{b}}^\top \otimes I_1) \widehat{\mathcal{A}}_1^{j+1/2,j+1/2} M_2 + \alpha_2^{-1} M_1 \widehat{\mathcal{A}}_2^{j+1/2,j+1/2} (\bar{\mathbf{b}} \otimes I_2) \right], \quad (120)$$

and that of the auxiliary fields in (99) reads as

$$\begin{aligned} \widehat{\mathcal{A}}_1^{j+1/2,j+1/2} &= \frac{1}{2} \left[ (\mathcal{H}_K \otimes I_1) \widehat{\mathcal{A}}_1^{j,j+1} + \widehat{\mathcal{A}}_1^{j,j} \right] + (\mathcal{G}_K \otimes I_1) \left[ \frac{1}{\rho} \mathbf{1}_K \otimes \left( \Lambda_1 \widehat{U}^{j+1/2} + \frac{\widehat{\Phi}_1^{j,j+1} - \widehat{\Phi}_1^{j,j}}{2} \right) \right], \\ \widehat{\mathcal{A}}_2^{j+1/2,j+1/2} &= \frac{1}{2} \left[ \widehat{\mathcal{A}}_2^{j+1,j} (\mathcal{H}_K \otimes I_2) + \widehat{\mathcal{A}}_2^{j,j} \right] + \left[ \frac{1}{\rho} \mathbf{1}_K^\top \otimes \left( \widehat{U}^{j+1/2} \Lambda_2 + \frac{\widehat{\Phi}_2^{j+1,j} - \widehat{\Phi}_2^{j,j}}{2} \right) \right] (\mathcal{G}_K \otimes I_2). \end{aligned} \quad (121)$$

Plugging-in the updates for the auxiliary fields from (121) in the discrete system (120) and simplifying, yields

$$\begin{aligned} M_1 \widehat{U}^{j+1/2} M_2 + \alpha_1^{-2} S_1 \widehat{U}^{j+1/2} M_2 + \alpha_2^{-2} M_1 \widehat{U}^{j+1/2} S_2 + \varpi^{(1/2)} \left[ \alpha_1^{-1} \Lambda_1 \widehat{U}^{j+1/2} M_2 + \alpha_2^{-1} M_1 \widehat{U}^{j+1/2} \Lambda_2 \right] \\ = M_1 \widehat{U}^j M_2 + \mathcal{B}_{a_1}^{j+1/2} + \mathcal{B}_{a_2}^{j+1/2}, \end{aligned} \quad (122)$$

where the history terms are given by

$$\begin{aligned} \mathcal{B}_{a_1}^{j+1/2} &= \alpha_1^{-1} \frac{1}{\rho} (\mathbf{b}^\top \mathcal{G}_K \mathbf{1}_K) \left( \frac{\widehat{\Phi}_1^{j+1,j} - \widehat{\Phi}_1^{j,j}}{2} \right) M_2 + \frac{1}{2} \alpha_1^{-1} \left[ (\mathbf{b}^\top \mathcal{H}_K \otimes I_1) \widehat{\mathcal{A}}_1^{j,j+1} + (\mathbf{b}^\top \otimes I_1) \widehat{\mathcal{A}}_1^{j,j} \right] M_2, \\ \mathcal{B}_{a_2}^{j+1/2} &= \alpha_2^{-1} \frac{1}{\rho} (\mathbf{b}^\top \mathcal{G}_K \mathbf{1}_K) M_1 \left( \frac{\widehat{\Phi}_2^{j+1,j} - \widehat{\Phi}_2^{j,j}}{2} \right) + \frac{1}{2} \alpha_2^{-1} M_1 \left[ \widehat{\mathcal{A}}_2^{j+1,j} (\mathcal{H}_K \mathbf{b} \otimes I_2) + \widehat{\mathcal{A}}_2^{j,j} (\mathbf{b} \otimes I_2) \right]. \end{aligned} \quad (123)$$

The simplifications noted in Remark 4 can also be applied here for the history terms. We omit the details because the adaption is straightforward. The computation of the history terms require diagonal-to-diagonal update of fields  $\widehat{\mathcal{A}}_1^{j,j}$  and  $\widehat{\mathcal{A}}_2^{j,j}$  which can be obtained by TR-based discretization of (99) as follows:

$$\begin{aligned} \widehat{\mathcal{A}}_1^{j+1,j+1} &= (\mathcal{H}_K \otimes I_1) \widehat{\mathcal{A}}_1^{j,j+1} + \left[ \frac{2}{\rho} (\mathcal{G}_K \mathbf{1}_K) \otimes \left( \Lambda_1 \widehat{U}^{j+1/2} + \frac{\widehat{\Phi}_1^{j,j+1} - \widehat{\Phi}_1^{j,j}}{2} \right) \right], \\ \widehat{\mathcal{A}}_2^{j+1,j+1} &= \widehat{\mathcal{A}}_2^{j+1,j} (\mathcal{H}_K \otimes I_2) + \left[ \frac{2}{\rho} (\mathcal{G}_K \mathbf{1}_K)^\top \otimes \left( \widehat{U}^{j+1/2} \Lambda_2 + \frac{\widehat{\Phi}_2^{j+1,j} - \widehat{\Phi}_2^{j,j}}{2} \right) \right]. \end{aligned} \quad (124)$$

Moreover, the updates above require off-diagonal samples of the auxiliary fields which can be obtained by solving the dynamical system in (110). The TR-based discretization of this system reads as

$$\begin{aligned} (M_1 + \alpha_1^{-2} S_1) \widehat{\mathcal{A}}_2^{j+1/2,j} &= M_1 \widehat{\mathcal{A}}_2^{j,j} - \alpha_1^{-1} [b_0 \Lambda_1 \widehat{\mathcal{A}}_2^{j+1/2,j} - (\mathbf{b}^\top \otimes I_1) \widehat{C}^{j+1/2,j}], \\ \widehat{\mathcal{A}}_1^{j,j+1/2} (M_2 + \alpha_2^{-2} S_2) &= \widehat{\mathcal{A}}_1^{j,j} M_2 - \alpha_2^{-1} [b_0 \widehat{\mathcal{A}}_1^{j,j+1/2} \Lambda_2 - \widehat{C}^{j,j+1/2} (\mathbf{b} \otimes I_2)], \end{aligned} \quad (125)$$

and that of the auxiliary field in (109) work out to be

$$\begin{aligned} \widehat{C}^{j+1/2,j} &= \left[ \frac{1}{\rho} (\mathcal{G}_K \mathbf{1}_K) \otimes (\Lambda_1 \widehat{\mathcal{A}}_2^{j+1/2,j}) + (\mathcal{H}_K \otimes I_1) \widehat{C}^{j,j} \right], \\ \widehat{C}^{j,j+1/2} &= \left[ \frac{1}{\rho} (\mathcal{G}_K \mathbf{1}_K)^\top \otimes (\widehat{\mathcal{A}}_1^{j,j+1/2} \Lambda_2) + \widehat{C}^{j,j} (\mathcal{H}_K \otimes I_2) \right]. \end{aligned} \quad (126)$$

Plugging-in these updates in the discrete system (125) and collecting the latest time-step of the field yields

$$\begin{aligned} \Gamma_{a_2} : \quad & (M_1 + \alpha_1^{-2} S_1 + \alpha_1^{-1} \varpi^{(1/2)} \Lambda_1) \widehat{\mathcal{A}}_2^{j+1/2,j} = M_1 \widehat{\mathcal{A}}_2^{j,j} + \alpha_1^{-1} (\mathbf{b}^\top \mathcal{H}_K \otimes I_1) \widehat{C}^{j,j}, \\ \Gamma_{a_1} : \quad & \widehat{\mathcal{A}}_1^{j,j+1/2} (M_2 + \alpha_2^{-2} S_2 + \alpha_2^{-1} \varpi^{(1/2)} \Lambda_2) = \widehat{\mathcal{A}}_1^{j,j} M_2 + \alpha_2^{-1} \widehat{C}^{j,j} (\mathcal{H}_K \mathbf{b} \otimes I_2). \end{aligned} \quad (127)$$

The computation of the history terms above will require diagonal-to-diagonal update of auxiliary field  $\widehat{C}^{j,j}$  which can be achieved via  $\widehat{C}^{j,j} \rightarrow \widehat{C}^{j,j+1} \rightarrow \widehat{C}^{j+1,j+1}$ . The TR-based discretization of the systems (109) leads to

$$\begin{aligned} \widehat{C}^{j,j+1} &= \left[ \frac{2}{\rho} (\mathcal{G}_K \mathbf{1}_K)^\top \otimes (\widehat{\mathcal{A}}_1^{j,j+1/2} \Lambda_2) + \widehat{C}^{j,j} (\mathcal{H}_K \otimes I_2) \right], \\ \widehat{C}^{j+1,j+1} &= \left[ \frac{2}{\rho} (\mathcal{G}_K \mathbf{1}_K) \otimes \frac{1}{2} (\Lambda_1 \widehat{\mathcal{A}}_2^{j+1,j+1} + \Lambda_1 \widehat{\mathcal{A}}_2^{j,j+1}) + (\mathcal{H}_K \otimes I_1) \widehat{C}^{j,j+1} \right]. \end{aligned} \quad (128)$$

The computation of history terms  $\mathcal{B}_{a_1}^{j+1/2}$  and  $\mathcal{B}_{a_2}^{j+1/2}$  also require the off-diagonal samples  $\widehat{\Phi}_1^{j,j+1}$  and  $\widehat{\Phi}_2^{j+1,j}$  which can be obtained by solving the dynamical system in (90). The TR-based discretization of this system reads as

$$\begin{aligned} (M_1 + \alpha_1^{-2} S_1) \widehat{\Phi}_2^{j+1/2,j} &= M_1 \widehat{\Phi}_2^{j,j} - \alpha_1^{-1} [b_0 \Lambda_1 \widehat{\Phi}_2^{j+1/2,j} - (\mathbf{b}^\top \otimes I_1) \widehat{\mathcal{A}}_1^{j+1/2,j} \Lambda_2], \\ \widehat{\Phi}_1^{j,j+1/2} (M_2 + \alpha_2^{-2} S_2) &= \widehat{\Phi}_1^{j,j} M_2 - \alpha_2^{-1} [b_0 \widehat{\Phi}_1^{j,j+1/2} \Lambda_2 - \Lambda_1 \widehat{\mathcal{A}}_2^{j,j+1/2} (\mathbf{b} \otimes I_2)], \end{aligned} \quad (129)$$

and that of the auxiliary fields in (99) reads as

$$\begin{aligned} \widehat{\mathcal{A}}_1^{j+1/2,j} &= \left[ \frac{1}{\rho} (\mathcal{G}_K \mathbf{1}_K) \otimes (\Lambda_1 \widehat{\Phi}_2^{j+1/2,j}) + (\mathcal{G}_K \otimes I_1) \widehat{\mathcal{A}}_1^{j,j} \right], \\ \widehat{\mathcal{A}}_2^{j,j+1/2} &= \left[ \frac{1}{\rho} (\mathcal{G}_K \mathbf{1}_K)^\top \otimes (\widehat{\Phi}_1^{j,j+1/2} \Lambda_2) + \widehat{\mathcal{A}}_2^{j,j} (\mathcal{G}_K \otimes I_2) \right]. \end{aligned} \quad (130)$$

Plugging-in these updates in the discrete system (129) and collecting the latest time-step of the field yields

$$\begin{aligned} \Gamma_{a_2} : \quad & (M_1 + \alpha_1^{-2} S_1 + \alpha_1^{-1} \varpi^{(1/2)} \Lambda_1) \widehat{\Phi}_2^{j+1/2,j} = M_1 \widehat{\Phi}_2^{j,j} + \alpha_1^{-1} (\mathbf{b}^\top \mathcal{G}_K \otimes I_1) \widehat{\mathcal{A}}_1^{j,j} \Lambda_2, \\ \Gamma_{a_1} : \quad & \widehat{\Phi}_1^{j,j+1/2} (M_2 + \alpha_2^{-2} S_2 + \alpha_2^{-1} \varpi^{(1/2)} \Lambda_2) = \widehat{\Phi}_1^{j,j} M_2 + \alpha_2^{-1} \Lambda_1 \widehat{\mathcal{A}}_2^{j,j} (\mathcal{G}_K \mathbf{b} \otimes I_2). \end{aligned} \quad (131)$$

The algorithmic steps for the solving the IBVP in (2) using NP-TR method are enumerated below.

**Step 1:** Solve the dynamical system in (127) and (131) corresponding to auxiliary fields for one step, say,  $j \rightarrow (j+1)$  using the previously computed values of the auxiliary field on the segments (as described in Fig. 3).

**Step 2:** Compute the history functions on each of the boundary segments of the domain  $\Omega_i$  to obtain

$$\begin{aligned} \mathcal{B}_{a_1}^{j+1/2} &= \alpha_1^{-1} \frac{1}{\rho} (\mathbf{b}^\top \mathcal{G}_K \mathbf{1}_K) \left( \frac{\widehat{\Phi}_1^{j+1,j} - \widehat{\Phi}_1^{j,j}}{2} \right) M_2 + \frac{1}{2} \alpha_1^{-1} [(\mathbf{b}^\top \mathcal{H}_K \otimes I_1) \widehat{\mathcal{A}}_1^{j,j+1} + (\mathbf{b}^\top \otimes I_1) \widehat{\mathcal{A}}_1^{j,j}] M_2, \\ \mathcal{B}_{a_2}^{j+1/2} &= \alpha_2^{-1} \frac{1}{\rho} (\mathbf{b}^\top \mathcal{G}_K \mathbf{1}_K) M_1 \left( \frac{\widehat{\Phi}_2^{j+1,j} - \widehat{\Phi}_2^{j,j}}{2} \right) + \frac{1}{2} \alpha_2^{-1} M_1 [\widehat{\mathcal{A}}_2^{j+1,j} (\mathcal{H}_K \mathbf{b} \otimes I_2) + \widehat{\mathcal{A}}_2^{j,j} (\mathbf{b} \otimes I_2)]. \end{aligned}$$

**Step 3:** Solve the discrete linear system in (122) to compute the solution at  $(j + 1)$ -th time step, i.e.,  $\widehat{U}^{j+1/2}$ .

**Step 4:** Update the arrays storing the values of the auxiliary fields  $\widehat{\mathcal{A}}_1$  and  $\widehat{\mathcal{A}}_2$  with the  $(j + 1)$ -th time step values using (124). The auxiliary field  $\widehat{C}$  at the corners is updated using (128).

## 6. Numerical Experiments

In this section, we will present several numerical tests to analyze the accuracy of the numerical schemes developed in this work to solve the IBVP (2). These numerical tests consist of analyzing the error evolution behaviour and empirical convergence of the considered IBVP. In order to visualize the reflections in the numerical solution, we also present some contour plots at different instants of time.

### 6.1. Exact solutions

The exact solutions admissible for our numerical experiments are such that the initial profile must be effectively supported within the computational domain. We primarily consider the wavepackets which are a modulation of a Gaussian envelop so that the requirement of effective initial support can be easily met. In this class of solutions, we consider the Chirped-Gaussian and the Hermite-Gaussian profiles.

Table 1: Chirped-Gaussian profile with  $A_0 = 2$  and  $c_0 \in \{4, 8, 12, 16\}$ .

$G(\mathbf{x}, t) = A_0 \sum_{j=1}^n G(\mathbf{x}, t; \mathbf{a}_j, \mathbf{b}_j, \mathbf{c}_j), \quad \mathbf{c}_j = c_0(\cos \theta_j, \sin \theta_j)$				
Type	$n$	$(\mathbf{a}_j \in \mathbb{R}^2)_{j=1}^n$	$(\mathbf{b}_j \in \mathbb{R}^2)_{j=1}^n$	$\boldsymbol{\theta} \in \mathbb{R}^n$
IIA, IIB	4	$\mathbf{a}_1 = (1/2.5, 1/2.4),$ $\mathbf{a}_2 = (1/2.3, 1/2.2),$ $\mathbf{a}_3 = (1/2.7, 1/2.6),$ $\mathbf{a}_4 = (1/2.2, 1/2.5)$	$\mathbf{b}_j = (1/2)\mathbf{1}$	IIA: $\boldsymbol{\theta}_A = (0, \pi/2, \pi, 3\pi/2),$ IIB: $\boldsymbol{\theta}_B = \boldsymbol{\theta}_A + (\pi/4)\mathbf{1}$

#### 6.1.1. Chirped-Gaussian profile

Using the function defined by

$$\mathcal{G}(x, t; a, b) = \frac{1}{\sqrt{1 + 4i(a + ib)t}} \exp\left[-\frac{(a + ib)}{1 + 4i(a + ib)t}x^2\right], \quad a > 0, \quad (132)$$

one can define the family solutions referred to as chirped-Gaussian profile by

$$G(\mathbf{x}, t; \mathbf{a}, \mathbf{b}, \mathbf{c}) = \mathcal{G}(x_1 - c_1 t, t; a_1, b_1) \mathcal{G}(x_2 - c_2 t, t; a_2, b_2) \exp\left(+i\frac{1}{2}\mathbf{c} \cdot \mathbf{x} - i\frac{1}{4}\mathbf{c} \cdot \mathbf{c} t\right), \quad (133)$$

where  $\mathbf{a} \in \mathbb{R}_+^2$  determines the effective support of the profile at  $t = 0$ ,  $\mathbf{b} \in \mathbb{R}^2$  is the *chirp* parameter and  $\mathbf{c} \in \mathbb{R}^2$  is the velocity of the profile. Using linear combination, one can further define a more general family of solutions with parameters  $A_0, c_0 \in \mathbb{R}$ ,  $\boldsymbol{\theta} \in \mathbb{R}^n$ ,  $(\mathbf{a}_j \in \mathbb{R}_+^2)_{j=1}^n$  and  $(\mathbf{b}_j \in \mathbb{R}^2)_{j=1}^n$  given by

$$G(\mathbf{x}, t; c_0, A_0; (\mathbf{a}_j)_{j=1}^n, (\mathbf{b}_j)_{j=1}^n, \boldsymbol{\theta}) = A_0 \sum_{j=1}^n G(\mathbf{x}, t; \mathbf{a}_j, \mathbf{b}_j, \mathbf{c}_j), \quad \mathbf{c}_j = c_0(\cos \theta_j, \sin \theta_j). \quad (134)$$

Let the constant vector  $(1, 1, \dots) \in \mathbb{R}^n$  be denoted by  $\mathbf{1}$ , then the specific values of the parameters of the solutions used in the numerical experiments can be summarized as in Table 1. The energy content of the profile within the computational domain  $\Omega_i$  over time is

$$E_{\Omega_i}(t) = \int_{\Omega_i} |G(\mathbf{x}, t)|^2 d^2 \mathbf{x} \Big/ \int_{\Omega_i} |G(\mathbf{x}, 0)|^2 d^2 \mathbf{x}, \quad t \geq 0. \quad (135)$$

The profiles are chosen with non-zero speed  $c_0$  so that the field hits the boundary of  $\Omega_i$ . In case of a square computational domain, the type ‘A’ class of solutions are directed to the segments of the boundary normally while type ‘B’ class of solutions are directed to the corners. The behavior of the  $E_{\Omega_i}(t)$  for  $t \in [0, 5]$  is shown in Fig. 4.

Table 2: Hermite-Gaussian profile with $A_0 = 2$ and $c_0 \in \{4, 8, 12, 16\}$ .				
$G(\mathbf{x}, t) = A_0 \sum_{j=1}^n G(\mathbf{x}, t; \mathbf{m}_j, \mathbf{a}_j, \mathbf{c}_j), \quad \mathbf{c}_j = c_0(\cos \theta_j, \sin \theta_j)$				
Type	$n$	$(\mathbf{a}_j \in \mathbb{R}^2)_{j=1}^n$	$(\mathbf{m}_j \in \mathbb{N}_0^2)_{j=1}^n$	$\boldsymbol{\theta} \in \mathbb{R}^n$
IIA, IIB	4	$\mathbf{a}_1 = (1/2.5, 1/2.4),$ $\mathbf{a}_2 = (1/2.3, 1/2.2),$ $\mathbf{a}_3 = (1/2.7, 1/2.6),$ $\mathbf{a}_4 = (1/2.2, 1/2.5)$	$\mathbf{m}_1 = (1, 2),$ $\mathbf{m}_2 = (2, 1),$ $\mathbf{m}_3 = (2, 1),$ $\mathbf{m}_4 = (1, 2)$	$\boldsymbol{\theta}_A = (0, \pi/2, \pi, 3\pi/2),$ $\boldsymbol{\theta}_B = \boldsymbol{\theta}_A + (\pi/4)\mathbf{1}$

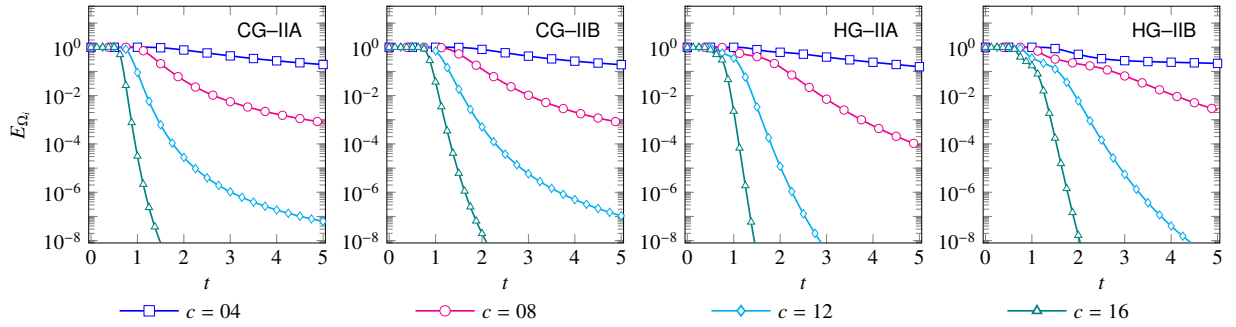


Figure 4: The figure shows the evolution of the relative energy content as defined in (135) of the chirped-Gaussian and Hermite-Gaussian profiles considered in Table 1 and Table 2. Here the computational domain is  $\Omega_i = (-10, 10)^2$ .

### 6.1.2. Hermite-Gaussian profile

Consider the class of normalized Hermite-Gaussian functions defined by

$$\mathcal{G}_m(x, t; a) = \gamma_m^{-1} H_m \left( \frac{\sqrt{2a} x}{w(t)} \right) \sqrt{\frac{\mu(t)}{a}} \exp \left[ -\mu(t) x^2 - i m \theta(t) \right], \quad m \in \mathbb{N}_0 = \{0, 1, \dots\}, \quad (136)$$

where  $a > 0$ ,

$$w(t) = \sqrt{1 + (4at)^2}, \quad \frac{1}{\mu(t)} = \frac{1}{a} + i4t = \frac{1}{a} w(t) \exp[i\theta(t)], \quad (137)$$

and the normalization factor is given by  $\gamma_m^2 = 2^m (m!) \sqrt{\pi} (2a)^{-1/2}$ . The Hermite polynomials are evaluated using the following relations

$$H_{n+1}(x) = 2xH_n(x) - 2nH_{n-1}(x), \quad H'_{n+1}(x) = 2(n+1)H_n(x), \quad (138)$$

with  $H_0(x) = 1$  and  $H_1(x) = 2x$ . Using these functions, we can define a family of solutions referred to as Hermite-Gaussian profile by

$$G(\mathbf{x}, t; \mathbf{m}, \mathbf{a}, \mathbf{c}) = \mathcal{G}_{m_1}(x_1 - c_1 t, t; a_1) \mathcal{G}_{m_2}(x_2 - c_2 t, t; a_2) \exp \left( +i \frac{1}{2} \mathbf{c} \cdot \mathbf{x} - i \frac{1}{4} \mathbf{c} \cdot \mathbf{c} t \right), \quad (139)$$

where  $\mathbf{m} \in \mathbb{N}_0^2$  is the order parameter,  $\mathbf{a} \in \mathbb{R}_+^2$  determines the effective support of the profile at  $t = 0$  and  $\mathbf{c} \in \mathbb{R}^2$  is the velocity of the profile. Once again, using linear combination, one can further define a more general family of

solutions with parameters  $A_0, c_0 \in \mathbb{R}$ ,  $\theta \in \mathbb{R}^n$ ,  $(\mathbf{m}_j \in \mathbb{N}_{0+}^2)_{j=1}^n$  and  $(\mathbf{a}_j \in \mathbb{R}_+^2)_{j=1}^n$  given by

$$G(\mathbf{x}, t; c_0, A_0; (\mathbf{m}_j)_{j=1}^n, (\mathbf{a}_j)_{j=1}^n, \theta) = A_0 \sum_{j=1}^n G(\mathbf{x}, t; \mathbf{m}_j, \mathbf{a}_j, \mathbf{c}_j), \quad \mathbf{c}_j = c_0(\cos \theta_j, \sin \theta_j). \quad (140)$$

As in the last case, we set  $\mathbf{1} = (1, 1, \dots) \in \mathbb{R}^n$ , then the specific values of the parameters of the solutions used in the numerical experiments can be summarized as in Table 2. The energy content of the profile within the computational domain  $\Omega_i$  over time is  $E_{\Omega_i}(t)$  as defined by (135) with the appropriate profile in the integrand. The profiles are chosen with non-zero speed  $c_0$  so that the field hits the boundary of  $\Omega_i$ . In case of a square computational domain, the type ‘A’ class of solutions are directed to the segments of the boundary normally while type ‘B’ class of solutions are directed to the corners. The behavior of the  $E_{\Omega_i}(t)$  for  $t \in [0, 5]$  is shown in Fig. 4.

Table 3: Numerical parameters for studying the evolution error

Computational domain ( $\Omega_i$ )	$(-10, 10) \times (-10, 10)$
Maximum time ( $T_{max}$ )	5
No. of time-steps ( $N_t$ )	5000 + 1
Time-step ( $\Delta t$ )	$10^{-3} = T_{max}/(N_t - 1)$
Number of LGL-points $((N + 1) \times (N + 1))$	$200 \times 200$

Table 4: Numerical parameters for studying the convergence error for the HF methods

Computational domain ( $\Omega_i$ )	$(-10, 10) \times (-10, 10)$
Maximum time ( $T_{max}$ )	5
Set of no. of time-steps ( $\mathbb{N}_t$ )	$\{2^8, 2^9, \dots, 2^{16}\}$
Time-step	$\{\Delta t = T_{max}/(N_t - 1), N_t \in \mathbb{N}_t\}$
Number of LGL-points $((N + 1) \times (N + 1))$	$200 \times 200$

## 6.2. Tests for evolution error

In this section, we consider the IBVP (2) where the initial condition corresponds to the exact solutions described in Sec. 6.1. In this work, we have developed two discrete versions of the DtN maps, namely, HF and NP. Each of these methods have a variant determined by the choice of time-stepping method used in the temporal discretization so that the complete list of methods to be tested can be labelled as NP-BDF1, HF-BDF1 (corresponding to the one-step method BDF1), HF-BDF2 (corresponding to the multi-step method BDF2), and, NP-TR, HF-TR (corresponding to the one-step method TR). Moreover, HF methods have two variants namely, CQ and CP, depending on the discretization scheme used for time-fractional operators. For all Padé based methods, we use diagonal Padé approximants of order 30. The numerical parameters used in this section are summarized in Table 3. The numerical solution is labelled according to that of the boundary maps. The error in the evolution of the profile computed numerically is quantified by the relative  $L^2(\Omega_i)$ -norm:

$$e(t_j) = \left( \int_{\Omega_i} |u(\mathbf{x}, t_j) - [u(\mathbf{x}, t_j)]_{\text{num}}|^2 d^2 \mathbf{x} \right)^{1/2} \left/ \left( \int_{\Omega_i} |u_0(\mathbf{x})|^2 d^2 \mathbf{x} \right)^{1/2} \right., \quad (141)$$

for  $t_j \in [0, T_{max}]$ . The integral above will be approximated by Gauss quadrature over LGL-points.

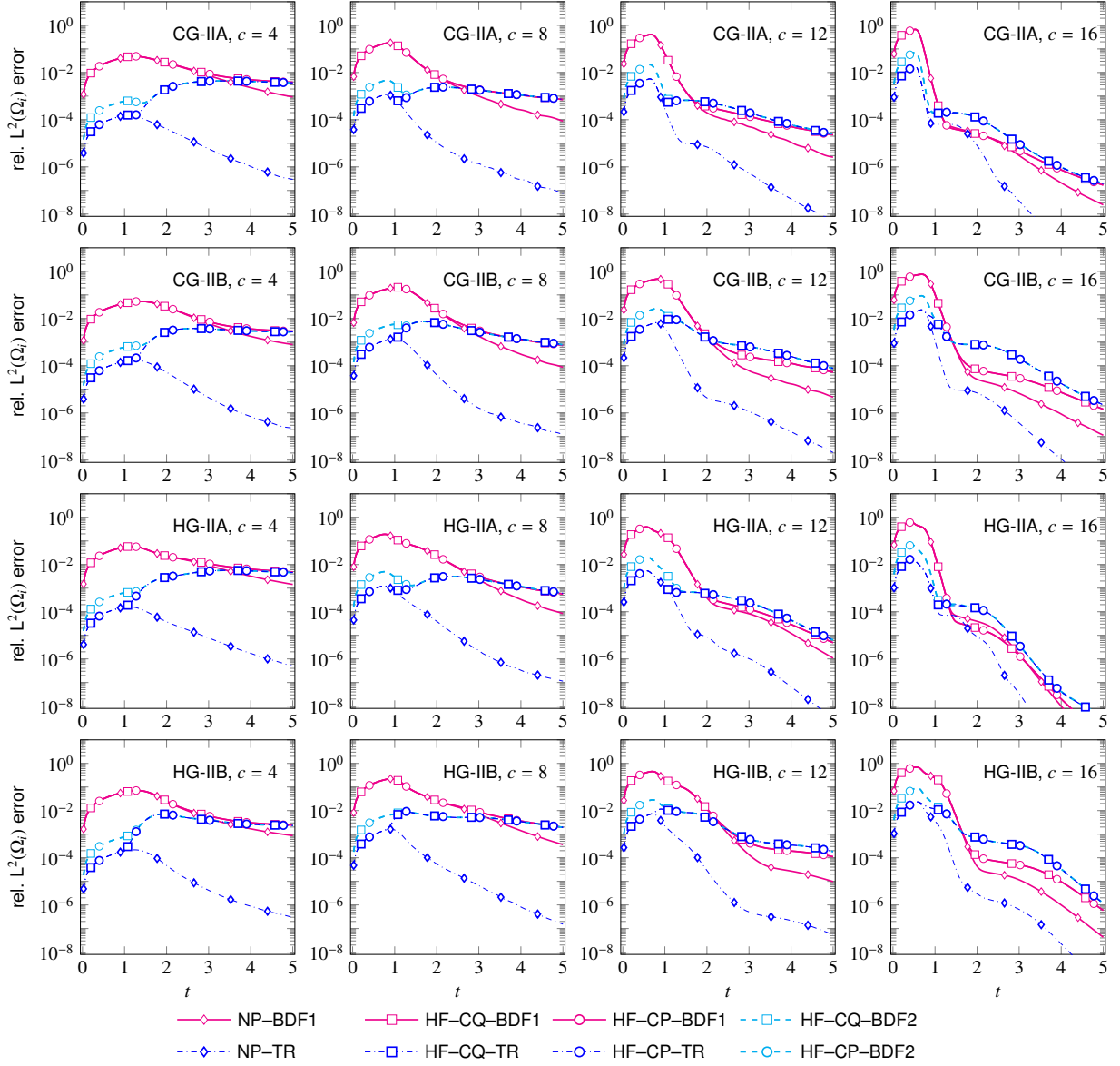


Figure 5: The figure shows a comparison of evolution of error in the numerical solution of the IBVP (2) with various approximations of the TBCs for the chirped-Gaussian and Hermite-Gaussian profiles with different values of the speed ‘c’ (see Table 1 and Table 2). The numerical parameters and the labels are described in Sec. 6.2 where the error is quantified by (141).

The numerical results for the evolution error on  $\Omega_i$  corresponding to the chirped-Gaussian and Hermite-Gaussian profiles are shown in Fig. 5. Note that the TR based methods perform better than the BDF based methods which is clear from the error peaks in Fig. 5. Let us observe that BDF1 method is incapable of distinguishing between NP and HF methods which points towards the fact that higher order method is needed to exploit the superior accuracy of NP method to that of HF. Also, for some initial time-steps, second order HF methods follow NP-TR but soon they become less accurate due to accumulation of error. Particularly for HF methods, the error behaviour improves for the case of faster moving profiles. The performance of NP-TR turns out to be best among all the methods considered in this test. There is not much significant difference in the results for evolution error on  $\Omega_i$  corresponding to the chirped-Gaussian

profile and Hermite-Gaussian profile.

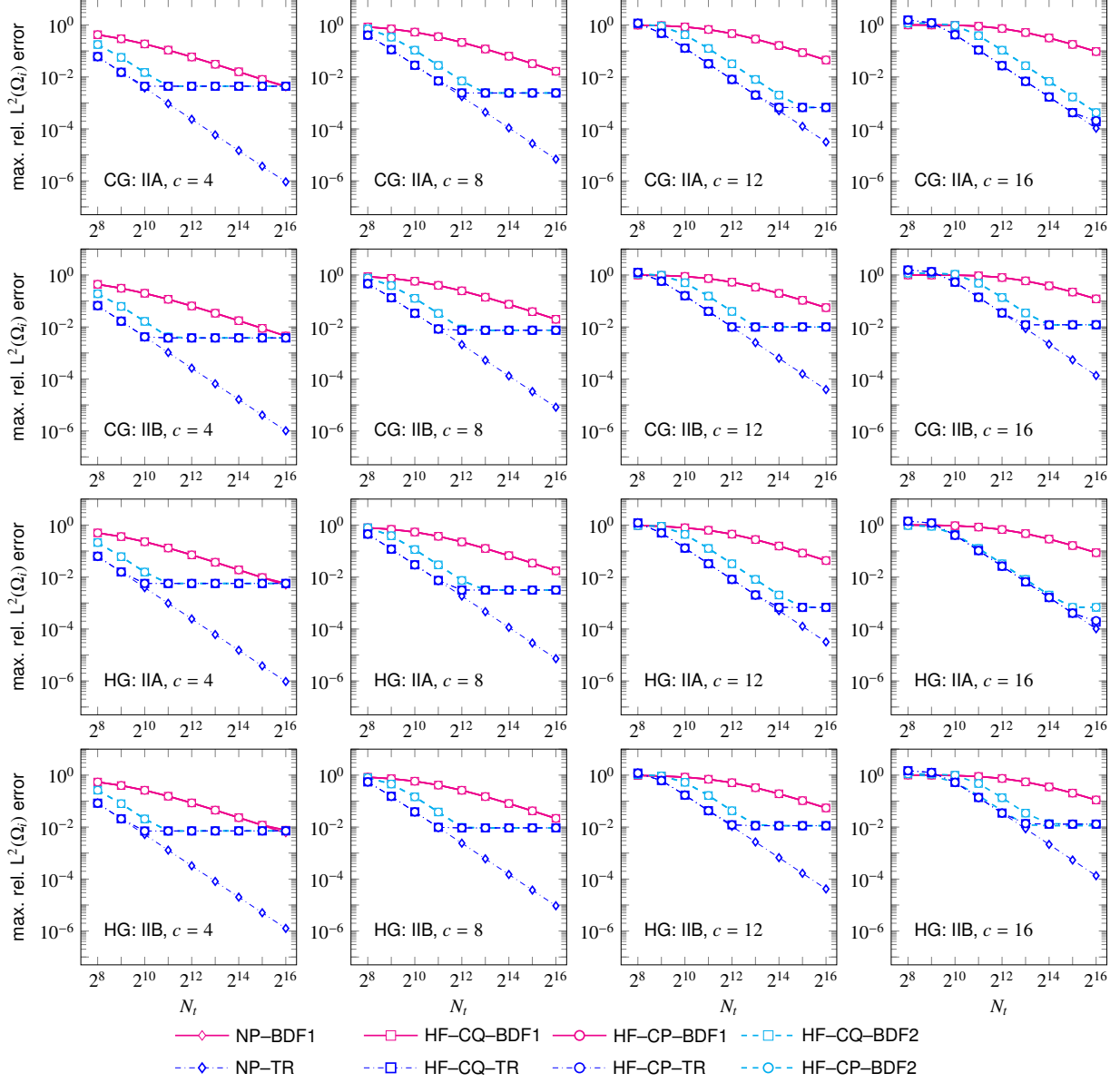


Figure 6: The figure shows a comparison of convergence behaviour in the numerical solution of the IBVP (2) with various approximations of the TBCs for the chirped-Gaussian profile and Hermite-Gaussian profile with different values of the speed 'c' (see Table 1 and Table 2). The numerical parameters and the labels are described in Sec. 6.3 where the error is quantified by (142).

The contour plots depicting  $4 \log_{10} |u(x, t)|$  and  $8 \log_{10} |u(x, t)|$  corresponding to the chirped-Gaussian and Hermite-Gaussian profiles are shown in Figs. 7 and 8, respectively. There are some visible reflections in the contour plots as expected for the maps obtained under high-frequency approximation. Moreover, TR based methods better resolve the contour levels in comparison to BDF based methods.

### 6.3. Tests for convergence

In this section, we analyze the convergence behaviour of the numerical schemes for the IBVP in (2) where the initial condition corresponds to the exact solutions described in Sec. 6.1. The error used to study the convergence behaviour is quantified by the maximum relative  $L^2(\Omega_i)$ -norm:

$$e = \max \{e(t_j) \mid j = 0, 1, \dots, N_t - 1\}, \quad (142)$$

for  $t_j \in [0, T_{max}]$ . To analyze the convergence behaviour of NP and CP-HF methods, we use diagonal Padé approximants of order 30. The Table 4 lists the numerical parameters for studying the convergence behaviour of NP and HF methods. The complete list of the methods tested for convergence is as follows: NP-BDF1, NP-TR, CQ-BDF1, CQ-BDF2, CQ-TR, CP30-BDF1, CP30-BDF2, CP-TR.

The numerical results for the convergence behaviour on  $\Omega_i$  corresponding to the chirped-Gaussian and the Hermite-Gaussian profiles are shown in Fig. 6. It can be seen that the diagonal Padé approximant based methods, namely, NP30, CP30, and CQ based methods show stable behaviour for the parameters specified in Table 4. In the log-log scale, we can clearly identify the error curve to be a straight line before it plateaus. The orders can be recovered from the slope which we found consistent with the order of the underlying time-stepping methods. The TR methods perform better than the BDF1 and BDF2 methods which is obvious from the slope of the error curves in Fig. 6. Particularly for HF-based methods, we note that the error background decreases with increase in the value of  $c$  for IIA-type profiles which are moving towards the segments of the domain while the error background remains unchanged with the increase in the value of  $c$  for IIB-type profiles which are directed towards the corners of the domain. In addition, faster moving profiles show better convergence in comparison to slow moving profiles as evident from the error curves in Fig. 6, particularly for IIA-type profiles. Our novel Padé approach based methods perform equally well for both IIA and IIB-type profiles. Finally, let us observe that there is no significant difference in the results for convergence on  $\Omega_i$  corresponding to the chirped-Gaussian profile and the Hermite-Gaussian profile.

## 7. Conclusion

In this work, we presented an efficient numerical implementation of the transparent boundary operator and its various approximations for the case of free Schrödinger equation on a rectangular computational domain which presents unique challenges on account of the presence of corners. More specifically, we addressed the spatial and temporal discretization of the IBVP obtained as a result of imposing BCs obtained under high-frequency approximation of the TBCs along with suitable corner conditions. The recipe was then extended to the IBVP obtained as a result of imposing the TBCs.

In quite a standard fashion, the use of convolution quadrature scheme for the fractional operators yields a numerical algorithm which scales in complexity (in terms of number of operations as well as memory storage) with the time-steps. In contrast, the use of Padé approximant based rational approximation (in a manner which treated the corners of the boundary adequately) yields algorithms that do not scale in complexity with the number of time-steps. The performance of these algorithms were demonstrated using time-stepping methods upto second order of convergence. We were able to empirically confirm the stability and convergence behavior of the proposed algorithms. Further, the approach developed in this work makes the system amenable to higher-order time-stepping methods in the class of linear one-step and multi-step methods<sup>3</sup>. Let us emphasize that for the first time, we are able to carry out a comparison of the high-frequency approximation of the transparent operator with the exact form confirming the nature of underlying approximations. We believe that these insights would be useful in understanding the behavior of the high-frequency approximations for more general systems for which exact TBC is not available. We note that, within the pseudo-differential approach, corners in the boundary of the computational domain can be adequately treated only under the high-frequency approximation [8]; therefore, we hope that the approach developed in this work would be relevant for the case of general Schrödinger equation.

Finally, let us observe that there are several open problems that have not been addressed in this work. For instance, the well-posedness of the IBVP under the nonreflecting BCs and its various approximations on the rectangular domain

<sup>3</sup>It remains to be explored if one can also employ the exponential integrators [17–19] which allow for larger step-sizes for the time-stepping scheme.



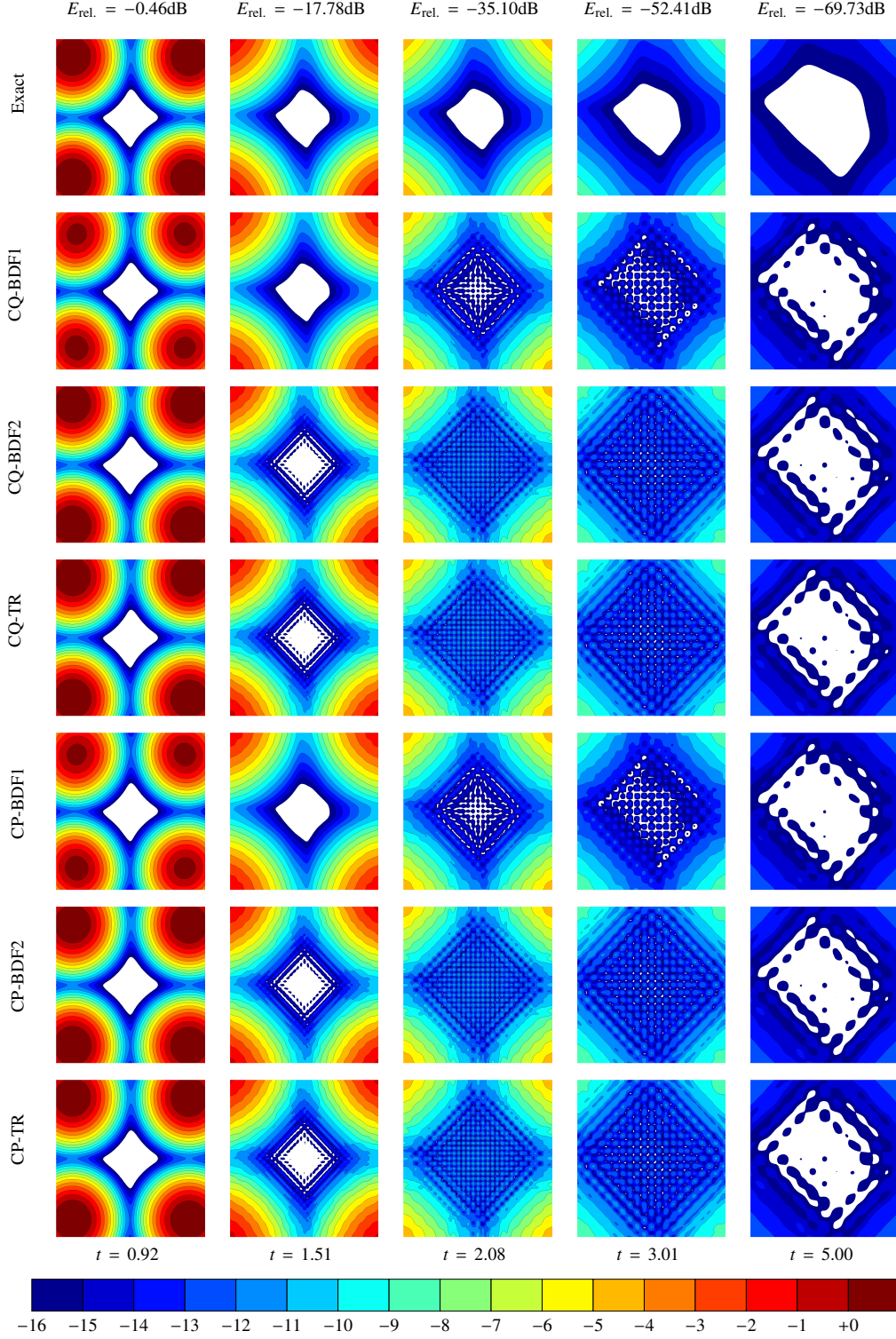


Figure 7: The figure shows contour plots of  $4 \log_{10} |u(x, t)|$  with various TBCs for the IIB-type chirped-Gaussian profile (see Table 1) for  $c = 12$  at different instants of time. The numerical parameters and the labels are described in Sec. 6.2.

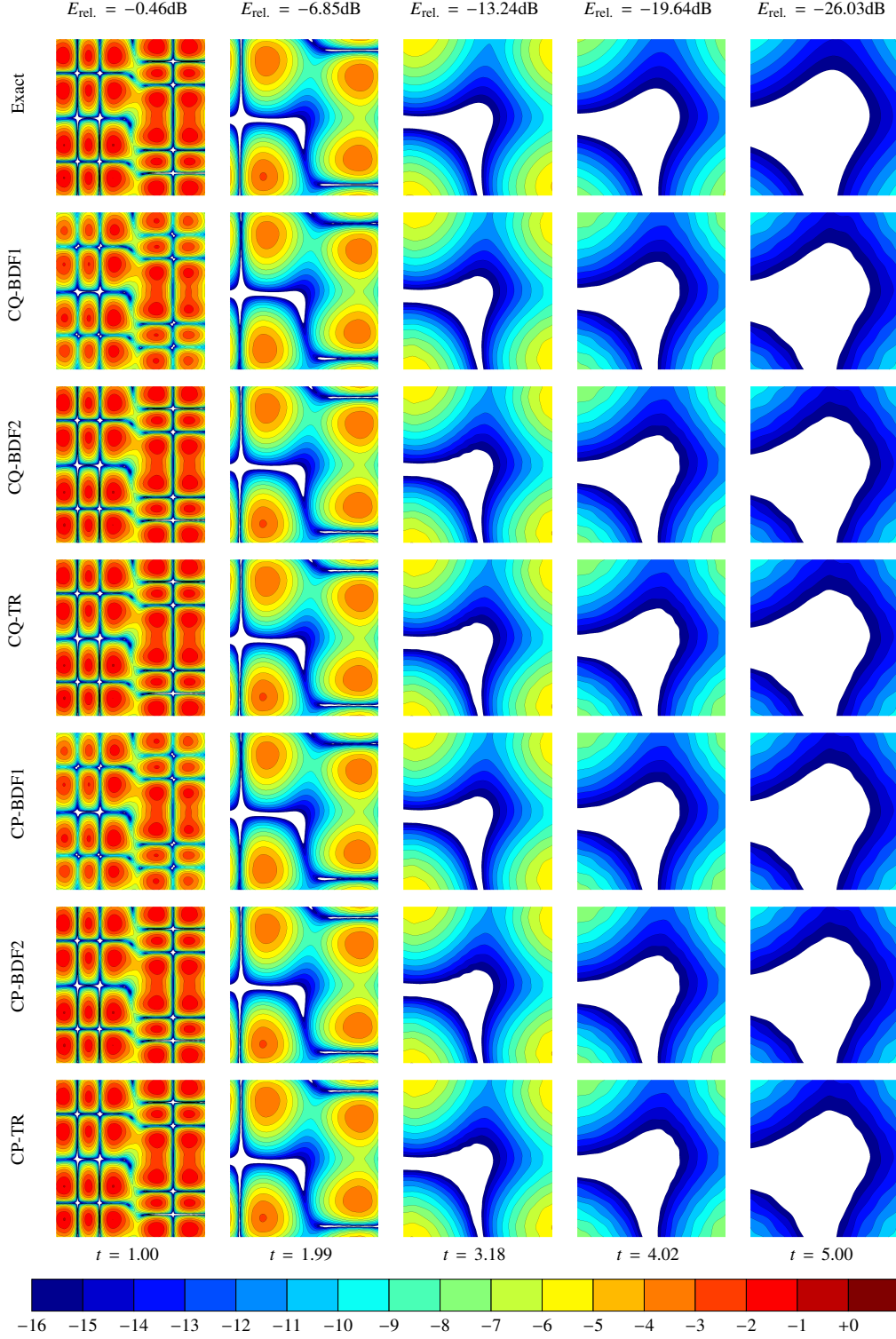


Figure 8: The figure shows contour plots of  $8 \log_{10} |u(\mathbf{x}, t)|$  with various TBCs for the IIB-type Hermite-Gaussian profile (see Table 2) for  $c = 8$  at different instants of time. The numerical parameters and the labels are described in Sec. 6.2.

is left as an open problem. A rigorous analysis of the proposed numerical schemes for stability and convergence are deferred to a future publication. We note that the high-frequency BCs do not yield a convergent numerical scheme for the IBVP. However, the stability of the Padé approximant based approach for the spatially discrete system follows from the standard results for autonomous dynamical systems. Extension of this approach to the TBC is left as an open problem.

## Acknowledgements

I, senior research fellow (grant no. 09/086(1431)/2019-EMR-I), am thankful to CSIR, India, for providing me financial assistance. I would like to thank IIT Delhi for providing the computational resources.

## References

- [1] X. Antoine, A. Arnold, C. Besse, M. Ehrhardt, A. Schädle, [A review of transparent and artificial boundary conditions techniques for linear and nonlinear Schrödinger equations](#), Comm. Comput. Phys. 4 (4) (2008) 729–796. URL <https://hal.archives-ouvertes.fr/hal-00347884>
- [2] D. Lee, S. T. McDaniel, Ocean Acoustic Propagation by Finite Difference Methods, Modern Applied Mathematics and Computer Science, Pergmon Press, New York, 1988.
- [3] M. Levy, Parabolic equation methods for electromagnetic wave propagation, Vol. 45 of IEE Electromagnetic Waves Series, Institution of Electrical Engineers (IEE), London, 2000.
- [4] Y. S. Kivshar, G. P. Agrwal, Optical Solitons: From Fibers to Photonic Crystals, 1st Edition, Academic Press, San Diego, California, 2003.
- [5] A. Schädle, Non-reflecting boundary conditions for the two-dimensional Schrödinger equation, Wave Motion 35 (2) (2002) 181–188. doi:10.1016/S0165-2125(01)00098-1.
- [6] H. Han, Z. Huang, [Exact artificial boundary conditions for Schrödinger equation in  \$\mathbb{R}^2\$](#) , Comm. Math. Sci. 2 (1) (2004) 79–94. URL <https://projecteuclid.org/euclid.cms/1250880210>
- [7] J. Szeftel, Design of absorbing boundary conditions for Schrödinger equations in  $\mathbb{R}^d$ , SIAM Journal on Numerical Analysis 42 (4) (2005) 1527–1551.
- [8] V. Vaibhav, On the nonreflecting boundary operators for the general two dimensional Schrödinger equation, J. Math. Phys. 60 (1) (2019) 011509. doi:10.1063/1.5030875.
- [9] X. Antoine, C. Besse, Construction, structure and asymptotic approximations of a microdifferential transparent boundary condition for the linear Schrödinger equation, J. Math. Pures Appl. 80 (7) (2001) 701–738. doi:10.1016/S0021-7824(01)01213-2.
- [10] X. Antoine, C. Besse, V. Mouysset, Numerical schemes for the simulation of the two-dimensional Schrödinger equation using non-reflecting boundary conditions, Math. Comput. 73 (248) (2004) 1779–1799. doi:10.1090/S0025-5718-04-01631-X.
- [11] X. Antoine, C. Besse, P. Klein, Absorbing boundary conditions for the two-dimensional Schrödinger equation with an exterior potential. Part I: Construction and a priori estimates, Math. Models Methods Appl. Sci. 22 (10) (2012) 1250026. doi:10.1142/S0218202512500261.
- [12] X. Antoine, C. Besse, P. Klein, Absorbing boundary conditions for the two-dimensional Schrödinger equation with an exterior potential. Part II: Discretization and numerical results, Numer. Math. 125 (2) (2013) 191–223. doi:10.1007/S00211-013-0542-8.
- [13] L. D. Menza, Transparent and absorbing boundary conditions for the Schrödinger equation in a bounded domain, Numer. Funct. Anal. Optim. 18 (7) (1997) 759–775. doi:10.1080/01630569708816790.
- [14] R. M. Feshchenko, A. V. Popov, Exact transparent boundary condition for the parabolic equation in a rectangular computational domain, J. Opt. Soc. Am. A 28 (3) (2011) 373–380. doi:10.1364/JOSAA.28.000373.
- [15] S. Yadav, V. Vaibhav, Transparent boundary condition and its effectively local approximation for the Schrödinger equation on a rectangular computational domain (2024). [arXiv:2403.07787](#).
- [16] S. Yadav, V. Vaibhav, Nonreflecting boundary condition for the free Schrödinger equation in 2d, in: 2023 Photonics and Electromagnetics Research Symposium (PIERS), 2023, pp. 328–337. doi:10.1109/PIERS59004.2023.10221299.
- [17] S. Blanes, F. Casas, J. Ros, Improved high order integrators based on the Magnus expansion, BIT Numer. Math. 40 (3) (2000) 434–450. doi:10.1023/A:1022311628317.
- [18] S. M. Cox, P. C. Matthews, Exponential time differencing for stiff systems, J. Comput. Phys. 176 (2) (2002) 430–455. doi:10.1006/jcph.2002.6995.
- [19] M. Hochbruck, C. Lubich, On Magnus integrators for time-dependent Schrödinger equations, SIAM J. Numer. Anal. 41 (3) (2003) 945–963. doi:10.1137/S0036142902403875.
- [20] C. Canuto, M. Y. Hussaini, A. Quarteroni, T. A. Zang, Spectral Methods: Fundamentals in Single Domains, Springer-Verlag, Heidelberg, 2007. doi:10.1007/978-3-540-30726-6.
- [21] W. Gautschi, Numerical Analysis, Birkhäuser, Boston, 2012. doi:10.1007/978-0-8176-8259-0.
- [22] E. Hairer, C. Lubich, G. Wanner, Geometric Numerical Integration: Structure-Preserving Algorithms for Ordinary Differential Equations, 2nd Edition, Springer Series in Computational Mathematics, Springer-Verlag, Berlin, 2006. doi:10.1007/3-540-30666-8.

## Appendix A. Autonomous System

The dynamical system defined by (63) and (64) can be stated as an autonomous ODE given by

$$\partial_t \mathcal{V} = \mathcal{M} \mathcal{V}, \quad (\text{A.1})$$

where the vector-valued dependent variable  $\mathcal{V}$  comprises of blocks

$$\begin{aligned} \mathcal{V}_0 &= \text{vec}(\widehat{U}) = \widehat{U}, \\ \mathcal{V}_{k+1} &= \text{vec}(\widehat{\mathcal{A}}_{k,1}) = \widehat{\mathcal{A}}_{k,1}, \quad \mathcal{V}_{K+k+2} = \text{vec}(\widehat{\mathcal{A}}_{k,2}) = \widehat{\mathcal{A}}_{k,2}, \quad k = 0, 1, \dots, K, \end{aligned} \quad (\text{A.2})$$

and the constant matrix  $\mathcal{M}$  is defined in the following paragraphs. Let us label the coefficients appearing in (64) as follows:

$$\begin{cases} \gamma_{0,1} = e^{i\pi/4} \frac{1}{2} d_0 \sqrt{\beta_1} \beta_2, & \gamma_{0,2} = e^{i\pi/4} \frac{1}{2} d_0 \sqrt{\beta_2} \beta_1, \\ \gamma_{k,1} = -e^{-i\pi/4} \sqrt{\beta_1} \left( b_k + i \frac{1}{2} \beta_2 d_k \right), & \gamma_{k,2} = -e^{-i\pi/4} \sqrt{\beta_2} \left( b_k + i \frac{1}{2} \beta_1 d_k \right), \quad k = 1, \dots, K. \end{cases} \quad (\text{A.3})$$

Setting  $\eta_0 = 0$ , the dynamical system corresponding to the auxiliary field (63) can be stated as

$$\partial_t \widehat{\mathcal{A}}_{k,1} = -\eta_k^2 \widehat{\mathcal{A}}_{k,1} + (I_2 \otimes \Lambda_1) \widehat{U}, \quad \partial_t \widehat{\mathcal{A}}_{k,2} = -\eta_k^2 \widehat{\mathcal{A}}_{k,2} + (\Lambda_2 \otimes I_1) \widehat{U}, \quad k = 0, 1, \dots, K. \quad (\text{A.4})$$

Introducing the modified stiffness matrices  $S'_p = S_p + e^{-i\pi/4} (b_0 / \sqrt{\beta_p}) \Lambda_p$ ,  $p = 1, 2$ , the dynamical system in (64) can be stated as

$$\begin{aligned} i(M_2 \otimes M_1) \partial_t \widehat{U} &= \left[ \beta_1 (M_2 \otimes S'_1) + \beta_2 (S'_2 \otimes M_1) + \frac{3}{4} \sqrt{\beta_1 \beta_2} (\Lambda_2 \otimes \Lambda_1) \right] \widehat{U} \\ &+ \gamma_{0,1} (S_2 \otimes I_1) \widehat{\mathcal{A}}_{0,1} + \gamma_{0,2} (I_2 \otimes S_1) \widehat{\mathcal{A}}_{0,2} + \sum_{k=1}^K \left[ \gamma_{k,1} (M_2 \otimes I_1) \widehat{\mathcal{A}}_{k,1} + \gamma_{k,2} (I_2 \otimes M_1) \widehat{\mathcal{A}}_{k,2} \right]. \end{aligned} \quad (\text{A.5})$$

The form of the dynamical system (A.4) and (A.5) dictates the matrix entries of the block matrix  $\mathcal{M}$  which comprises non-null matrix entries on the diagonal, the first row and the first column. It is straightforward to see that the diagonal entries of  $\mathcal{M}$  are given by

$$\begin{aligned} \mathcal{M}_{0,0} &= -i(M_2 \otimes M_1)^{-1} \left[ \beta_1 (M_2 \otimes S'_1) + \beta_2 (S'_2 \otimes M_1) + \frac{3}{4} \sqrt{\beta_1 \beta_2} (\Lambda_2 \otimes \Lambda_1) \right], \\ \mathcal{M}_{k+1,k+1} &= -\eta_k^2 (I_2 \otimes I_1), \quad \mathcal{M}_{K+k+1,K+k+1} = -\eta_k^2 (I_2 \otimes I_1), \quad k = 0, 1, \dots, K. \end{aligned} \quad (\text{A.6})$$

The entries in the first row of  $\mathcal{M}$  are given by

$$\begin{aligned} \mathcal{M}_{0,1} &= -i\gamma_{0,1} (M_2 \otimes M_1)^{-1} (S_2 \otimes I_1), \quad \mathcal{M}_{0,K+2} = -i\gamma_{0,2} (M_2 \otimes M_1)^{-1} (I_2 \otimes S_1), \\ \mathcal{M}_{0,k+1} &= -i\gamma_{k,1} (M_2 \otimes M_1)^{-1} (M_2 \otimes I_1), \quad \mathcal{M}_{0,K+k+2} = -i\gamma_{k,2} (M_2 \otimes M_1)^{-1} (I_2 \otimes M_1), \quad k = 1, \dots, K. \end{aligned} \quad (\text{A.7})$$

The entries in the first column of  $\mathcal{M}$  are given by

$$\mathcal{M}_{k+1,0} = (I_2 \otimes \Lambda_1), \quad \mathcal{M}_{K+k+1,0} = (\Lambda_2 \otimes I_1), \quad k = 0, 1, \dots, K. \quad (\text{A.8})$$

The boundedness of the system matrix  $\mathcal{M}$  under any suitable matrix norm follows from the standard results of Legendre-Galerkin method [20]. Based on the formalism, it suffices to employ any zero-stable method [21, 22] in order to arrive at a stable time-stepping scheme for the ODE in (A.1). A detailed discussion of these aspects is deferred to a future publication. Before we conclude, let us acknowledge that a similar analysis for the novel-Padé method can be carried out yielding a system of three coupled non-autonomous systems on account of the presence of three different temporal variables. The stability analysis of such system is not so straightforward and, therefore, deferred to a future publication which would also explore the possibility of employing exponential integrators [17–19] for such systems.